Knee Kinematics of Total Knee Replacement Patients: Pre and Post Operative Analysis Using Computer Generated Images

Christopher Barr BSc(hons) MRes

This thesis was submitted in accordance with the regulations governing the award of degree of Doctor of Philosophy in Bioengineering

Bioengineering Unit

University of Strathclyde

Glasgow

2011

Declaration

'This thesis is the result of the author's original research. It has been composed by the author and has not been previously submitted for examination which has led to the award of a degree.'

'The copyright of this thesis belongs to the author under the terms of the United Kingdom Copyright Acts as qualified by University of Strathclyde Regulation 3.50. Due acknowledgement must always be made of the use of any material contained in, or derived from, this thesis.'

Signed:

Date:

For Jamie

Acknowledgements

Firstly I would like to thank the subjects who took part in this study, and made it possible.

I would like to thank the staff and students at the Bioengineering Unit for their intellectual and emotional support throughout the course of this project, especially Steve and Vicky for introducing me to bodybuilder, John Davie and Steve in the workshop, Prof Nicol for his guidance, Prof Grant for her emotional support, and to Maggi, Alison, Shiv, Dave, Susie and Jules for the essential support network within the student group.

Thanks to the staff at Glasgow Royal Infirmary, especially Mr Mark Blythe and his orthopaedic team, Dr Sambrook and the radiology team, and their secretaries, Grace and Trish, who seemed to keep the whole hospital running.

Thanks to the staff at Glasgow Victoria Infirmary for keeping me on this earth.

Thanks to my family, especially my parents for all their support throughout the course of this work.

Finally, thanks to my wife Alison, who throughout the course of this project moved in with me, married me, moved to Australia with me, and supported my in absolutely everything.

Abstract

Introduction: Osteoarthritis (OA) is one of the leading causes of disability, and the knee is the most commonly affected joint in the body. The last resort for treatment of knee OA is Total Knee Replacement (TKR) surgery. Despite numerous advances in prosthetic design, patients do not reach normal function after surgery. Current surgical decisions are made on 2D radiographs and patient interviews. **Aims:** The aim of this study was to compare knee kinematics pre and post TKR surgery using computer animated images of patient specific models under every day conditions. **Methods:** 7 subjects were recruited for the study. Subjects underwent 3D gait analysis during 4 every day activities, and medical imaging of the knee joint pre and one month post surgery. A 3D model was created from each of the scans, and the kinematic gait analysis data was used to animate the images. **Results**: Improvements were seen in range of motion in all 4 activities 1 year post surgery. The preoperative 3D images provide detailed information on the anatomy of the osteoarthritic knee. The postoperative images demonstrate potential future problems associated with the implant. Although not accurate enough to be of clinical use, the animated data can provide a valuable insight into what conditions cause damage to both the osteoarthritic and prosthetic knee joint. As the animated data does not require specialist training to view, the images can be utilised across the fields of health professionals and manufacturing in the assessment and treatment of patients pre and post knee replacement surgery. Future improvements in the collection and processing of data may yield clinically useful data. **Conclusion**: Although not yet of clinical use, the potential application of 3D animations of the knee joint pre and post surgery is widespread.

Table of Contents

Chapter 1. Introduction

The population of over 65 year olds in the UK is predicted to increase by 53% from 2001 to 2031, leading to a likely increase in the number of people who have chronic illnesses (Majeed and Aylin 2005). Increases in life expectancy and ageing populations are expected to make osteoarthritis the fourth leading cause of disability by the year 2020 (Woolf and Pfleger 2003). The knee is the weight bearing joint most commonly affected by OA (Hunt et al 2008). In the UK approximately 10% of those over 50 years old suffer from knee osteoarthritis, twice as many as those who suffer from hip osteoarthritis (Dieppe, 2000). Knee replacement surgery is usually the last option in treatment of any disease of the knee, as it is a major operation and could result in complications both during and after surgery (Mizner and Snyder-Mackler 2005), but is the treatment of choice for severe degenerative joint disease (Fantozzi et al 2003). 96% of knee replacement cases in England indicated OA as the reason for surgery (Sibanda et al 2008). TKR subjects do not achieve normal knee function (Jones and Holt 2008). Failure of the prostheses occurs in approximately 9% of cases (Kurtz 2005) and less severe problems, such as pain or limited flexion, occur in 20-40% of cases (Delp et al 1998).

Results from gait laboratories are not well understood by clinicians (Baker 2006). New information gained from 3D visualisation of the knee joint could lead to improved clinical outcomes by providing valuable information for both making and evaluating treatment decisions (Sheehan Siesler and Alter 2008).

A better understanding of kinematics of the knee joint could lead to improved surgical procedures, better implant design, and an increase in the life of the implant. Assessment of in vivo kinematics in 3D could aid in the studying of the diseased and replaced knee joint and could aid in studying of new designs. These factors could lead to improved operation results, quality of

life for the patient, and ultimately reduce the cost burden on the health service.

Aims and Objectives

The aim of this project was to show a comparison of knee kinematics in pre- and post- operative total knee replacement surgery, using computer animation to represent a patient specific model of the knee joint interactions under every day conditions.

In order to do this, the project objectives were to:

- Conduct gait analysis on subjects with osteoarthritis of the knee who were awaiting knee replacement surgery.
- To make patient specific 3-dimensional computer models of the affected knee joint from MR imaging.
- To utilise current virtual reality packages to animate the movements of the knee joint as measured from the gait analysis, allowing a visualisation of the interactions of the femur and tibia during everyday actions of walking, ascending and descending stairs, and rising from a chair.
- To repeat this process one year after TKR surgery, and to compare the results pre- and post-operatively.

Chapter 2. Background

The knee

The anatomy of the knee has been well documented and descriptions are available in numerous anatomy text books (Gray 1918, Tortora 2008). To surmise (figure 2.1), the femur is the longest and heaviest bone in the human body. Proximally it articulates with the pelvis, and distally with the tibia and patella. Distally, the medial and lateral condyles articulate with the medial and lateral condyles of the tibia respectively. Between the condyles is the intercondylar fossa (Gray 1918). Medially, the femoral condyle consists of the arcs of two circles, the anterior facet articulates with the tibia in extension, and the posterior in over 20° flexion. Laterally, the epicondyle consists of almost entirely a single arc, similar in radius to that of the posterior arc on the medial epicondyle (Iwaki et al 2000).

The tibia articulates proximally with the distal condyles of the femur, and with the fibula. Distally it articulates with the fibula and the talus bone of the ankle. The Medial side of the tibia consists of two angled flats that articulate with the two arc facets of the femur, whist laterally, the tibia is roughly flat (Iwaki et al 2000).

The patella is a small rounded bone on the anterior of the joint. The broad superior end is the base, and the pointed inferior end is the apex. The posterior surface contains two articular facets, which articulate with the medial and lateral condyles of the femur. The patellar increases the leverage of the tendon of the quadriceps by providing a mechanical advantage to the quadriceps.

The anterior cruciate ligament (ACL) extends posteriorly and laterally from the area anterior to the intercondylar eminence of the tibia to the posterior part of the medial surface of the lateral condyle of the femur. The posterior cruciate ligament (PCL) extends anteriorly and medially from a depression

on the posterior intercondylar area of the tibia and lateral meniscus to the anterior part of the medial surface of the medial condyle of the femur.

The medial meniscus is a semicircular piece of fibrocartilage whose anterior end is attached to the anterior intercondylar fossa of the tibia anteriorly to the ACL, and whose posterior is attached to the posterior intercondylar fossa of the tibia between the attachments of the PCL and the lateral meniscus. The lateral meniscus is a near circular piece of fibrocartilage whose anterior end is attached anteriorly to the intercondylar eminence of the tibia and is lateral and posterior to the ACL. The posterior end is attached posteriorly to the intercondylar end of the medial meniscus.
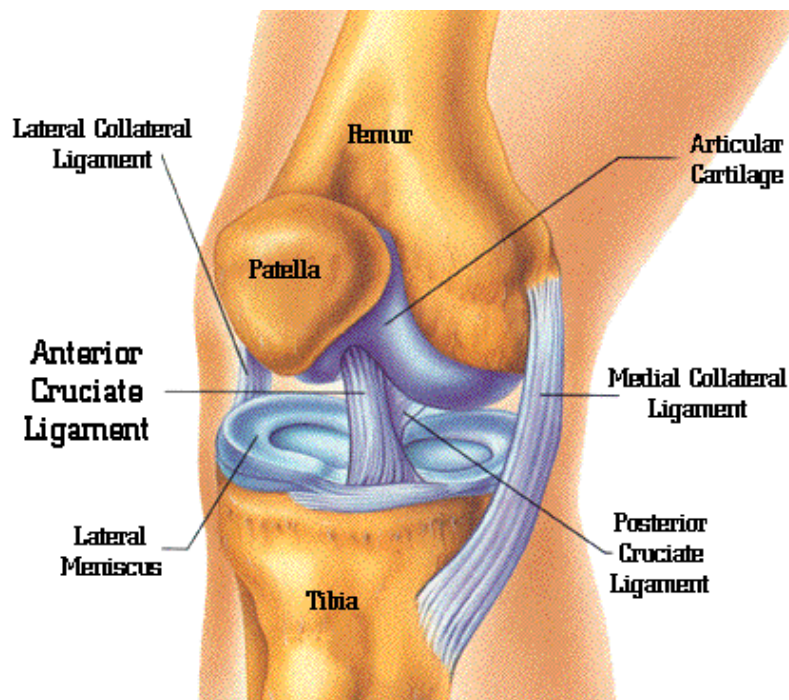

Figure 2.1 Diagram of the gross anatomy of the knee joint.

Image from http://wazajournal.com/media/2010/02/kneeanat1.gif accessed February 2011

Osteoarthritis

Osteoarthritis (OA) is a degenerative joint disease, which mostly affects the elderly population, and is the most common form of arthritis (Felson et al 2000). It is a disease that affects the cartilage in joints, which, along with the synovium, gradually wears down and allows bone to rub on bone (Shiozaki et al, 1999). OA results in bony remodelling, capsular stretching, cartilage loss, and weakness of articulating muscles (Felson 2006) and leads to pain and loss of function primarily in the knees and hips (Woolf and Pfleger 2003). The factors that influence osteoarthritis are not well understood (Andriacchi et al 2000). Currently, assessment is based on clinical examination of symptoms and radiographic assessment (Andriacchi and Alexander 2000).

In the UK approximately 10% of those over 50 years old suffer from knee osteoarthritis, twice as many as those who suffer from hip osteoarthritis (Dieppe, 2000). In the USA, approximately 12% of the population aged 55 or over show radiographic osteoarthritis of the knee, and many without radiographic symptoms also probably have OA (Felson, 2006). Radiographic assessment is the primary method of evaluation (Davies and Glasgow, 2000), however a number of studies question the relationship between radiographic assessment and the symptoms associated with osteoarthritis, believing that the condition is dependent on neuromuscular status rather than knee damage (Dieppe 2000). Indeed, there is no standardised method in which radiographs are requested, and many surgeons request x-rays in only one plane, and in non-weight bearing conditions (Davies and Glasgow, 2000). The prevalence of osteoarthritis increases with age, as the disease is irreversible (Silman and Hochberg 1993), rising to 18% for females over 65 years old (Kaufman et al 2001).

Although no one is certain of the cause of osteoarthritis, there are a number of accepted risk factors, including age, obesity, injury, genetic predisposition, and gender, with females being more at risk, and obesity being a higher risk factor in females than males (Matsuda et al 1998). Recent investigations

however suggest that these factors place a patient more at risk for the initiation rather than the progression of the disease (Dieppe, 2000), although onset and initiation of the disease both increase with body mass index (Matsuda et al 2004). The warning signs of the onset of osteoarthritis are complaints of steady or intermittent pain when moving, stiffness or swelling of the joint when resting, a tenderness in the joint, a crunching feeling or sound when in motion, and radiographic evidence of cartilage loss, bone damage or bone growth spurs (Andriacchi and Alexander 2000). Osteoarthritis was estimated to be the 8th leading non-fatal burden of disease in the world in 1990, and is expected to rise to 4th by 2020 (Woolf and Pfleger 2003).

Non-steroidal anti-inflammatory drugs (NSAIDS) and other analgesics are commonly used to treat osteoarthritis, with a positive result with respect to many knee-scoring systems used clinically (Andriacchi et al 2000). However these systems rely heavily on pain reporting. Andriacchi et al noted that the decrease in pain is associated with an increase in joint loading due to the removal of the pain protective reflex by the analgesic action, which may actually worsen osteoarthritis in such patients. More recently, there are a number of studies into preventative medicine, in particular with the use of nutritional supplements such as glucosamine, and essential fatty acids (EFA's) from sources such as cod liver oil (Curtis et al 2004). Benefits have been shown in the clinical trials described by Curtis, and there is some evidence of the benefits of other nutritional supplements, however there is little scientific proof at the cellular or molecular level to explain their mechanisms of action.

Knee Replacement Surgery

Knee replacement surgery is usually the last option in treatment of any disease of the knee, as it is a major operation and could result in complications both during and after surgery (Mizner and Snyder-Mackler

2005), but is the treatment of choice for severe degenerative joint disease (Fantozzi et al 2003). 96% of cases indicated OA as reason for surgery in England (Sibanda et al 2008), and 94% of cases from the Mayo clinic in The USA indicate OA as the underlying diagnosis. (Singh et al 2010).

In England between 2003 and 2006, 85% of knee replacement procedures were cemented, 7% cementless, and 5% were unicondylar (Hospital Episode Statistics (HES) database) (Sibanda et al 2008). There are a number of companies world-wide that produce different variations of prostheses, including the substitution or retention of the posterior cruciate ligament, and those with a fixed or mobile bearing, for a choice of rotational stability (Harrington et al 2009, Duffy et al 2008).

While some papers have reported a significant clinical difference in posterior cruciate retaining versus sacrificing designs, other authors have reported no difference (Fantozzi et al 2003). The national joint registry for England and Wales reported in 2007 that TKR in England and Wales was done by using 86 different prosthesis brands (Sibanda et al 2008).

TKR is performed more on females than males, with incidence of TKR in the UK increasing from 28.7 to 99.4 cases per 100,000 males and from 42.5 to 138.7 cases per 100,000 females between 1991 and 2006 (Culliford et al 2010). From 1990 to 2002, total numbers of both primary and revision surgery in the USA have increased threefold from 129,000 to 381,000, which is 4 times the increase of primary THR surgery (Kurtz et al 2005). The growth of primary TKR is viewed as recognition of the effectiveness of the procedure, but is also postulated that the reason knee surgery is increasing more than hip surgery is partly due to the rising prevalence of obesity (Kurtz et al 2005). Life expectancy in the UK increased over the period 1991 to 2009, from 73.4 years to 77.9 years for males and from 78.9 years to 82.0 years for females (statistics.gov.uk). Given this it is probable that the increase in TKR procedures is in part due to the ageing population. It is not clear at what stage, in life or the disease that it is best to undertake knee

replacement surgery, but it is vital that the surgery is done at a time that will maximise the value to the patient and reduce the chance of the need for revision surgery (Kennedy et al 2003). TKR has excellent post-operative results, with a marked reduction in pain, increased ability to carry out activities of daily living and thus increase the quality of life for the patient (Tanaka et al 2000). However, the surgery is not shown to lead to levels of functionality that compare with the normal population (Mizner and Snyder-Mackler 2005). Jones and Holt (2008) developed an objective tool to assess the clinical outcome of TR surgery. They used a simplex plot based on the Dempster-Shafer theory to assess outcomes of gait analysis. By classifying the outcome in 4 groups – dominant normal, non-dominant normal, non-dominant OA, and dominant OA – they found that preoperatively and in 3, 6, and 12 months postoperatively TKR subjects do not achieve normal knee function. Success of the prosthesis depends at least partly on the design and alignment. (Delp et al 1998). Improvements in cut alignments improve procedural outcomes; however 8% of tibial cuts are malaligned by more than 4 degrees in the coronal plane (Delp et al 1998), and incorrect positioning increases the wear and tear of the prosthesis. (Stulberg. Loan and Sarin, 2002).

Failure of the prosthesis is usually due to polyethylene wear, component loosening, instability, infection, arthrofibrosis, malalignment or malposition (Sharkey et al 2002). Less severe problems, such as pain or limited flexion, occur in 20-40% of cases (Delp et al 1998). The ultimate aim is to have longevity of the implant by reducing component loosening, as it will reduce the risk of the need for revision surgery and allow the procedure to be carried out on a younger patient group (Catani et al 2003). A recent study (Longstaff et al 2009) classified alignment success by a cumulative score of errors in 6 different alignment parameters. Of 146 TKR implants conducted in a single hospital, 46 had a cumulative error score $\geq 6°$. Those who had a score less than $6°$ had a significantly better functional outcome as measured by the Knee Society Score at 1 year than those with a score over $6°$. Alignments

for cutting are made on standard bone geometry, however as the literature demonstrates a high percentage of alignment error (Longstaff et al 2009), it is possible that bone deformation in OA can adversely affect the precision of angular cuts made in TKR surgery.

In the USA, revision surgery cases for TKR increased from 12,000 in 1990 to 35,000 cases in 2002. This represents an increase of 166% to 5.4 cases per 100,000 population (Kurtz 2005). Revision rates in England between 2003 and 2006 were 0.4% within 1 year, and 1.4% within 3 years, irrespective of whether the implant was cemented or cementless (Sibanda et al 2008). If a reduction in revision surgery of 1% (from 8.4% to 7.4%) could be achieved, it would result in a reduction of 4500 procedures per year in the USA, saving an estimated US$53-94m (Kurtz 2005).

A history of arthroplasty development (Andriacchi et al 1982) and specifications for modern implants (www.depuy.com) can be found elsewhere. In summary, the end of the femur is replaced with a smooth metal surface, which fits onto a tibial plate. This plate is made of a type of plastic, which may be supported by a metal backing. The two components are usually fixed to the bone with surgical cement. Alternatively, components maybe coated with hydroxyapatite (Uvehammer, Kärrholm and Carlsson 2007), which encourages bone to grow into them to help hold the components in place.

The femoral component of the prosthesis is rounded to maximise the contact area, thus reducing the stress placed on the polythene insert. This also helps reduce excess loading on the medial or lateral edges that can be caused by varus or vulgus thrust during gait. There is also a smooth ridge to allow the patella to move smoothly from flexion to extension, and to be comfortable at high flexion angles (figure 2.2).

Figure 2.2 Sigma Knee System from Depuy
(https://www.healthbase.com/hb/pages/fixed-bearing-knee-replacement.jsp
accessed February 2011)

The tibial trays are modular, and have either a rough, porous surface to allow bone growth and attachment, or are cemented. The tray is most commonly made of titanium, allowing it to be strong yet thin, meaning a minimal amount of bone resection is needed. The insert contains a locking lip to prevent polyethylene creep. The insert is symmetrical to allow for an even distribution of load across the tibial plateau. The cemented type has an undercut to allow cement to seal around the edge of the implant. The cement creates a seal around the implant, and protects against debris entering the bone/cement/implant interfaces.

3D Gait Analysis

Gait analysis can be conducted for any number of conditions for analysis of numerous aspects of gait. Kinematic data can be used to collect data on the gait cycle, using a variety of motion analysis software or video cameras.

Force plates or localised transducers can be used to assess the forces through the joints of the body. Gait has been analysed using fluoroscopy (Komistek et al 2005), comparison to one and two plane x-rays (Li et al 1993), CT and MRI scans (Otake et al 2002) with varying degrees of success. Analysis can be conducted on anything from straight walking (Deluzio and Astephen 2007) to the kinetics and kinematics of gymnastics (Mills et al 2005), and how patients with certain afflictions can perform certain tasks, such as an arthritic patient climbing into a car (Pudlo et al 2009). Many comparisons have been made of control subjects and patients (Desailly et al 2009), and gait analysis has even been used on chickens by vets (Sandilands et al 2011). Yet, there is no standardised method for the use of a gait laboratory, marking of the subject, or analysis of the data. As a result of this, a comparison of inter-laboratory results is difficult. Regardless of the method used, gait data is collected in a set fashion.

As first demonstrated by Muybridge in 1887, dynamic gait analysis is conducted using some form of photography, and the method that gait analysis is currently based on was first devised by Braune and Fisher in 1895 (Cappozzo, 1984). Braune and Fisher were the first to represent the body as a set of rigid segments, and used stereometry to reconstruct the 3-dimensional position of a segments instantaneous position in a laboratory coordinate system. This works on the basis that three non-collinear points on the segment can define its full position.

Forces acting on a body can be described as being either internal or external. External forces are the only truly measurable forces, and this was first fully demonstrated by Eberhart et al in 1947 (Cappozzo, 1984). This group constructed and utilised a dynamometric platform that could measure ground reaction forces in all six degrees of freedom, three forces and three moments. Internal forces can be calculated by a series of measurements,

assumptions, and calculations, using mass, centre of gravity, and inertial properties. The intersegmental forces can be calculated by using assumptions of a linked chain of rigid bodies.

Rotation of one body segment around another is normally reported as absolute orientation in a global coordinate system or as relative orientation with a reference frame embedded in one segment (Wu and Cavanagh 1995). Another method that is relatively standardised is the use of the Grood and Suntay (1983) coordinate system for calculation of joint angles. In this system, two axes are fixed body axes, one in body A and one in body B. The third axis is a cross-product of the first two, and so is called a floating axis, as it is not fixed in either body, and moves relative to each segment. For each of these methods there is a corresponding Euler angle (Sheehan and Mitiguy 1999). Euler angles are less complicated, but must be calculated in a specific order. Euler angles are more commonly used when the data is to be utilised in computer graphics packages (Ma et al 2004)

Gait analysis is now at a mature stage of development, with systems delivering the level of accuracy needed in conventional gait analysis (Baker 2006). Improvements are aimed at the ease and speed in which data is collected and interpreted, and decreasing the costs and skill levels needed to use gait analysis systems (Whittle 2002 3rd ed), and to make the data clinically relevant (Schwartz et al 2004). Clinical relevance can be described as 'if this is normal how many degrees does it have to deviate by before it is significant' (Schwartz et al 2004). If analysis conceals errors important information can be lost, conversely, if limitations are not known small deviations may be considered meaningful or over interpreted (McGinley et al 2009). The biggest effect on results is misplacement of the lateral and medial epicondyle markers (Stagni et al 2006). McGinley et al (2009) reviewed 3D gait measurements in previous studies. They found that while the biggest errors in calculation of knee kinematics are in the transverse

plane, clinically acceptable errors can be achieved, but not always are. Thus, Natural variability should not be confused with experimental error. The main error in calculation of knee joint angles derives from malalignment of axes resulting in cross talk, and movement of markers relative to the underlying bone resulting in skin motion artefact (SMA) (Leardini et al 2005, Della Crosse et al 2005). Instrumental errors are negligible with proper calibration, but SMA and anatomical landmark misplacement are critical (Stagni et al 2006). SMA effect results in the frontal and transverse planes more than the sagittal plane (Lu and O'Connor 1999). SMA has a level of error at least an order of magnitude higher than sterophotogrammetric errors, but the effects of SMA can be reduced by choosing placement of a cluster of markers at a point of minimum relative motion, with proximal thigh markers being more prone to SMA than distal. (Cappozzo et al 1996). SMA errors can be further reduced by using a double calibration method, where a calibration is conducted at both maximum and minimum knee flexion, reducing errors to within $3°$. (Cappello et al 1997).

Hip joint centre location is problematic in gait analysis, as the hip cannot be directly palpated and externally marked due to its anatomical position, and therefore must be calculated. The most common method used to calculate the hip joint centre is based on cadaveric anthropometric studies by Bell et al (1990), resulting in the hip joint centre estimation to be identified within 26mm of its true position. While mislocation of the hip joint centre can result in large errors in hip kinematics, mislocation of up to 30mm has been shown to effect calculated knee kinematics by as little as $1.5°$ (Stagni et al 2000).

Gait in Osteoarthritis

Healthy elderly people have less flexion/extension and more internal rotation than young healthy subjects, possibly due to weaker muscles, poorer tone, and compensatory motions (Marin et al 1999). It has been hypothesised that patients with osteoarthritis change their gait in a compensationary manner to

minimise loading on the joint, thus reducing pain (Kaufman et al 2001). Few studies have quantified changes in gait associated with osteoarthritis, and most are on a level walking surface (Astephen et al 2008). Dynamic assessment of loading during gait is a better predictor of clinical outcome than static measurements, and the presence of either a varus or vulgus deformation has no effect on whether the disease progresses or not (Andriacchi et al 2000). Patients with OA walk slower than healthy controls during both level walking and stair ascent and descent, even at early stages of the disease (Kaufman et al 2001).

Gait in TKR

Evaluation of gait is seen as being one of the most important post-operative tasks (Tanaka et al 2000). Numerous studies have compared cemented or cementless implants (Tanaka et al 2000), fixed and mobile bearing tibial implants (Ball et al 2010), cruciate sacrificing and cruciate retaining surgeries (Saari et al 2004), unilateral or bilateral compartment replacements (Mattsson et al 1990) and have reported by using standardised scoring systems (Deluzio et al 1999), assessment of range of motion (Ng et al 2007), functional living outcomes (Bourne 2008), and angles and forces (Andriacchi et al 2000). Depending on the methodologies used and outcomes measured, many conflicting views on the success or otherwise of TKR have been reported. Chao et al (1980) conducted a study measuring pre and post-operative gait and knee motion data in patients with TKA, as well as a control group. Their results demonstrate that there is a marked improvement in knee function, pain control and correction of deformity after TKA. Deluzio et al (1999) compared pre and post-operative data for unicompartmental arthroplasty patients using gait analysis and the knee scoring system (KSS). The KSS marked a score out of 200, and the gait analysis score was out of 8. The gait score was calculated on a number of measured parameters, and given a point if they fell within the "normal" range

for that parameter. Both the pre and post-operative results from these tests had a very good correlation, however, the pre-operative correlation was better, possibly due to the fact that the gait score is purely functional whereas the KSS relies rather heavily on subjective pain scoring. In 1987, Berman et al studied gait both pre and post-operatively in 16 patients with unilateral TKA with unilateral involvement.   Post-operatively, all patients showed significant improvements in stance time, single support time, step length, double support time, velocity and swing/stance time ratio (but not swing time). Levels also improved from poor pre-operatively to excellent in the follow up study. Mattsson et al (1990) examined pre and 1year post-operative data on patients with ether uni- or bi- compartmental knee replacements.   Those patients with unicompartmental Knee replacement showed significant improvements as assessed by the British Orthopaedic Association Assessment Chart (BOA), maximum walking speed, oxygen cost of walking, pain and perceived exertion when walking at maximum speed.

It is postulated that cemented prostheses are better as the patient can undertake full weight bearing during gait two weeks earlier than the cementless type (Tanaka et al 2000). However, Tanaka et al (2000) showed that, although earlier results were better due to the earlier stage that patients with cemented TKA could walk with full weight bearing, there was no significant difference in the gait of the patients with cementless prostheses after one year post-operative follow up. Saari et al (2004) compared cruciate sacrificing and cruciate retaining tibial inserts. No difference was found in maximum flexion, maximum extension or knee scoring system results between those with cruciate sacrificing implants, cruciate retaining implants or the control group. Oberg et al (1996) conducted a 6-month follow up on 118 patients who underwent TKA with a cemented prosthesis, assessing both everyday activities and more traditional orthopaedic variables.   The patient group showed significant improvement in 18 of the 20 variables (the other two were aimed at patients with hip replacement, and so this group had nothing to improve in), most marked in the variable of pain.   This study

showed marked improvements in functional and social variables related to activities of daily living. Gait analysis can also be used to calculate the external joint loading. Andriacchi et al (2000) found that the peak force on the medial compartment was about 2.5 times that of on the lateral compartment, and postulates that the increase in adduction moment may be associated with an increase in prevalence of osteoarthritis or in the progression of the disease.

Stair Negotiation

Stair climbing is of particular interest since stairs are encountered in daily living, and requires greater knee moments and ranges of motion than those required in level walking (Andriacchi et al 1982). Stair climbing is a demanding locomotor task that is an essential part of everyday living. For the elderly and those with disabilities of the lower limb, stair climbing can be a very demanding task. The ability to ascend stairs could dramatically improve the quality of life of a person with physical disabilities and lighten the workload of caregivers (Nadeau et al 2003).

An increased range of motion at the knee joint of up to 20° more than that seen in level walking is required to successfully negotiate stairs, meaning mild restrictions in range of motion can dramatically reduce functional performance (Nadeau et al 2003).

Chair Rise

Rising from a chair is an essential part of everyday life, movements involved in using a chair are also used in other aspects of everyday living such as getting into and out of bed and in toileting. Knee arthritis is one of the most common forms of illness in the elderly that affects their ability to rise from a sitting position (Su et al 1998). The forces across the knee joint are seven

times higher in rising from a chair than stair ascent or level walking (Saari et al 2004). Post TKR surgery, a reduction in functional range of motion of 30%-40% is seen when compared to age matched control groups (Mizner and Snyder-Mackler 2005).

Visualisation of the Knee Joint

It is important to visualise the knee joint in the diseased state as bone geometry can affect kinematics (Siesler and Sheehan 2006). Radiological imaging is used in osteoarthritis as a measurement of change in the joint, both before and after surgery (Rovati, 1999), as it shows the main pathological changes in osteoarthritis, such as cartilage loss as measured by joint space narrowing, osteophytes, bone sclerosis and cysts (Vignon, 1999). It is desirable to estimate the 3D pose from a 2D x-ray image (Mahfouz et al 2005). Radiographic assessment has been recommended as an outcome measure of osteoarthritis in clinical trials of potential structure modifying drugs (Buckland-Wright, 1999). However there is no agreement on how to assess radiographic data or define progression of osteoarthritis (Andriacchi et al 2000). The radiograph is still the gold standard by which OA of the knee is assessed, however it does not meet the needs as it provides an indirect and therefore unreliable method of measuring cartilage by way of measuring the joint space width (Teichtahl et al 2008). Further, they are 2-dimensional and so cannot measure 3-dimensional changes and structures.

CT scans of the knee joint have been used to create 3D computer aided design (CAD) models of the knee joint registered to radiographs (Asano et al 2001), or fluoroscopic images (Dennis et al 2001), but are not the most common method of scanning due to the risks associated with radiation exposure.

MRI is an excellent tool for visualising the pathological processes of the knee joint, as high-resolution images can view both osseous structures and soft

tissue such as the menisci and ligaments in multiple planes (Khanna et al, 2001). MRI has proven to be an accurate non-invasive assessment technique with several unique advantages such as recording of 3D coordinates and precise visualisations of bone and volume reconstruction (Wretenberg et al 2002). Recent advances in MRI technology have allowed for images to be recorded in open scanners during quasi-static load bearing (Johal et al 2005) and Cine phase contrast MRI has been used to study patellar elongation and strain by calculating from 3D velocity profiles for the tibia femur and patella (Sheehan and Drace 2000). MRI is a clinically useful method to determine the 3D position of the knee joint, comparing well to other methods using RSA/CT and 3D digitisation (McPherson et al 2005).

Studies using MRI have shown that there are variations in anatomical geometry in OA patients, and that these individual differences should be taken into account by surgeons when planning TKR surgery (Matsuda et al 2004). Spotting early changes may lead to novel targets for prevention and treatment (Teichtahl et al 2008). MRI and fluoroscopy are also being integrated into CAS in orthopaedics (Schep et al 2003).

Fluoroscopy is a method of imaging x-rays in real time, to produce an x-ray movie of motion. 3D images can be posed from fluoroscopy if the geometry of the item being imaged is known, such as in prosthetic implants. In general, fluoroscopy uses pattern matching algorithms to estimate the 3D pose of the joint from a 2D silhouette (Hossain et al 2008). Fluoroscopy can also be used to ensure reproducible positioning both within and between patient visits (Buckland-Wright, 1999). Fluoroscopy provides sufficient accuracy to detect relative motions of even a few degrees and translations of a few mm between the tibial and femoral components, but suffers from a limited field of view, exposing the patient to radiation and requires extensive analysis of images (Fantozzi et al 2003). Patient specific 3D images of the knee joint can be achieved by registering fluoroscopic images with CT scans (Dennis et al 2005). Fluoroscopy and motion analysis can show real time imaging of TKR kinematics without giving direct visualisations of contact

areas or surrounding tissues (Carpenter et al 2009). A mobile fluoroscope system that is capable of tracking movements as fast as jogging has also been developed (Liu et al 2007).

Computer based surgical simulation uses volumetric models generated from MRI (Gibson et al 1997). DiGioia et al (1998) provide an overview of the main types of computer-aided surgery. Briefly, there is a limited ability to couple pre-operative planning with intra-operative procedure. Image guided and surgical navigation systems bring imaging into the operating room and can provide the surgeon with vital intra-operative information. This procedure utilises CT or MRI data to provide precise patient specific imaging and planning. Computer assisted orthopaedic surgery provides patient specific pre-operative planning, with cause and effect type practice. Registration must take place to orientate the image with the patients' position (e.g. by surface matching). Tracking devices are attached to the surgical tools to map position and orientation during surgery. This system must also have a good human-computer interface. There are three main types of computer-aided surgery: Passive, where the planning is done pre-operatively and can make use of navigators or aiming devices, but the work is all done by the surgeon, semi-active, which utilises a template of the work, and active, an autonomous robotic system that works under the guidance of the surgeon.

The Clinical Need for an Improved Visualisation Tool

Gait analysis is still considered a research tool and efforts must be made to improve on the clinical usefulness and the time/cost of gait analysis (Simon 2004). Results from gait laboratories are usually reported as Euler or Cardan rotations or the Grood and Suntay convention of describing joint rotations, which are not well understood by clinicians or many bioengineers

(Baker 2006). New information gained from 3D visualisation of the knee joint could lead to improved clinical outcomes by providing valuable information for both making and evaluating treatment decisions (Sheehan and Siesler 2008). The increase in demand for TKR has necessitated the improvement in durability of knee prostheses (Hossain et al 2008). To improve diagnostic accuracy, and to reduce the impact of joint impairment on the function of the joint, 3D kinematics of the knee joint must be quantified (Seisler and Sheehan 2006). In vivo measurement of prosthetic kinematics can yield information vital for future prosthetic design (Hossain et al 2008)

Chapter 3. Methods

Subject Recruitment

Ethical approval for the project was gained from North Glasgow University Hospitals NHS Trust on 21st March 2003.

Subjects were first identified from the waiting lists of two surgeons at Glasgow Royal Infirmary (GRI). Case notes of the patients who were awaiting total knee replacement for osteoarthritis were then studied to assess suitability based on the following criteria for inclusion in the study:

- The patient had osteoarthritis of the knee
- The uninvolved knee was either not or only slightly affected, or had already been replaced, so as not to have a large impact on gait.
- The patient was over 50 years of age.
- The patient was not housebound and could walk more than 500 metres.
- The patient's symptoms were not so severe as to not be able to do the trials asked of them.
- Their operation was not in jeopardy due to co-morbidities.

Those patients who were deemed suitable for inclusion in the study from the analysis of the case notes were then contacted via a telephone call by the author to further assess suitability, to gauge interest in the study, and to check that there were no factors omitted from the case notes that would exclude them from the study. This included discussing the patient's daily functional abilities and mobility, pain levels and tolerance, as well as other factors affecting their waiting times, such as holidays. A time and date was then agreed for the author to visit the subjects to discuss in more detail the protocol of the project and to go through the consent forms (appendix I and

II). Once the subjects agreed to take part, an appointment was made for them to attend the Bioengineering Unit at Strathclyde University for gait analysis. Figure 3.1 shows the flow of patient recruitment for the study.
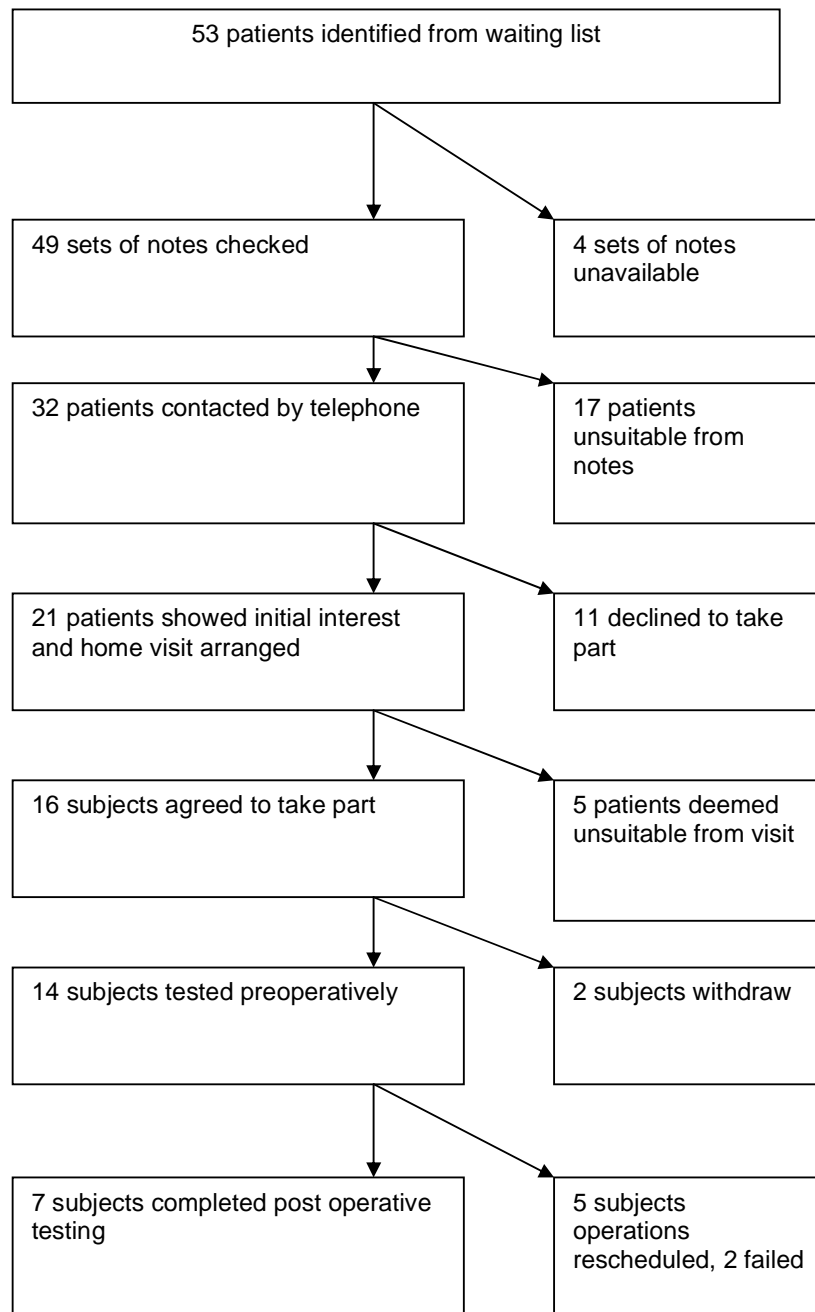
Figure 3.1 Flowchart of subject recruitment procedure

Motion Analysis

Vicon System

Motion analysis was conducted on a Vicon Motion Analysis 612 system from Oxford Metrics ®. An 8 camera setup was used, with the cameras positioned at varying heights and positions in order to allow the markers on the shank to be seen when the subject was standing on the ground, up to visualisation of the pelvis markers when the subject was at the top of the 4-step staircase. In total, the area of observation was 3.5m high, with a walkway of 5m and a width of 2.5m. Kinematic data was captured at a rate of 120Hz.

A calibration procedure was followed at the initial setup of the laboratory for each session. Firstly, a static calibration was carried out. This involved placing an L-frame with 4 markers a known distance from each other on the floor at the centre of the testing area. The L-frame allows the Vicon system to build up a representation of the test area, using the markers to determine the origin of the laboratory, the X and Y directions, and using the plane of XY to determine Z.

A dynamic calibration was then carried out. Two markers on a wand a known distance apart were waved in the test area, ensuring that the markers covered all the area the patient will be active in. This was done in such a way as to ensure that all eight cameras could see the markers in all positions in the testing area. The calibration was accepted if the reconstruction errors were less than 1mm for each camera, less than 0.75mm average error for all eight cameras, and the wand was visible to each camera more than 65% of the time.

The data was recorded on a PC using Vicon Workstation, via the Vicon Datastation.

Initial analysis of the Vicon workstation was conducted in order to assess the optimum camera and marker setup. Different camera positions and angles were used to obtain maximum exposures of the markers to as many cameras as possible. Numerous practice runs were also conducted to ensure a consistent system and calibration set up.

Marker Placement

In the first marker setup tests, 14mm markers were placed directly onto the anatomical landmarks. The first problem encountered with this approach was that the markers on the medial landmarks (medial malioi, medial tibial epicondyle, medial femoral epicondyle) were frequently occluded from view of the cameras. Some markers were also knocked off the skin during swing phase of gait. Markers placed over the left and right anterior superior iliac spines were occluded on overweight and obese subjects due to skin folds. The markers were also out of view of the cameras on all subjects during sit to stand.

The CAST method (Cappozzo et al 1995) was then assessed for suitability of use. In this method a cluster of at least 3 markers are placed onto a segment to track its motion. Anatomical points are then labelled, and their position in relationship to the cluster on the segment is calculated. The anatomical markers can then be removed, and virtually reconstructed at the data processing stage. For this study, a cluster of 4 markers for each segment was used to introduce a level of redundancy in the cluster. In order to visualise medial anatomical points, a wand marker system was used to allow for the creation of virtual points at the data processing stage. The wand marker system consists of a rod with two markers a known distance

apart, with the tip of the wand a known distance from its closest marker. The tip of the wand is then placed onto the anatomical point to be marked. At the data processing stage, the two markers create a vector, and a virtual marker is then calculated to be at the tip of the wand.

In order to remove any error caused by relative motion of markers within a cluster, each set of 4 marker clusters for the thigh and shank were mounted onto a rigid plastic plate, which was contoured to fit over the segments. The clusters were then attached to a nepoprene strap, and were secured onto the segment with Velcro. Medipore tape was then placed over the segment, strap and cluster, to ensure the strap and cluster did not slip. Clusters were positioned over the area of the segment deemed to have the least skin motion artefact, while optimising visualisation. Both clusters were placed distally and anteriorly or anteriolaterally (figure 3.2). The placement of the clusters agree with a pilot study by Stagni et al (2005).

The pelvis cluster markers were placed on the posterior of an orthopaedic belt attached to the waist with a Velcro strap. Markers were placed directly onto the belt, as it was only used for static calibration.

Each anatomical point of interest was palpated and marked on the subject with a skin pencil before calibration took place (figure 3.3).

Fig 3.2 marker clusters attached to each segment

Pelvis

The anterior and posterior superior iliac spines (LASIS, RASIS, LPSIS, RPSIS) were marked to identify the pelvis. This was to allow calculation of the hip joint centre (HJC).

Femur

The medial and lateral epicondyles of the femur (MFEP, LFEP) were identified and marked to allow the calculation of the distal end of the femur (DFEM).

Tibia

The medial and lateral epicondyles of the tibia (MTEP, LTEP) were marked to calculate the proximal end of the tibia (PTIB), as were the medial and lateral malleoi (MMAL, LMAL), to calculate the distal end of the tibia (DTIB).

The femur was defined as being from the HJC to DFEM, and the tibia was defined as PTIB to DTIB.
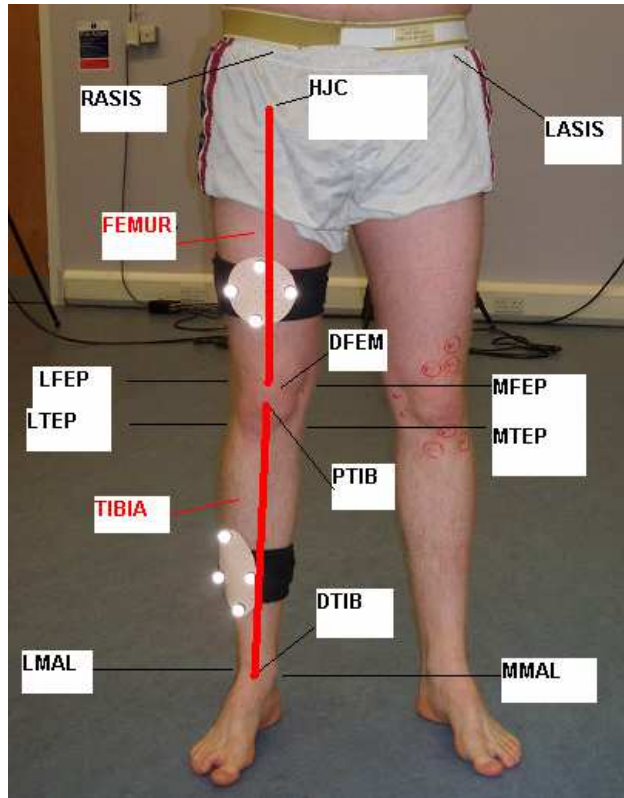
Figure 3.3 Identification of anatomical landmarks

Once all bony landmarks were identified, the patient stood in the middle of the test area to undergo a static calibration. The anatomical points were marked and identified with the wand marker. Each point was later reconstructed in Vicon Bodybuilder. The method of marking utilised allowed the subject to move freely without the danger of markers being obscured or knocked off during testing, especially on the medial aspect. This method

also reduces the errors involved due to skin movement relative to underlying bone (Cappozzo et al 1996) as only the movement of the clusters is recorded, and the relative position of the anatomical markers are calculated from their position. The strapping also reduced the effect of skin motion artefact by limiting skin motion (Stagni et al 2005).

As the current study was investigating the tibiofemoral joint, the tibia and femur first had to be defined. The tibia was defined as being from the centre of the proximal end if the tibia to the centre of the distal end. The femur was defined as being from the hip joint centre to the distal centre of the femur. The distal end if the tibia (DTIB) was defined as being the midpoint between the malioi, the proximal (PTIB) end was defined as being the midpoint of the tibial epicondyles, and the distal end of the femur (DFEM) was defined as being the midpoint of the femoral epicondyles. There are two main ways to define the hip joint centre: the helical axis method (Piazza et al 2004) or from anatomical references (Bell 1990). It was decided that in the present study the hip joint centre would be calculated from anatomical landmarks, as the subjects were not supple enough to rotate their legs as required for the helical axis method.

Patient Testing

Once the subject was marked up as described, they were asked to perform some simple everyday tasks.

Task One

Once the subjects were familiar in their surroundings and were comfortable, they were asked to perform the first task. The first task involved the subject walking from out with the test area through the middle and out to the other

side. This was done so that when the subject walked through the test area they were in a normal full stride. As test area was approximately five metres long, the subject took at least five steps in the test area. As this was the first test conducted, the subject was asked to repeat the task 3 times to ensure that they were comfortable. Due to the subject's condition, repeat tests to allow an averaging out of any errors were not conducted unless the data acquisition was poor, as most subjects reported pain and discomfort when walking for prolonged periods.

Task Two

Next, the subjects were asked to sit in a specially adapted chair. The chair backrest had been removed to allow the cameras in the Vicon system to see the markers on the pelvis, however armrests were still attached to assist the subject in rising or sitting if needed. Once the subject was sitting comfortably, they were asked to rise to a standing position as they would normally, and, after a small pause, return to a sitting position. Again, provided the data collected could identify the 12 markers on the clusters, the subject was not asked to repeat this movement.

Task Three

After the first two tasks were completed, the subject rested whilst a set of stairs was constructed in the test area. Each stair was 18cm high, 27cm deep, and 88cm wide, with 4 steps to a platform on the top, and handrails on either side. Once the subject was ready to continue, they were asked to ascend the stairs, turn on the platform at the top, and descend the stairs again. As with tests one and two, the subject was not asked to repeat the task provided the data was collected adequately.

Total time taken to test each subject, including marking, static calibration, and activities was approximately one hour.

BodyBuilder

A model was written in BodyBuilder from Vicon to analyse the kinematic data (Appendix III).

Identification of Points

Each marker from the clusters and the wand were named and identified. The point at the end of the wand was then identified as being a vector distance away from the markers on the wand, and a virtual point was created and named. The virtual point was then linked to the appropriate cluster. This method was repeated for each anatomical point of interest.

Segment Definition

Each segment was then defined, and joint centres calculated (figure 3.4). The four pelvis anatomical landmarks were identified first. These were the two anterior and posterior iliac spines (RASIS, LASIS, RPSIS, LPSIS). The hip joint centre was calculated as being 22% of the inter ASIS distance laterally from the midpoint of the ASIS ((LASIS+RASIS)/2), 30% of the inter ASIS distance distally, and 36% to the posterior, as adapted from cadaveric studies by Bell et al (1990).

The medial and lateral femoral epicondyles (MFEP, LFEP) were then identified. The distal femur was then calculated as being the midpoint of the epicondyles (DFEM=MFEP+LFEP/2).

The medial and lateral epicondyle of the tibia, and the medial and lateral malleoi were then identified (MTEP,LTEP,MMAL,LMAL). The proximal and distal ends of the tibia/shank section was calculated as being the respective midpoints (PTIB=MTEP+LTEP/2, DTIB=MMAL+LMAL/2).
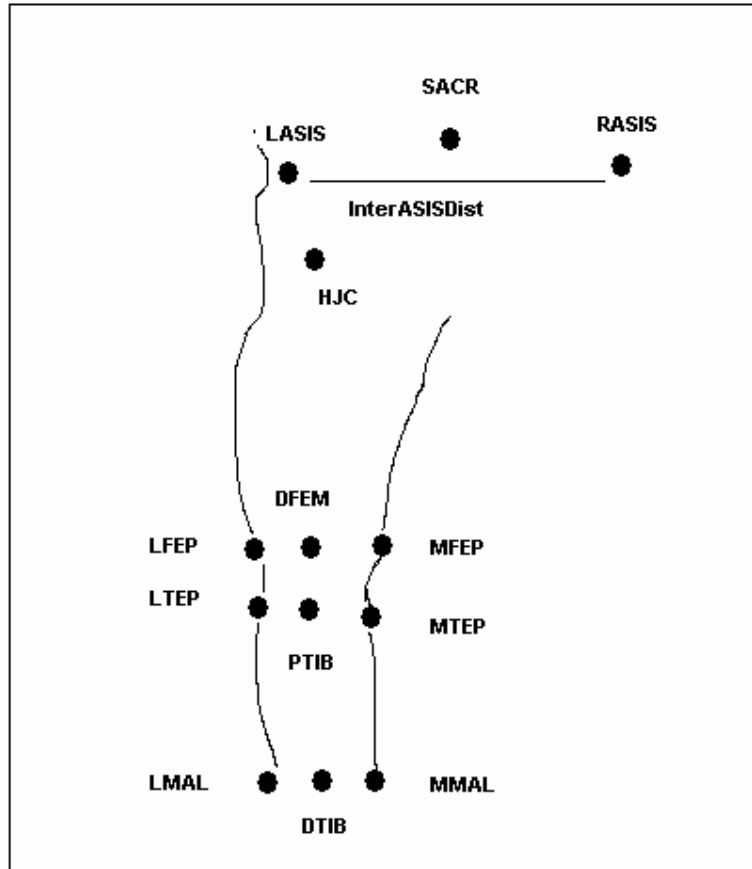

Figure 3.4 Representation of Marker Points

The long axis of the femur was defined in the bodybuilder code as being from the knee joint centre to the hip joint centre. The plane between the long axis and the medial and lateral epicondyles of the femur defined the second axis. The plane between the first and second axes then defined the third axis. A similar method was then used to define the tibia, with the first axis being from the ankle joint centre to the knee joint centre. The second axis was defined

as the plane from the first axis and the medial and lateral tibial epicondlyes. The third axis was the plane between the first and second axes. Stick figure representations of the femur and tibia were then created (figure 3.5). Visualisation of the calculated axes were then added to ensure the model was labelled correctly. Rotations at the knee joint were then calculated as being the rotation of the femur around the tibia, by the order of flexion/extension, varus/valgus, then internal/external rotation.
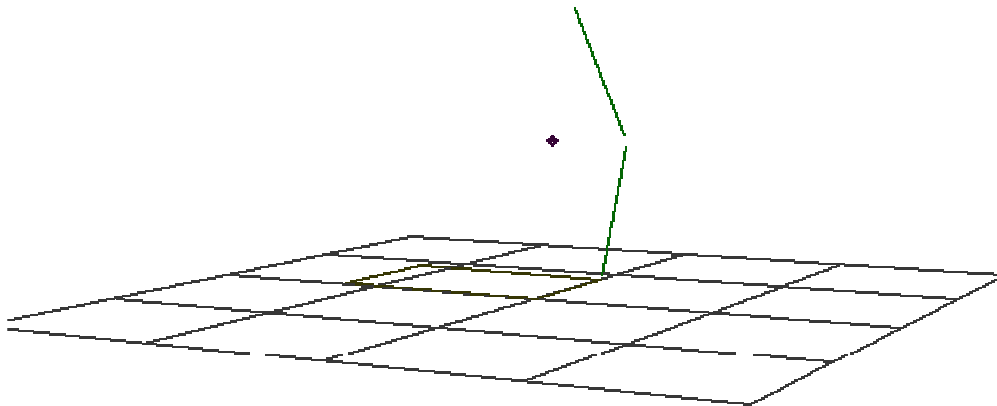
Figure 3.5 stick figure representation of the femur and tibia

Kinematics

Each of the virtual points were associated with their respective clusters. When the clusters move with the subject in motion, the virtual points are then recreated with respect to their position to the clusters. The HJC was first recreated with the pelvis cluster in the static trials. For the dynamic trials, the HJC was re-associated to the thigh cluster, so that any errors involved in

movement of the pelvis cluster were removed. Rotations were then calculated using Euler angles as being the rotation of the femur around the tibia. This was done in Euler as opposed to the more conventional Grood and Suntay method (Grood and Suntay 1983) as the data was to be later used for animation.

Rotations

The first section of data analysis was done on the rotations of the femur around the tibia. Each activity was time normalised and rotations in three directions were calculated. The motion of the knee in all activities was compared pre and post operatively, and these results were then compared with those previously reported in the literature.

Translations

The relative translations of the femur to the tibia for each subject in each trial were then calculated. This was defined as being the movement of the distal end of the femur relative to the proximal end of the tibia, as described above. The absolute translation and motion in each of the three planes was then compared pre and post operatively.

Double Calibration

In an attempt to quantify and further reduce the effect of skin motion artefact, a double calibration method was devised. The subject used for the initial testing of the double calibration method had cluster markers applied as described. Virtual markers were then pointed onto the 10 anatomical landmarks as described above, with the subject in a standing position. The subject was then asked to sit with their feet flat on the ground and the knee flexed at approximately $90°$, and the anatomical landmarks were then pointed to again. There was no difference in the position of the malioi

markers on the skin between the two positions. This is due to the ankle being in a similar position relative to the tibia in both standing and sitting calibration positions. Marking of the pelvis proved very difficult in the sitting position, and as the pelvis markers were only going to be used to calculate the hip joint centre in the static calibration using cadaveric data (Bell et al 1990), it was decided that the pelvis markers would only be marked once in the standing position. The largest variation in marks on the skin between the two calibration positions were seen in the four anatomical landmarks on the distal femur and the proximal tibia. By marking the skin in both standing and sitting positions, the measured difference between the two positions was 12mm in the LTEP, 10mm in the MTEP, 22mm in the MFEP, and 46mm in the LFEP.
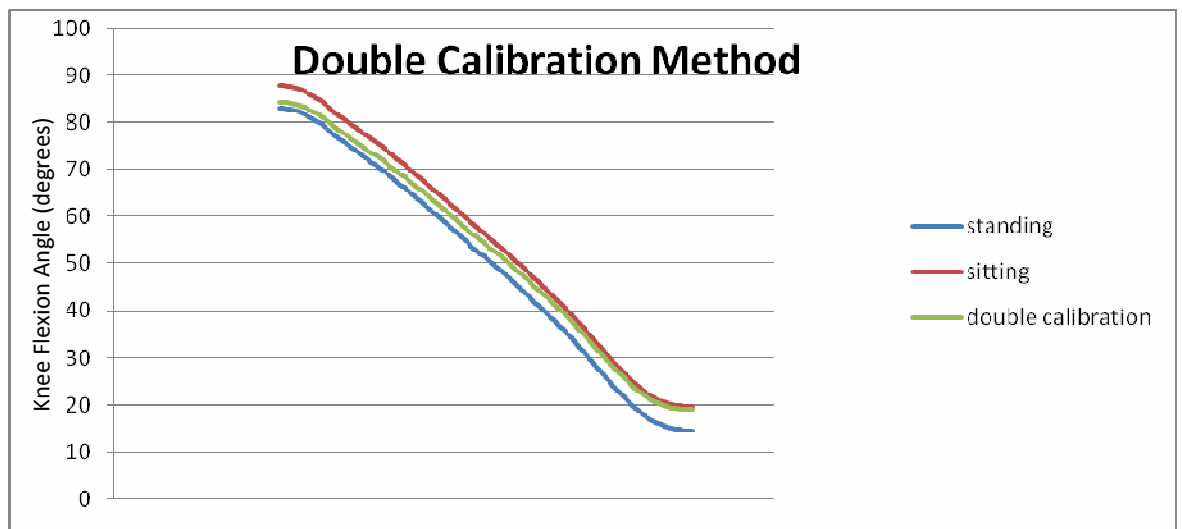
Figure 3.6 Difference in measured flexion angles using a double calibration method

When the two sets of calibration data were calculated through the BodyBuilder program, there was approximately 5° difference in the flexion angle. In theory, a graduated line weighted 100% to the standing calibration

line at 0° flexion and 100% to the sitting calibration at 90° flexion (figure 3.6), similar to the method used by Cappello et al (1997), would follow the true movement of the bone. This method proved successful in calculating the flexion angle, however there was no discernable pattern in the other 5 degrees of freedom to allow for an effective use of this method. It was therefore decided for the current study to measure all 6 degrees of freedom in the same way, and use a single calibration method in the standing position.

Medical Imaging

There were two main types of medical imaging equipment available for use in the current study that would allow for 3D imaging of the knee joint, MRI and CT. Due to ethical constraints, MRI was the preferred imaging technique. MRI has been used in numerous previous studies to investigate the bones of the knee in osteoarthritis, for example Wretenberg et al (2002) and Patel et al (2004). The MRI scans in the current study were taken to the standard specifications of the hospital.

After preoperative gait analysis was concluded, an appointment was made for the subject to attend Glasgow Royal Infirmary MRI department. Again, transport was provided.

A 1.5T MRI scanner (Phillips Gyroscan NT) was used to take 44 images, 2mm thick, with a resolution of 512, at the knee joint in the transverse plane (figure 3.7).

Previous to the appointment, the subjects were advised to ensure that they were not carrying any metallic objects, and were dressed comfortably. On attendance at the MRI department, the radiographer went through the

checklist provided to ensure that an MRI image could be taken safely (Appendix IV). This was checked prior to testing by the author to ensure that there were no delays on the day of testing.
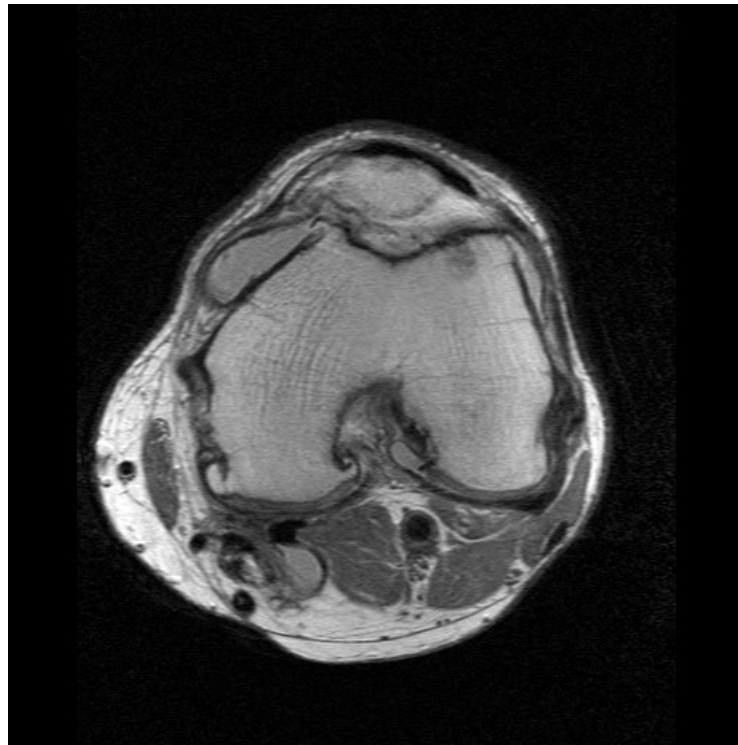

Figure 3.7 An example of a preoperative MR slice

Once it was ascertained that the scan could be conducted safely, the subject was taken into the scanning room by the radiographer, and asked to lie on the bed of the scanner. Once comfortable, the subject was asked to lie still for the duration of the scan. This lasted approximately seven minutes. The scan was later exported in DICOM format for analysis.

The first subject to be tested postoperatively attended the hospital for an MRI scan. This was done to assess the suitability of MRI for imaging the knee replacement.   MRI images were not suitable for imaging of the knee joint postoperatively, as scanning of the implant resulted in an image blackout (figure 3.8), making it impossible to surface the contours of the bone and implant.
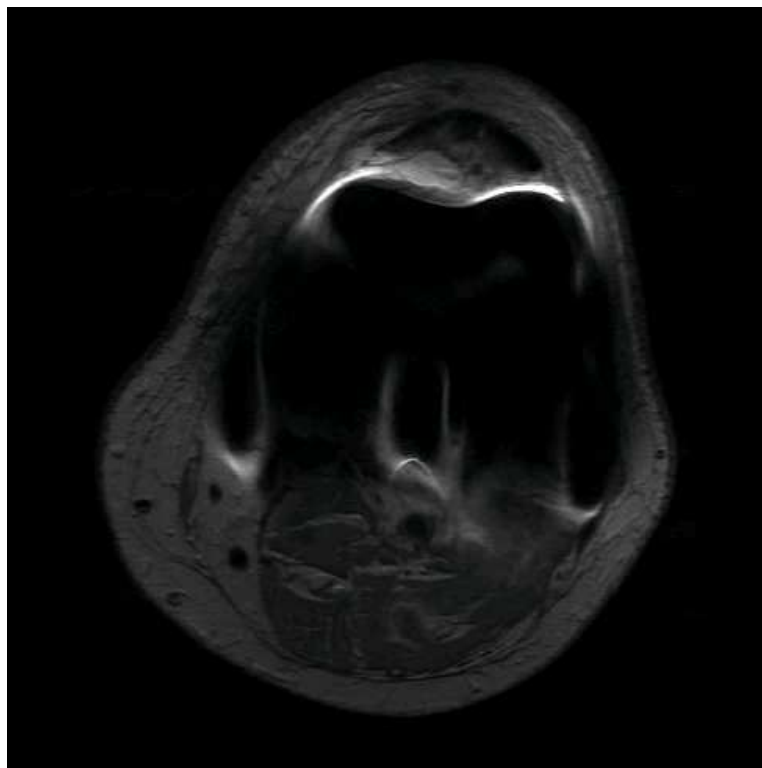
Figure 3.8 Image blackout in postoperative MRI

At the ethical consideration stage, an application was made and approved in order to allow the use of CT, only if MRI proved unsuitable in the postoperative imaging. As with the preoperative MRI scan, transport was arranged for each subject to attend Glasgow Royal Infirmary for the

postoperative CT scan. 144 images of 1mm thickness and resolution of 512 were taken in the transverse plane (figure 3.9). Again, this scan lasted approximately 7 minutes, and the data was later exported in DICOM format.

Figure 3.9 An example of a postoperative CT slice

Ideally, all subjects would have been scanned using the same medical imaging technique pre and post operatively. Each subject would also have been scanned from the hip joint centre to the ankle joint centre. A scan of this size would have taken between 45mins to one hour to complete. It was considered unethical and impractical to ask the subjects to remain perfectly still in the scanner bed for this length of time. Also, it would not have been viable to have appointments at the hospital lasting up to one hour. With each scan lasting 7mins, 4 of the 14 scans used in the final analysis of the current

study had to be stopped and restarted, as the subject moved during the collection of the data. No subject reported pain or discomfort during imaging.

All medical imaging scans were exported from the hospital scanners in DICOM format, meaning Digital Imaging and Communications in Medicine. This is a standard developed by the American College of Radiology Manufacturers Association to define the connectivity and communication protocols of medical imaging devices. The preoperative scans were taken in a 1.5 Tesla MR scanner, at 2mm intervals with a resolution of 512 and a pixel size of 0.3516. The postoperative scans were taken in CT, with slices of 1mm thickness and a resolution of 512 and a pixel size of 0.3867.

3D Imaging and Reconstruction

Software Analysis

CORELDRAW

The first package analysed for use in the 3D reconstruction was CORELDRAW from Microsoft. In this application, all images were inputted as a .JPG format, and built up to create a 3D image that could be manipulated through pitch yaw and roll. The version available was old and too basic to use. On analysis of the newer and updated COREL package, it was found that Microsoft had developed the software to be used in cartoon style animations, and the features in the original package were no longer available, rendering the package unsuitable for use in the current study.

SURFDriver

The next software package analysed was called SURFDriver. This package imports the images as .jpg files, and stack them in a numerically consecutive order. The user then inputs data relating to the file, such as the picture width, slice thickness, and pixel size.

The .jpg files were reconstructed into a 3-dimensional image using SURFdriver version 3.5.1 (© Moody and Lozanoff). This is a surface recognition package that builds up a 3-dimensional image from a series of 2-dimensional images, in the form of polygons.
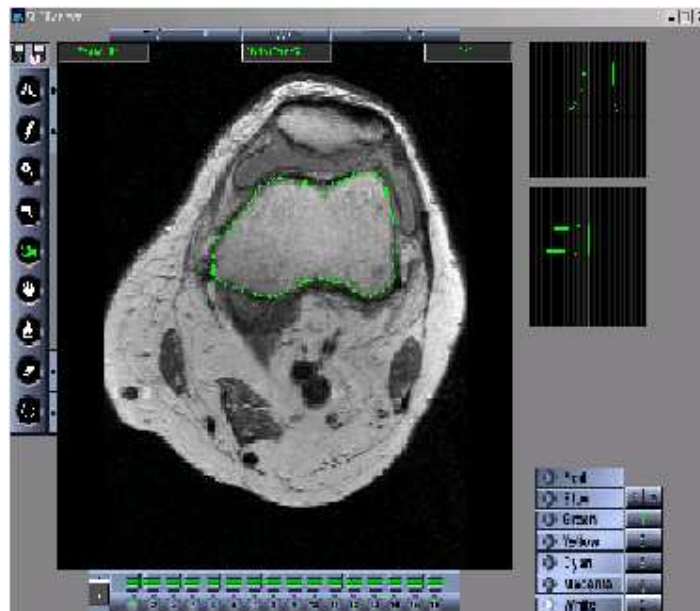
Figure 3.10 A screenshot from SURFdriver

Figure 3.10 shows a screenshot of a transverse slice of the femur in SURFdriver. The green line around the bone is the surface outline of the bone in this segment. This can be manipulated by the user, either by changing the surface recognition parameters, or manually.

For each patient, the images taken from the scan were converted to .jpg format for use in the reconstruction. Each image was to the same scale. The scale was measured by using a scale bar in the first slide, which was measured using the function provided in SURFdriver. Each slice had the same two initial characters, and were sequentially numbered. Once the first slide is selected for analysis, SURFdriver automatically selects the next file with the initial two characters and subsequent number, until such a time that the sequence ends or is broken. Once the slice width is measured using the scale bar, the slice thickness must be entered. In this case, the slice thickness was 2mm, as this was the thickness of slice collected at the time of the scan. SURFdriver also gives the option of only analyzing every nth frame, and fills gaps between. Although this is a useful tool when analyzing large amounts of data, or when accuracy is not critical, every slice was analyzed. Thus n, or the slice interval, was set to "1".

A number of options are available in the slice-editing window, as can be seen on the left hand side of the image in figure 3.10. The most efficient way to surface a slice is to use the Magic Wand tool. This option estimates the desired contour based on the threshold of the area that the user initially selects. The density and threshold can be set by the user. Increasing the threshold allows for a higher variation in the colour that the wand tool will include in its selection, whilst increasing density results in more vertices being created. Although this method was straightforward to use, selection of two areas with only a slight variation in shade produced two different contours, and was especially difficult to perfect in this situation, as osteoarthritic bones do not always appear uniform in colour.

The Pencil tool was the most accurate method to contour the bone. This involved the user tracing the edge of the bone with the cursor to produce the vertices. Once this was done, the Move Vertex tool could be used to alter

any vertices that were not produced as expected, and the Glue and Eraser tools were used to add or remove vertices where necessary.

Once all the slides had been contoured and saved, the object was surfaced. This process connects the vertices in each slice identified as being part of the final object. Once surfaced, an object can be viewed and exported.

Figure 3.11a shows the output from SURFdriver, a 3-dimensional model of the femur and tibia, built up from the patient specific MR scan. Figure 3.11b shows the same result in a wire frame representation. This shows more clearly the polygon build of the model. This completed model was then exported as a .dxf file, for later conversion into the animation package.
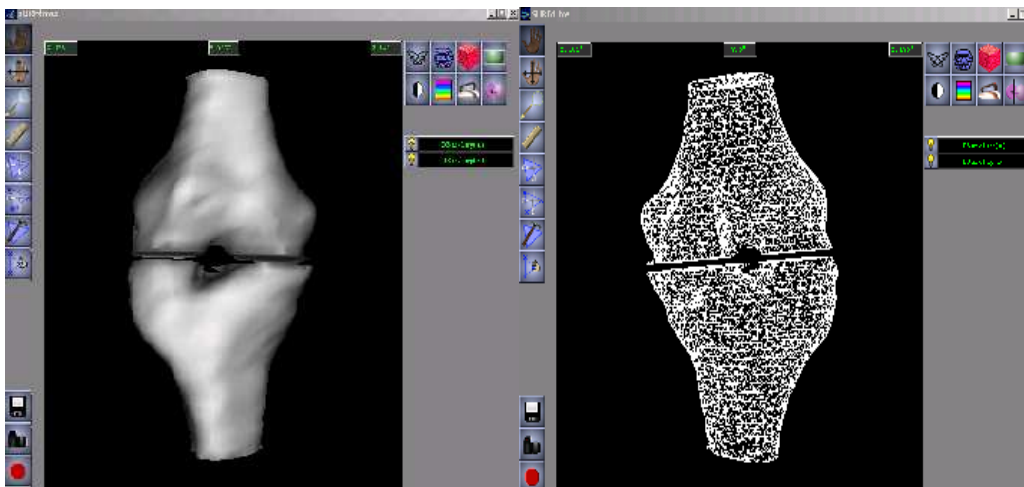
Figure 3.11a and Figure3.11b. The output from SURFdriver, showing a 3-dimendsional image of the femur and tibia, and a wire frame representation showing the build up of polygons.

This method of surfacing the medical imaging data suffered from many drawbacks. Firstly, the last slice of a section is 'levelled off'. This means that the areas of most interest when studying the knee joint could not be

included in the image, as the contact areas between the femoral epicondyles and the tibial plateau both appeared perfectly flat in the image. The power of this package was further reduced by the fact that the images were .jpg format, and as such could only be viewed in the transverse plane. This eliminated the opportunity to edit the image in the axial or frontal planes.

Secondly, as the data was imported as .jpg files, the size of the file had to be set by the user. Although SURFDriver offered a scaling tool to measure slice width, the actual results from this varied by 5%, which changed the height / width ratio and therefore the shape of the final surfaced image.

Finally, the completed image could not be exported into a suitable format, and a file conversion tool had to be used. This increased the workload and relied on an untested software system to accurately convert the files.

While the initial use of this package was of use in the development of the project methodology, it was decided that a more accurate and reliable method of surfacing the medical images should be found. Other packages with surfacing abilities were evaluated, and the package best suited for the current project was MIMICS from Materialize®.

MIMICS

MIMICS is a software system for interfacing with a medical scanner. CT and MRI scans can be segmented and visualised in the software. The major advantage that this system holds over SURFDriver is that the images are imported in DICOM format, which is easily exportable from both the MRI and CT scanners. This includes all the relevant image data including slice thickness and image resolution. The scan orientation is included, and the

medical headers such as patient name and identification number are also available.

MIMICS has some similar tools to SURFDriver, in that outlines of the bones can be segmented by a number of methods including pixel resolution detection, and by manual outlining of the bone. MIMICS has the added advantage that as well as surfacing in the transverse plane that the images are taken in, the image can also be viewed and edited in the other two planes (fig 3.12).
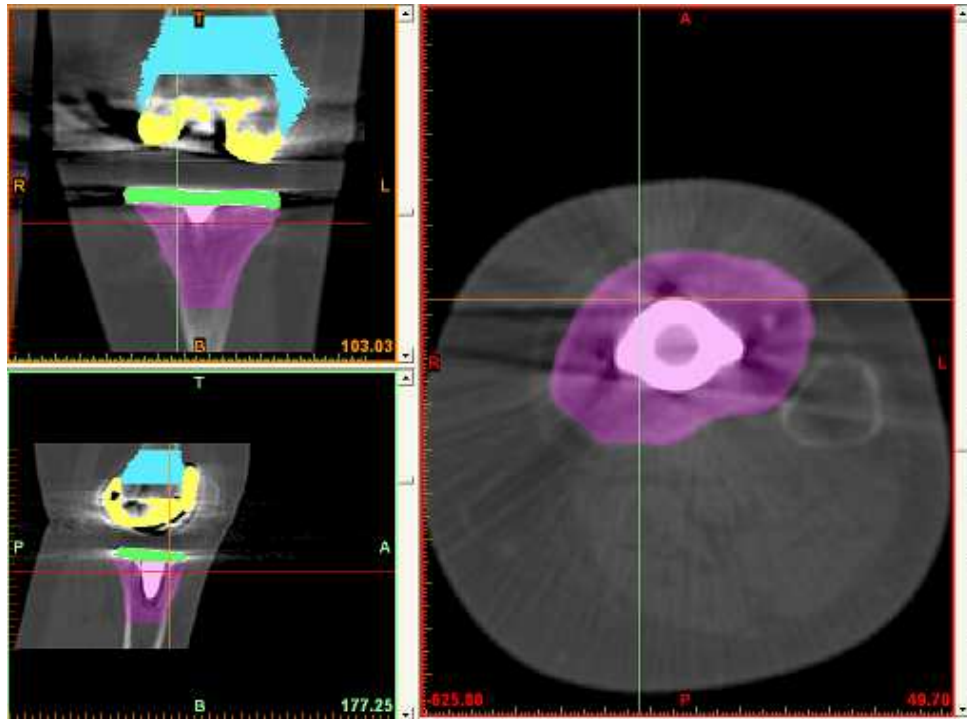

Figure 3.12 imaging in 3 planes in MIMICS

MIMICS has a number of export options, including exporting to .wrl files. MIMICS was the only software package assessed in the current study that had this option, which was important for use in the animation package later.
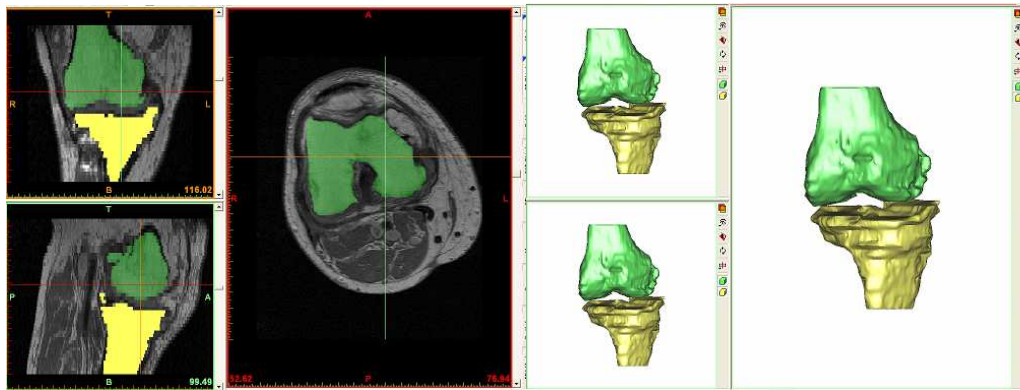
Figure 3.13 preoperative surfacing in Mimics and 3D reconstruction screen

Each scan was imported and orientated for use in the animation package. MIMICS allows for the scan slices to be visualised in the transverse plane, as they were taken, and in both the lateral and frontal planes. The bones were outlined in the transverse plane, and the accuracy of this was further checked using the images in the other two planes. In the preoperative scans, the femur and tibia were surfaced separately. In the postoperative scans, the bones were also surfaced separately, and the two components of the replacement were then surfaced individually. Figure 3.13 illustrates a 3D reconstruction of a preoperative knee. In this case, for subject 3, osteophytes can very clearly be seen on the femur. On the anterior aspect of the tibia the wear on the medial side can clearly be seen. This correlates

with the large hyperextension seen in this subject during preoperative motion analysis. Figure 3.14 shows the 3D reconstruction for the same knee postoperatively. In this image each bone and implant component is coloured differently to differentiate between them.
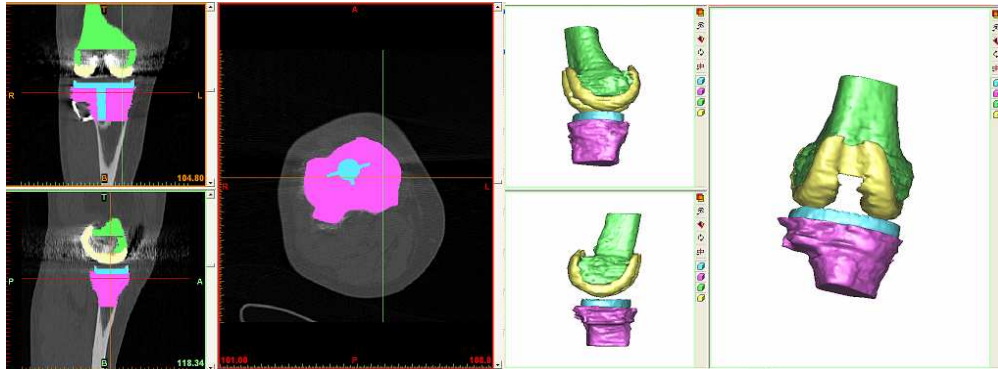

Figure 3.14 Postoperative Screenshot of Surfacing and 3D reconstruction screen

Registration of Points

An important aspect of 3D animation of human motion is the registration of anatomical landmark points onto the computer generated images.

The first attempt to register these points was done in the medical imaging scan. A marker from the Vicon system was placed in a custom made vial which was then filled with copper sulphate solution. This gives the effect that when it is placed in the MRI scanner, the copper sulphate solution shows white on the image, and the marker inside the solution shows black. When the marker in solution was scanned, the image showed up as expected.

The next stage was to have the markers placed on the anatomical landmarks prior to medical imaging. Firstly, when the subject was being marked in the motion analysis laboratory, marks were made on the skin where the virtual

points were placed. When the subject attended the hospital for medical imaging, a marker in copper sulphate solution was placed over the marks made for the MTEP, MFEP, LTEP, and the LFEP. The subject then underwent the MRI scan as per the protocol. This method had the drawback that it could only be done if the gait analysis and medical imaging were done on the same day. Also, although the skin around the knee joint could be marked in the gait laboratory, the markers to go into the scanner could not be placed on the skin until the subject was present at the MRI clinic, as the two departments were in different buildings. Initially, only one subject underwent a scan with the copper sulphate markers attached. On analysis of the scan data, it was found that there was an unquantifiable image shift relating to the copper sulphate. The copper sulphate solution used was the same as that reported elsewhere (Sheehan et al 1998). However, the standard method is to fill a capillary tube with a small volume of solution. In the current study there was approximately 10mm of solution in the vial around the marker.

In order to relate the anatomical landmarks palpated in the gait laboratory to the 3D images, a virtual palpitation tool was written in MATLAB. The xyz coordinate list of the bone surfaces exported from MIMICS were plotted into a 3 dimensional MATLAB graph. A user input function was then used to identify the most protruding point of each epicondyle in all three planes. This resulted in two sets of xyz coordinates, one relating to each epicondyle. This was done as these points relate to the positioning of the anatomical landmark markers utilised in motion analysis, palpated to be the most obtruding points of the femoral epicondyles. The midpoint of the epicondyles as identified in the graph was then calculated to give the centre of rotation of the joint, in the same way as calculated in BodyBuilder. Figure 3.15 shows an anterior view of an example of the graphical representation of the knee joint. The surface points are plotted as '+' signs to give a level of transparency to the image, and the epicondylar extremities and the resultant

centre of rotation are plotted as different coloured 'o' signs for easy identification.

Repeatability of the centre of rotation point is estimated to be within 0.5mm in the x (mediolateral) and y (anteroposterior) planes, and 1mm in the z (proximal-distal) plane. This process was repeated for each scan.
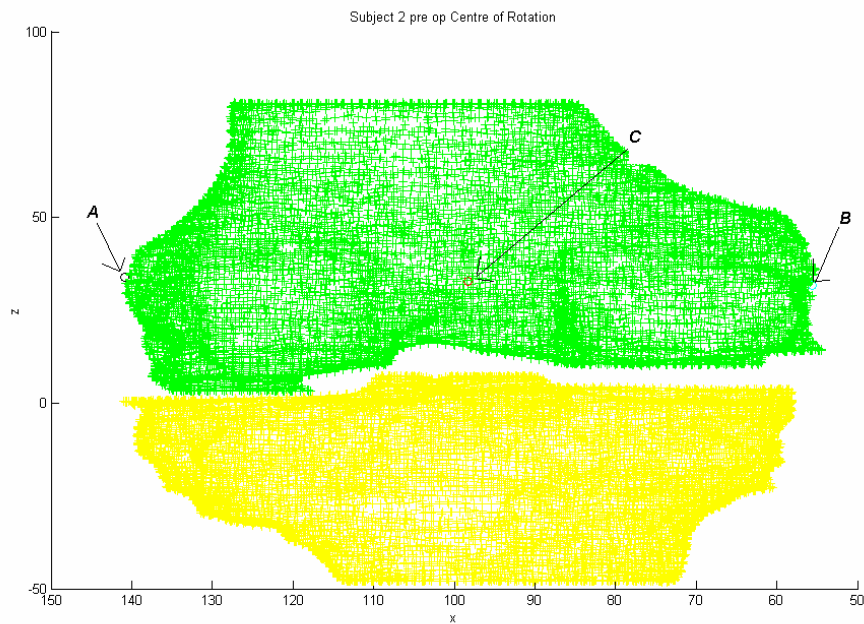

Figure 3.15 Centre of Rotation Calculation graph. The view in this graph is in the xz plane. The epicondyles are marked as circles and labelled (A and B). The calculated centre of rotation is marked as a circle and labelled (C).

3D animations

Virtual Reality Modelling Language (VRML)

The 3D model created in MIMICS was exported as a VRML file (.wrl). VRML is a branch of Web 3D technology, which is a higher archial scene description language that defines the geometry and behaviour of a 3-dimensional scene or 'world' (www.virtualrealms.com accessed December 2002). This requires a web browser with an additional software plug-in to be viewed. The plug-in used initially in this case was a freeware download called Cosmoplayer (© Install Shield Software Corp). This allows the user to 'navigate' in the virtual world created. For the purposes of this project, the viewer can select what position to watch the rotation of the knee from throughout the motion. In the duration of the study, Cosmoplayer was removed from publication as it was not compatible with newer versions of Microsoft Windows. A similar package called Swirlviewer was used instead (www.pinecoast.com accessed July 2005).

The numeric representation of VRML is a series of numbers describing the polygon structures that make up the shape of the knee. This representation of the polygons can be seen by opening a .wrl file in a word processing package, such as Microsoft Word or Notepad. Once this data is in .wrl format, the femoral and tibial segments are defined. A clock is then set in the .wrl file that corresponds to the time taken for the subject to complete the task under study. The rotations of the knee as described above are then defined and programmed into the virtual world. The centre of rotation is then defined as being the distal end of the femur as calculated in Matlab. Finally, the rotations are linked to the time that they occurred, via the clock described above, and the animation is produced. Appendix V has a sample of the VRML code. To save space the polygons and rotation data are omitted.

VRML files are organised as a list of xyz coordinates, with a corresponding set of coordinate indexed linkages. This has the effect of joining points in a triangular polygon mesh in order to produce a surface model. In this case, each segment that was surfaced in MIMICS was listed in a VRML file with separate coordinate listings and indexes. All data from each scan was then combined into one file to allow visualisation and subsequent animation. By defining each segment, they can be manipulated separately to produce the rotated animations of the knee joint seen later in this section. Below is the file layout in VRML. One example of the coordinate listing and of the coordinate index are included.

```
#VRML V2.0 utf8
DEF femur Transform {
        children [
                Shape {
                        appearance Appearance {
                                material Material {
                        }
                        }
                        geometry IndexedFaceSet {
                                coord Coordinate {
                                point [55.521 -74.8632      12.1206
]
                                }
                                coordIndex [97 156 135 -1
]
                        }
                }
```

```
                              ]
                              }


DEF tibia Transform {

        children [

                Shape {

                        appearance Appearance {

                                material Material {

                        }
                        }

                        geometry IndexedFaceSet {

                                coord Coordinate {

                        point [74.834 -96.1438        -57.0357


]

                        }

                                coordIndex [286 219 34 –1

]

                        }
                        }
                        ]
                        }
```

Rotations

The rotation angles of the knee were written to ASCII files from bodybuilder. These were calculated and written in the order XYZ. The rotations then had to be changed into a format suitable for use in VRML. This was done using a package called Dizzy V1.1 (© Vapour Technology, www.vapourtech.com accessed February 2004). This package uses quaternion mathematics to calculate the rotations. Quaternions are entities of the form w+xi+yj+zk where

sq(i) = sq(j) = sq(k) = ijk = -1

ij = k, jk = i, ki = j

ji = -k, kj = -i, ik = -j

The values of i, j, k are distinct, and neither quaternions themselves nor their components can be thought of as being complex numbers. Only some of the rules of arithmetic apply to quaternions. In particular, the commutative law does not apply. Given two quaternions a and b it is not in general true that ab = ba. When simplifying expressions, the rules given above are used instead. Quaternions have applications in physics and computer graphics. Quaternions are very useful in animation of biomechanics, as they efficiently solve 3 problems with the simpler Euler angles of yaw, pitch and roll: zero divide when manoeuvring vertically, gimbal lock and interpolation between 2 angles (http://c2.com/cgi/wiki?QuaternionMathematics accessed February 2004).

To program rotations in VRML, the data has to be in radians, and be given a magnitude in each direction, in the order of "X, Y, Z, Rotation". So, for

example, a pure rotation of 0.2 radians in the X direction should be written as: 1   0   0   0.2

When the X (1 0 0 rotation) Y (0 1 0 rotation) and Z (0 0 1 rotation) values are added together, one single X Y Z rotation value is given.

The XYZ angles were input into Dizzy in the same order they were calculated in body builder (XYZ), as Euler angles were used.   An example of the calculation is given below.

Input:	1	0	0	0.2
	0	1	0	0.1
	0	0	1	0.3
Output:	0.559	0.181	0.809	0.382

This example shows that a rotation with a 0.2rad magnitude in the X direction, 0.1rad magnitude in the Y direction, and a 0.3rad magnitude in the Z direction, has an overall rotation of 0.392rad, with a magnitude of 0.559x, 0.181y, and 0.809z. Figure 3.16 shows the package calculator used with the above calculation inputs.
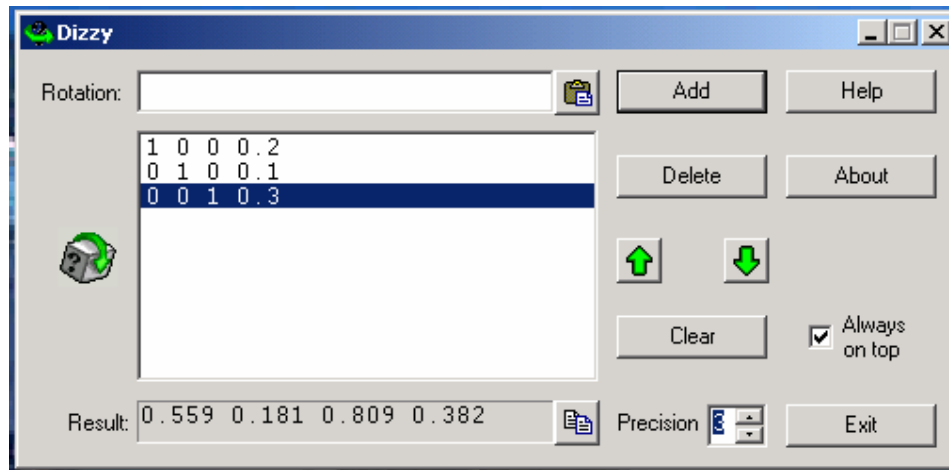
Figure 3.16 Dizzy Rotation Calculator

Every 10th set of data was calculated through Dizzy, so rotations were calculated for the animation purposes at 12Hz. This was done to limit the amount of data in the animation and to make for a smoother image. For further examples, see the results section of the CD, and view a .wrl file in a word processing package.

For each subject, the calculated rotations described above were added to the relevant VRML file, and the centre of rotation was included in the definition section of the code. The animations are included in appendix in the enclosed CD. Also included is the viewer plug in Swirlviewer and Instructions for use.

Chapter 4. Results

4.1 Individual Results

The results for each subject are presented individually. Flexion angles of the knee joint are reported for each task pre and post operatively, followed by range of motion in all three planes. As each subject was calibrated at each testing session, it is possible that an offset in the reporting of kinematic data exists due to mislocation of anatomical landmarks. Varus and internal rotations are reported, however there may be aspects of crosstalk affecting these results. The potential error associated with these results will be discussed later.

4.1.1 Subject 1

Subject 1 was fitted with a cruciate sacrificing (size 2) fixed bearing (size 3) knee implant from DePuy with a 10mm tibial spacer sized to the tibial component.
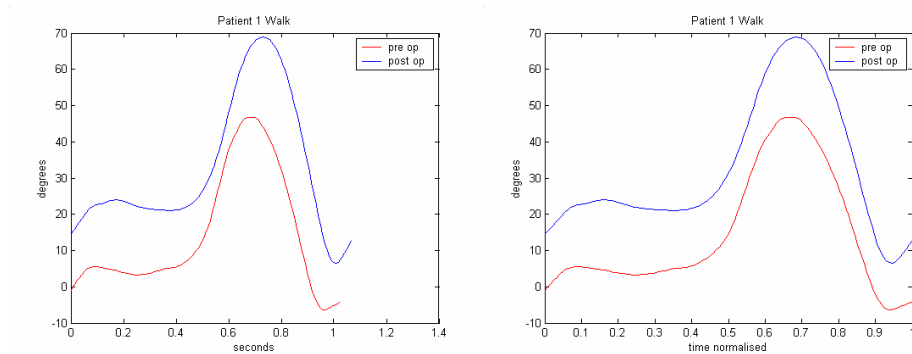
Figure 4.1 Flexion angles during level walking for subject 1

Subject 1 showed a minimal increase in time taken for a single stride during level walking. There was minimal change in the time to maximum flexion. Post operatively subject 1 increased maximum flexion angle by 22° to 67°, and showed an increased minimum flexion angle of 12°, removing a 6° hyperextension, resulting in an overall increase in range of motion of 10° (figure 4.1).
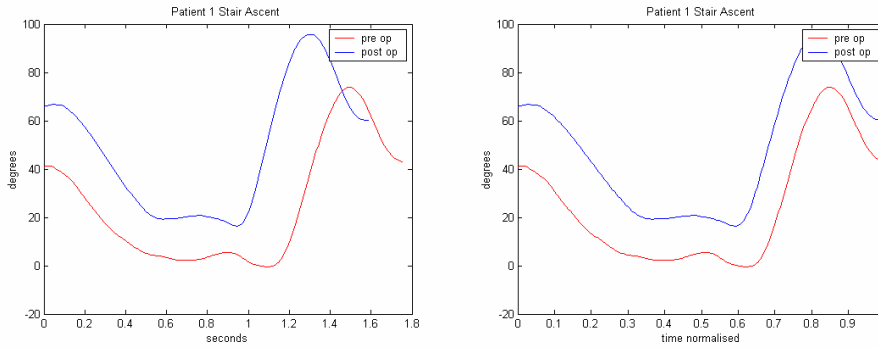
Figure 4.2 Flexion angle during stair ascent for subject 1

When ascending a stair, subject 1 took 0.2 seconds longer to reach maximum flexion and ascend one step preoperatively compared with postoperatively. Maximum flexion increased by 22° to 96° postoperatively, and minimum flexion increased to 16° from a slight hyperextension, resulting in an overall increase in range of motion of 5° (figure 4.2).
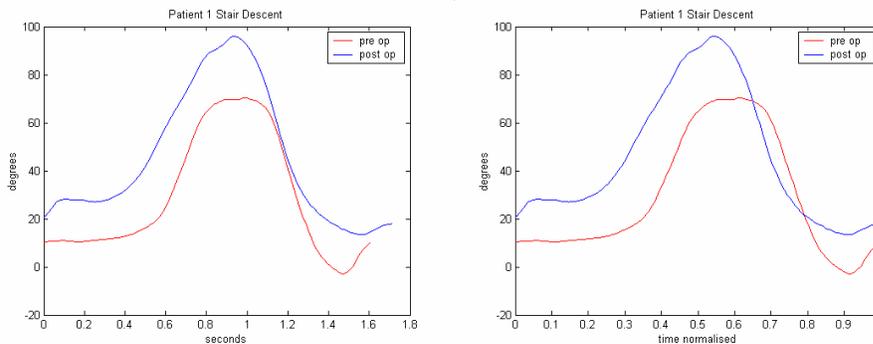
Figure 4.3 Flexion angle when descending a stair for subject 1

In stair descent subject 1 increased maximum flexion by 7° to 96°, and increased minimum flexion by 5° to 10°, meaning there was only a slight

increase in range of motion of 2°. There was minimal difference in time taken to complete a step and to reach peak flexion (Figure 4.3).
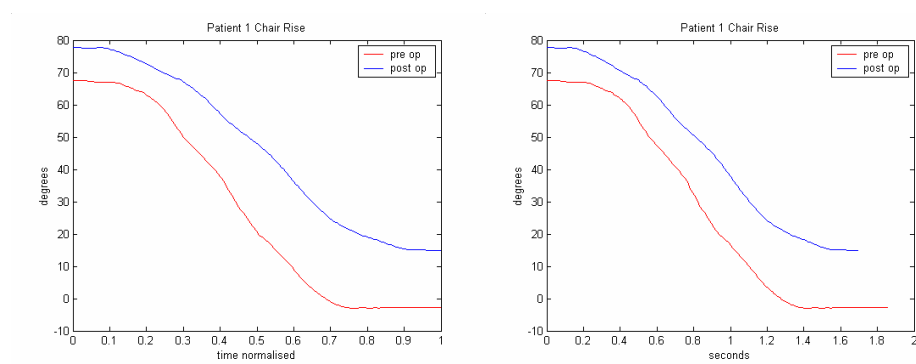
Figure 4.4 Flexion angle during chair rise for subject 1

A similar pattern is seen in rising from a chair in subject 1, with a 10° increase in maximum flexion angle to 78°, and a 17° increase in minimum flexion angle, removing a 3° hyperextension on standing upright. Again there was little impact on time taken to complete the movement (figure 4.4).
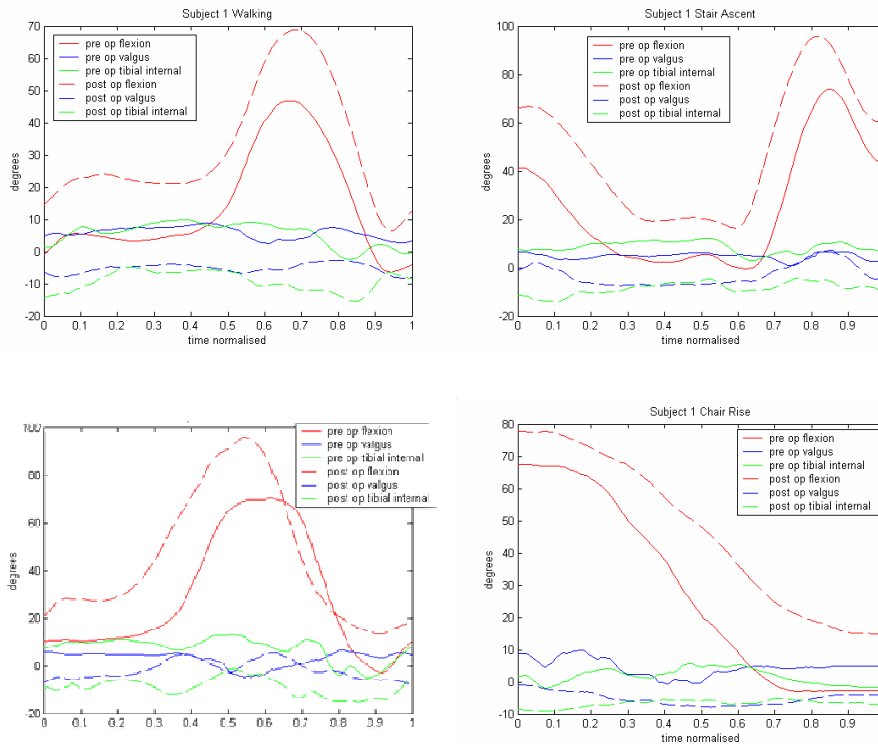
Figure 4.5 Pre and post operative angles in 3 planes for subject 1 during level walking (a) stair ascent (b) stair descent (c) and chair rise (d)

During level walking, the knee was in valgus preoperatively, and varus postoperatively. Preoperatively, the tibia was internally rotated until just before hyperextension, when it externally rotated slightly. Postoperatively, the tibia was always externally rotated. There was no difference in the pattern or range of rotation in varus or internal rotation (figure 4.5a).

As with level walking for subject 1 the tibia was again in internal rotation preoperatively and external rotation postoperatively during stair ascent. The knee was in valgus throughout stair ascent preoperatively. Postoperatively, the knee was in valgus when flexion was greater than 60° and varus when flexion was less than 60° (Figure 4.5b).

When descending a staircase preoperatively, the knee was in valgus for most of the step, rotating slightly into varus at maximum flexion, whereas the opposite was true postoperatively. Preoperatively the knee was internally rotated whereas postoperatively it was externally rotated, although the pattern of rotational motion was similar (figure 4.5c).

When rising form a chair, subject 1 modified their knee kinematics from a valgus internal rotation preoperatively to a varus external rotation postoperatively (figure 4.5d).

4.1.2 Subject 2

Subject 2 was fitted with a cruciate retaining (size 4) fixed bearing (size 4) knee from DePuy with a 10mm tibial spacer sized to the femoral implant.
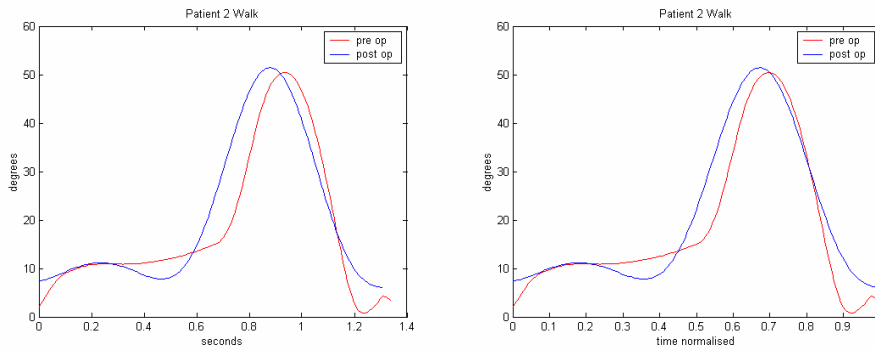
Figure 4.6 Flexion angle during level walking for subject 2

During level walking, there was less than 1° change in maximum flexion angle. Minimum flexion angle increased from 1° to 6°, meaning that there was a slight overall reduction in range of motion of 5°. Time taken to complete one step did not change, while maximum flexion angle was reached slightly earlier in the step (figure 4.6).
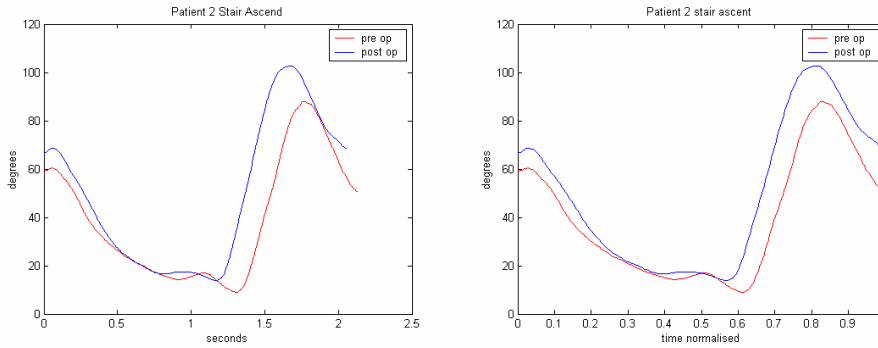
Figure 4.7 Flexion angle during stair ascent for subject 2

When ascending a staircase, subject 2 increased their maximum flexion angle from 87° preoperatively to 103° postoperatively. There was also a slight increase in minimum flexion angle of 5° to 14°, resulting in an overall increase in range of motion of 9°. As with level walking, maximum flexion was reached slightly earlier postoperatively (figure 4.7).
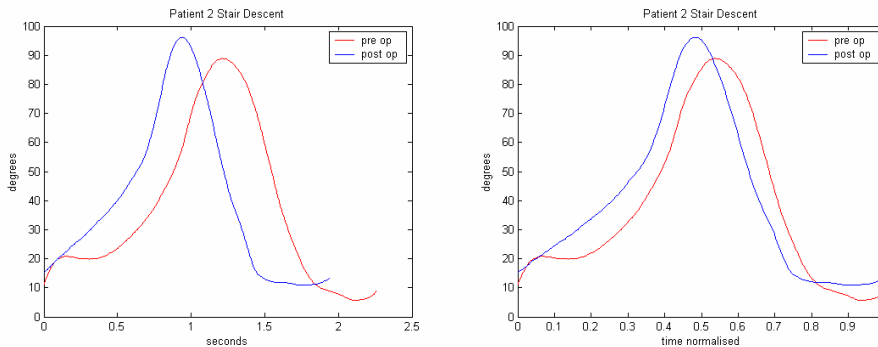

Figure 4.8 Flexion angle during stair descent for subject 2

When descending a staircase, subject 2 showed an increase in maximum flexion angle of 7° postoperatively, peaking at a m aximum of 96°. Minimum flexion angle also increased, from 5° preoperatively to 10° postoperatively.

Subject 2 took nearly 0.5 seconds less to complete the action postoperatively compared to preoperatively, and maximum flexion also occurred earlier (figure 4.8).
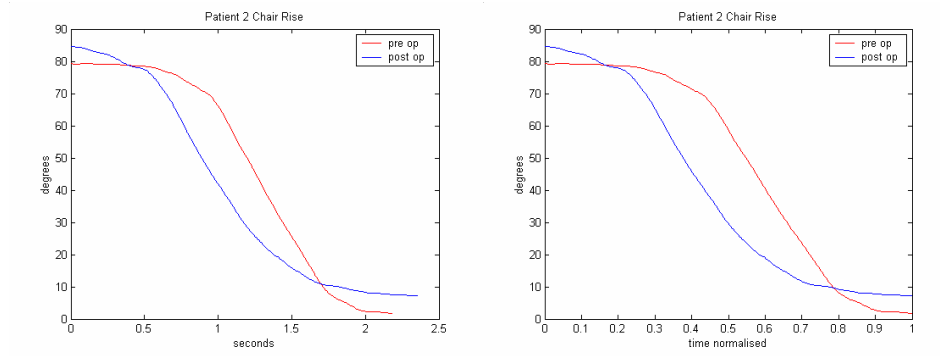

Figure 4.9 Flexion angle during chair rise for subject 2

When rising from a chair, there was a minimal difference in range of motion, as the 5° increase in maximum flexion to 84° was countered by an increase in minimum flexion to 7° (figure 4.9).
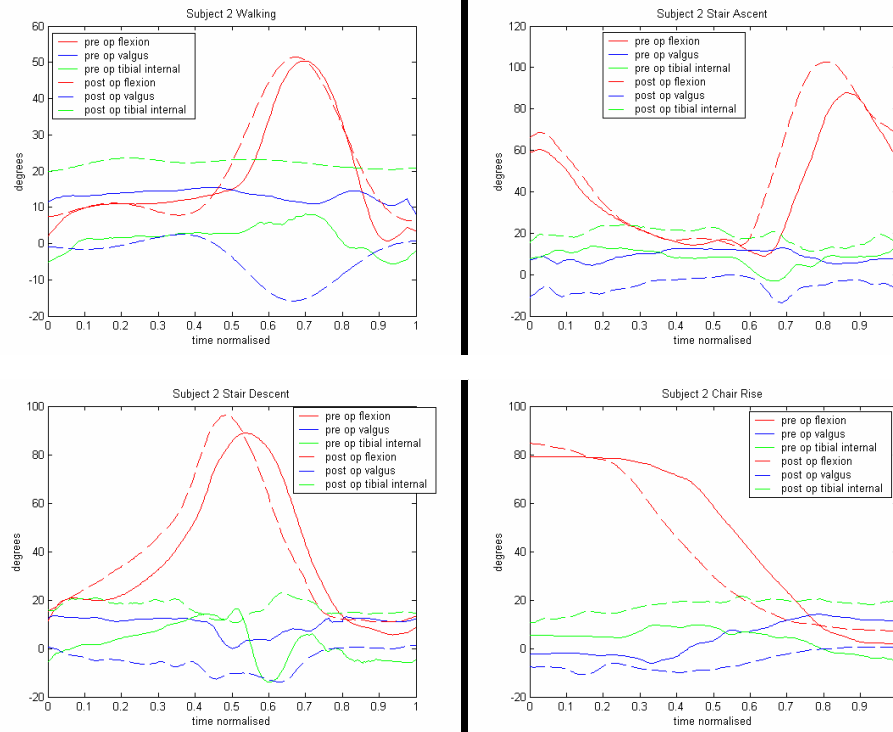
Figure 4.10 Pre and post operative angles in 3 planes for subject 2 during level walking (a) stair ascent (b) stair descent (c) and chair rise (d)

Preoperatively during level walking, the knee was mostly in valgus, and rotated further into valgus as flexion increased. Internal rotation also increased with flexion, showing an external rotation when flexion was lower than 10°. Postoperatively the knee was in varus, rotating further into varus at maximum flexion, and the tibia was internally rotated with little variation throughout the action (figure 4.10a).

When ascending a staircase, the knee was rotated in valgus preoperatively and varus postoperatively. Although the knee was predominantly internally rotated in both pre and postoperative situations, internal rotation was more pronounced postoperatively (figure 4.10b).

During preoperative stair descent, subject 2 is mostly in valgus. The magnitude of the valgus angle decreases at maximum flexion. This is coupled with an internal rotation that becomes external at maximum flexion. Postoperative rotation is varus and internal (figure 4.10c).

When rising from a chair preoperatively, the knee was in varus and internally rotated when sitting, rotating to a valgus external position when rising. Although a similar pattern of motion was seen postoperatively, the knee remained in varus, and was more internally rotated (Figure 4.10d).

4.1.3 Subject 3

Subject 3 was implanted with a cruciate sacrificing (size 4) fixed bearing (size 3) knee from DePuy, with a 10mm tibial spacer sized to the tibial implant.
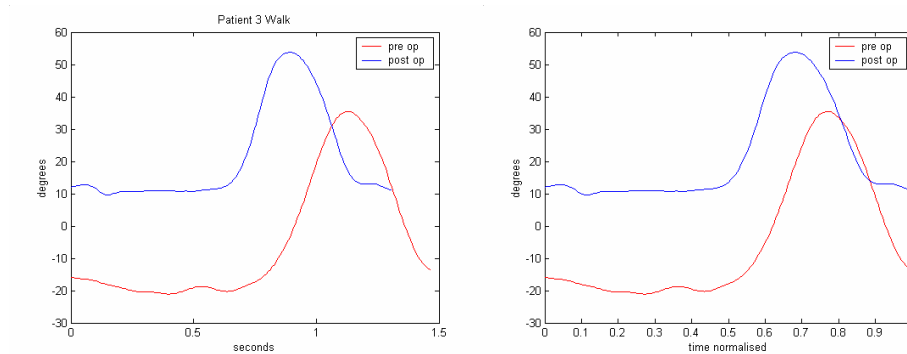

Figure 4.11 Flexion angle during level walking for subject 3

During level walking subject 3 increased their knee flexion from a preoperative maximum of 35° by 19 ° postoperatively. Minimum flexion angle increased from 21° hyperextension preoperatively to 10 degrees flexion postoperatively. Subject 3 also took 0.3 seconds less to complete a step, and reached maximum flexion earlier in the gait cycle (figure 4.11).
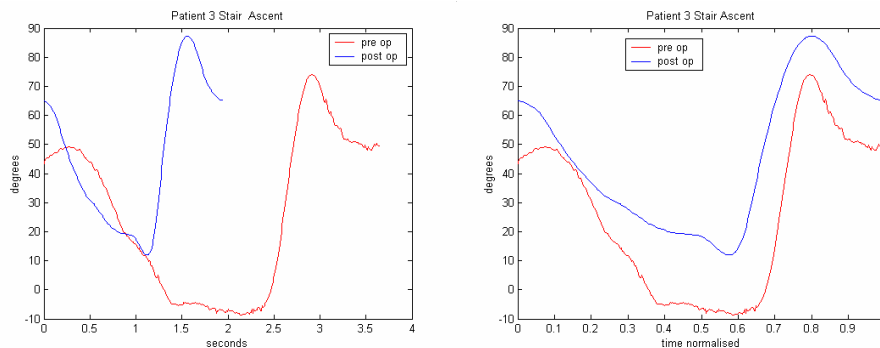

Figure 4.12 Flexion angle during stair ascent for subject 3

During stair ascent, subject 3 showed a 13° increase in maximum flexion angle postoperatively to 87°, and a 20° increase in minimum flexion angle, which corrected a 9° preoperative hyperextension and resulted in a reduced range of motion. Stair ascent took 1.5 seconds less postoperatively, although peak flexion occurred at the same stage of the motion (figure 4.12).
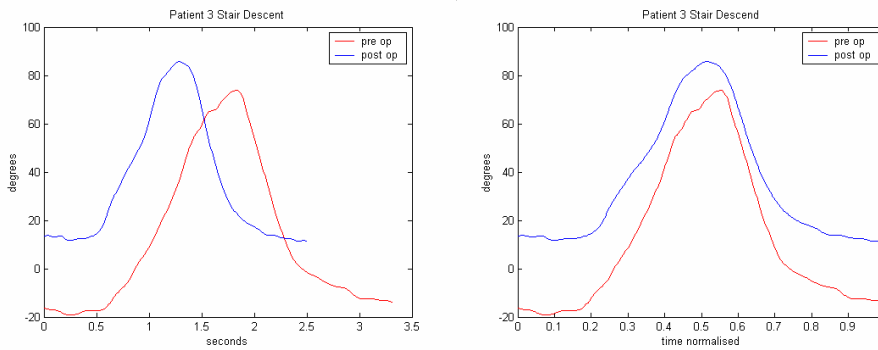

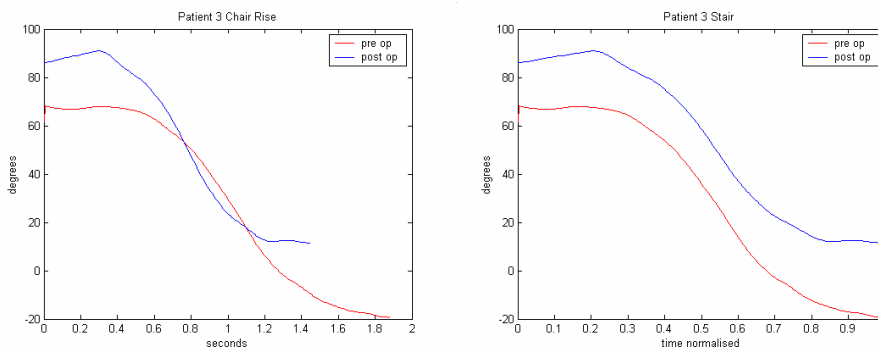Figure 4.13 Flexion angle during stair descent for subject 3

Figure 4.14 Flexion angle during chair rise for subject 3

During stair descent, subject 3 increased their maximum flexion angle from 74° to 86°. A preoperative hyperextension of 19° was corrected to an 11° minimum flexion angle postoperatively. Again, this had the effect of reducing the range of motion. As with stair ascent, there was a reduction in time taken to clear the step, this time of 1 second. Maximum flexion occurred at the same stage of the cycle pre and postoperatively (figure 4.13).

As with the previous 3 motions, when rising from a chair subject 3 demonstrated an increase in maximum flexion angle and a corrected hyperextension postoperatively, by increasing flexion by 22° and 30° respectively. Again, movement was quicker, by 0.5 seconds (figure 4.14).
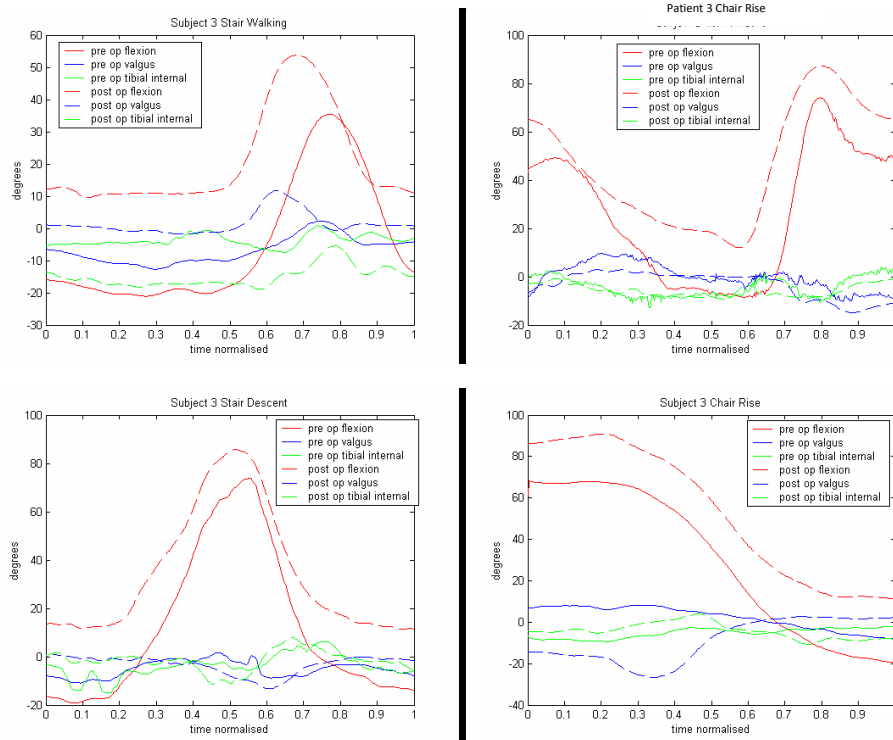

Figure 4.15 Pre and post operative angles in 3 planes for subject 3 during level walking (a) stair ascent (b) stair descent (c) and chair rise (d)

During preoperative level walking, the knee was in varus and rotated to a slight valgus angle at maximum flexion, and was externally rotated, rotating towards neutral at maximum flexion. The pattern of rotation was similar postoperatively but was more valgus and external (figure 4.15a).

During stair ascent, subject 3 rotated their knee from a slight varus to slight valgus angle, coupled with an external rotation. There was little change postoperatively, but the movement was smoother (figure 4.15b).

When descending a staircase, preoperatively the knee was in varus, rotating to a slight valgus at maximum flexion. The knee was externally rotated during flexion and rotated internally during extension. Postoperative rotations followed a similar pattern, but were generally more valgus and internal (figure 4.15c).

When rising from a chair preoperatively, the knee was in valgus, and rotated towards varus during extension, coupled with an initial external rotation that rotated towards neutral. Postoperatively, the knee was in varus when sitting, and rotated further into varus at beginning of extension, before rotating into valgus as the knee moved further into extension. Tibial rotation ws similar postoperatively (figure4.15d).

4.1.4 Subject 5

Subject 5 was fitted with a cruciate sacrificing (size 3) fixed bearing (size 3) implant form DePuy with a 10mm tibal spacer sized to the tibial implant.
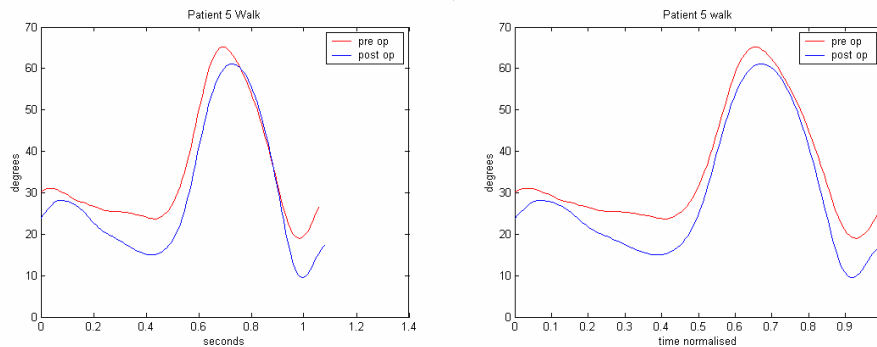

Figure 4.16 Flexion angle during level walking for subject 5

Subject 5 showed a decrease in maximum flexion angle postoperatively of 4°, from 65° preoperatively during level walking. Minimum flexion angle showed an improved extension postoperatively to 9° flexion from 19° preoperatively, resulting in an overall increase of 6° in range of motion (figure 4.16).
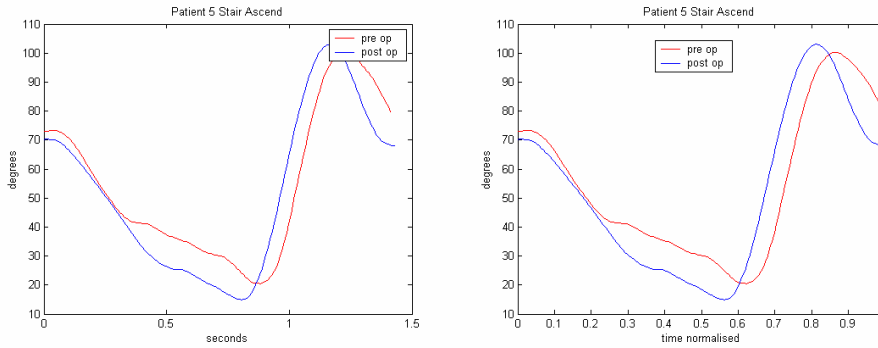
Figure 4.17 Flexion angle during stair ascent for subject 5

When ascending a staircase, subject 5 increased their maximum flexion angle by 3° to 103° postoperatively compared to preoperatively. At the same time, minimum flexion postoperatively reduced to 15° from 20° preoperatively, resulting in an overall increase in range of motion of 8°. Although heel strike and maximum flexion occurred earlier, there was no change in the overall time taken to complete the task (figure 4.17).
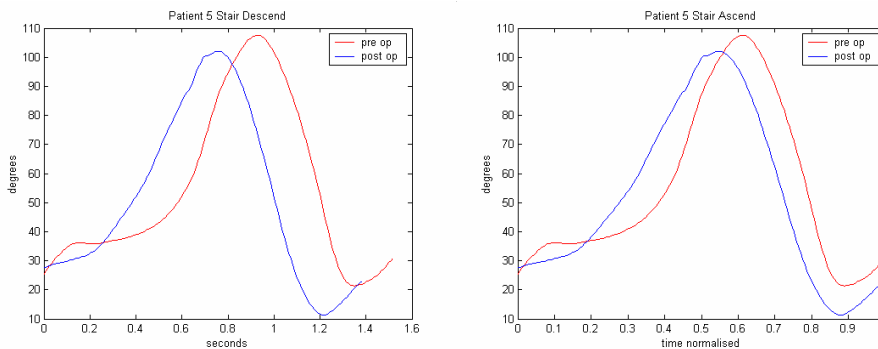
Figure 4.18 Flexion angle during stair descent for subject 5

Preoperatively, subject 5 had a maximum flexion angle of 107°. Postoperatively this reduced by 5°. Minimum flexion angle reduced from 21° preoperatively to 11° postoperatively, resulting in an overall increase in range

of motion of 5°. Time taken to complete the task was 0.2 seconds less postoperatively (figure 4.18).

Figure 4.19 Flexion angle during chair rise for subject 5

When rising from a chair, subject 5 increased maximum flexion angle when sitting to 82° postoperatively from 76° preoperatively. This was coupled with an improvement in extension of 10° to 11°, resulting in an overall increase in range of motion of 16°. Time taken to complete the task was 0.4 seconds less postoperatively (figure 4.19).

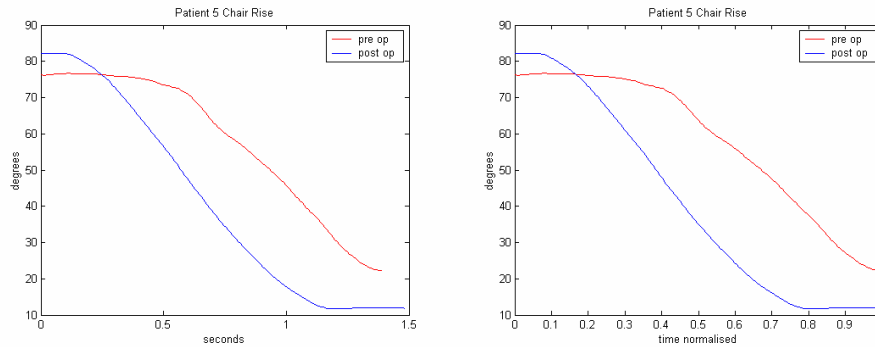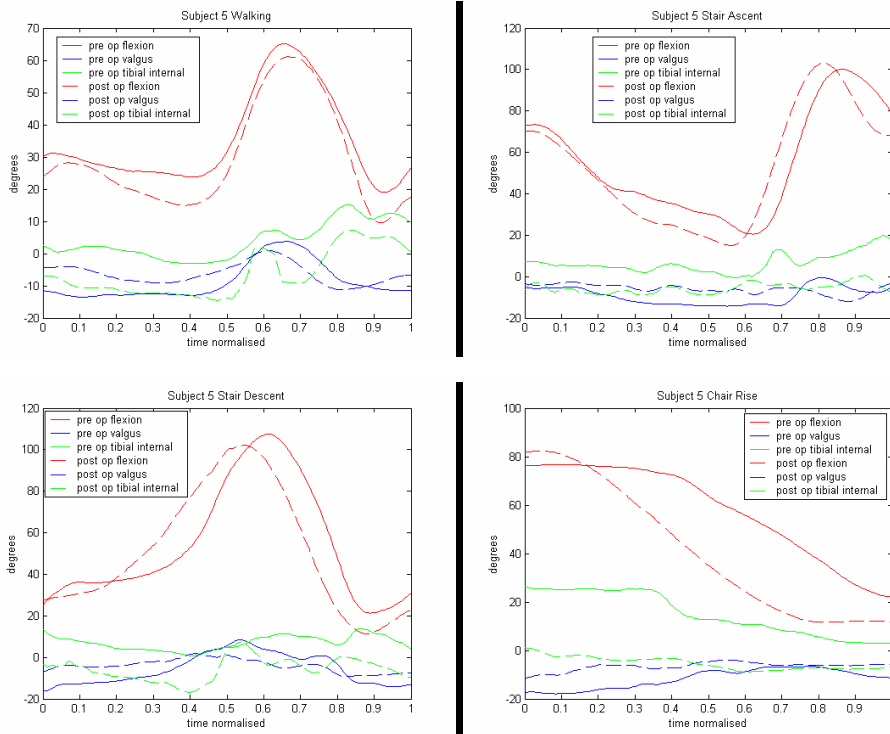Figure 4.20 Pre and post operative angles in 3 planes for subject 5 during level walking (a) stair ascent (b) stair descent (c) and chair rise (d)

During level walking, there was an initial varus rotation at heel strike that rotated towards neutral at maximum flexion in both pre and postoperative conditions, although there was less varus rotation postoperatively. The knee was rotated externally at heel strike preoperatively, and internally rotated at heel strike postoperatively. The pattern of rotation was similar in both pre and postoperative testing, and rotated externally during extension (figure 4.20a).

When ascending a staircase, the knee was in varus at heel strike both pre and postoperatively. Preoperatively, the knee rotated to varus until the beginning of flexion, where it then rotated towards neutral at full flexion. The knee then returned to varus by the next heel strike. Postoperatively, there was less varus rotation after heel strike, and during flexion did not rotate

towards neutral. Preoperatively, there was an external rotation at heel strike that rotated internally until the beginning of flexion, where it then rotated externally. Postoperatively the knee was rotated internally, with minimal movement in this plane (figure 4.20b).

When descending a staircase, the knee was in varus at heel strike and rotated into valgus during flexion then back to varus during extension. Postoperatively the pattern of rotation was similar, although the range was less, and closer to a neutral angle throughout. External rotation seen preoperatively was modified to an internal rotation postoperatively (figure 4.20c).

When rising from a chair, there was a varus knee angle preoperatively, which was reduced postoperatively, and a large internal rotation preoperatively that was close to neutral postoperatively (figure 4.20d).

4.1.5 Subject 11

Subject 11 was fitted with a cruciate sacrificing (size 4) rotating platform (size 4) knee implant from DePuy with a 10mm tibial spacer sized to the femoral component.
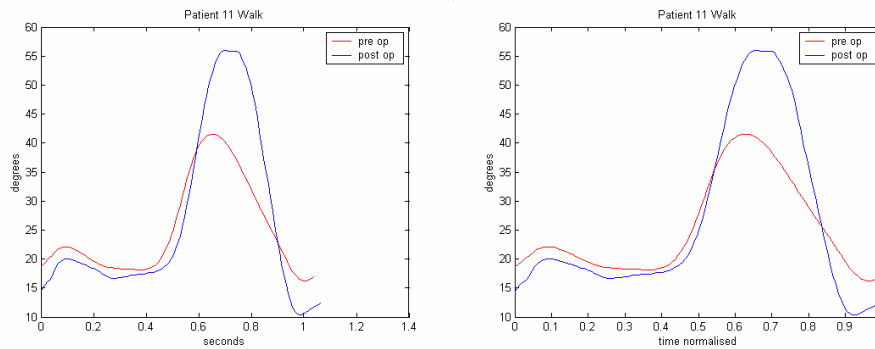
Figure 4.21 Flexion angle during level walking for subject 11

During level walking, subject 11 had a maximum flexion angle of 41° preoperatively, which increased to 56° postoperatively, while minimum flexion angle decreased from 16° to 10°. This resulted in an overall increase in range of motion of 21°. Time to maximum flexion and total time taken to complete the task was unchanged (figure 4.21).

Figure 4.22 Flexion angle during stair ascent for subject 11

During stair ascent, maximum flexion angle increased from 56° preoperatively to 75° postoperatively, and minimum flexion angle decreased from 16° to 14°. As seen in level walking, there was an overall increase of 21° in range of motion and no difference in the total time taken to complete the task. Preoperatively there was only one flexion peak, as the subject could only ascend the stairs one at a time, whereas postoperatively the subject could flex their knee further in order to clear each step (figure 4.22).
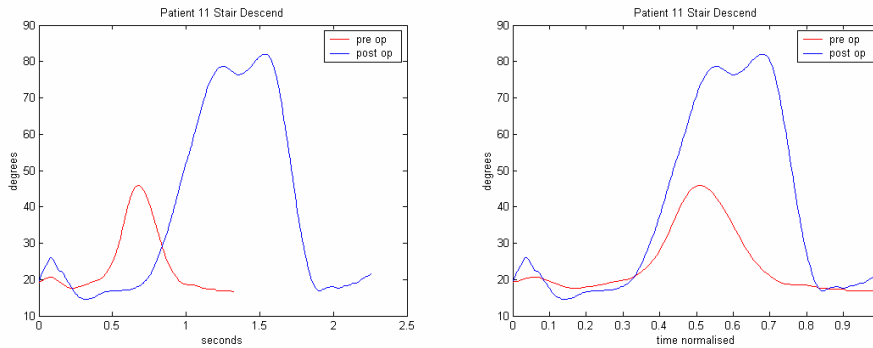
Figure 4.23 Flexion angle during stair descent for subject 11

During stair descent, subject 11 had a maximum flexion angle of 46° preoperatively and 82° post operatively. Minimum flexion angle decreased from 16° to 14°, resulting in an overall increase in range of motion of 38°. Time taken to complete the task increased by 0.5 seconds, again this was because the patient could clear each step postoperatively (figure 4.23).
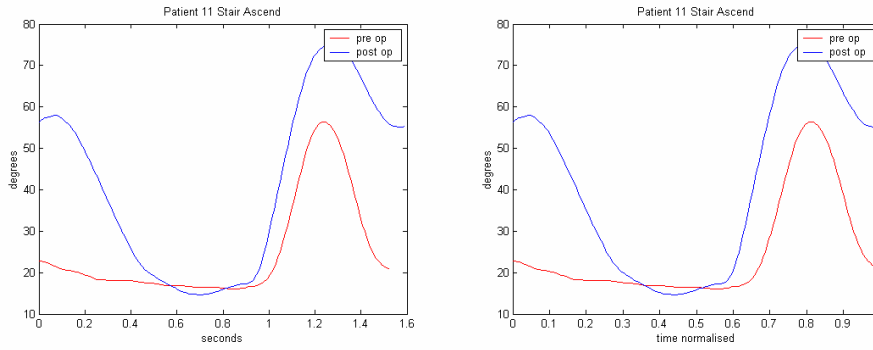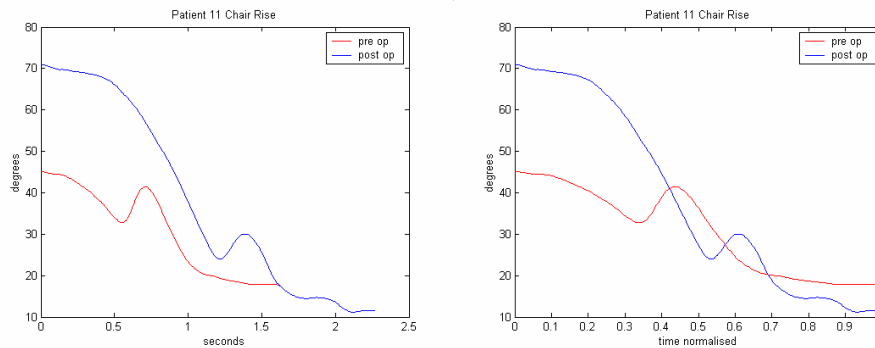

Figure 4.24 Flexion angle during chair rise for subject 11

When rising from a chair, maximum flexion angle increased from 45° preoperatively to 71° postoperatively, and minimum flexion angle decreased from 18° to 11°, giving an overall increase in range of motion 33°. In both pre and postoperative chair rise tasks, subject 11 sat with the affected leg in a more extended position than the non-affected leg, so that it was further forward. When rising from a chair, the subject appeared to take most of their weight on the non-affected leg at the beginning of the motion, and then pulled the affected leg towards their body so that it was in line with the non-affected leg. This motion can be seen in the two peaks of flexion in the above graph (figure 4.24).
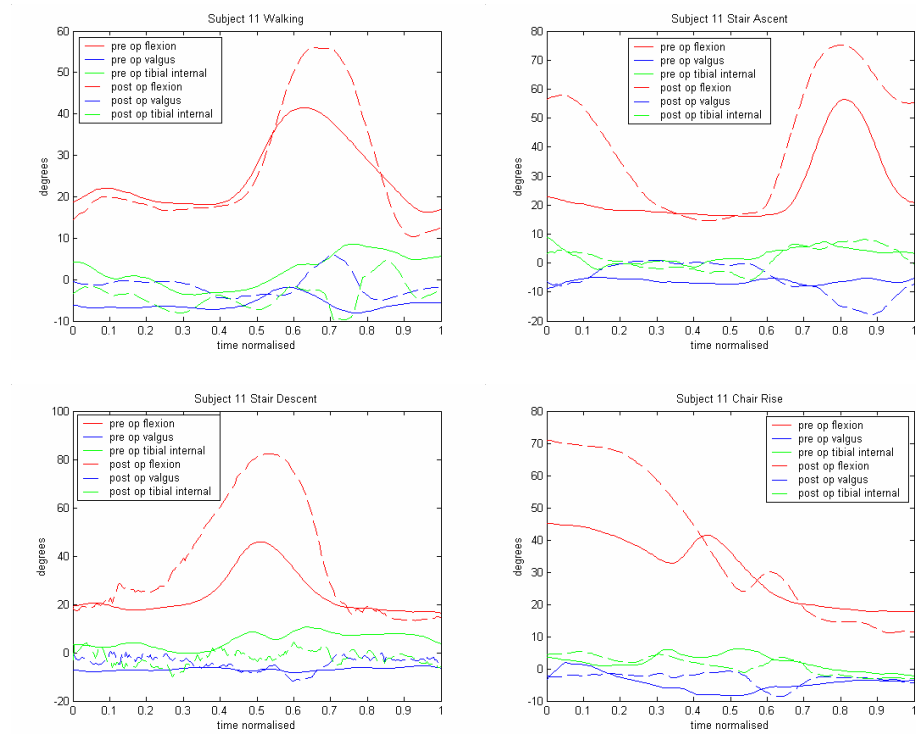
Figure 4.25 Pre and post operative angles in 3 planes for subject 11 during level walking (a) stair ascent (b) stair descent (c) and chair rise (d)

During level walking, subject 11 had a similar pattern of rotation pre and post operatively, which was more varus and internal preoperatively. The knee rotated into valgus during flexion, and back into varus during extension (figure 4.25a).

When ascending a staircase, there was a varus rotation preoperatively. Postoperatively, there was a change in the pattern of the varus rotation, in

the most part due to the change in ability to clear each step. The knee rotated further into varus at the higher flexion angle seen postoperatively. The knee rotated internally with flexion both pre and postoperatively (figure 4.25b).

In both stair ascent (figure 4.25c) and chair rise (figure 4.25d), subject 11 showed only small variations in varus and internal rotation, rotating to peak with peaks in flexion.

4.1.6 Subject 13

Subject 13 was fitted with a cruciate sacrificing (size 5) rotating platform (size 5) knee from DePuy with 10mm tibial spacer, sized to the femur.
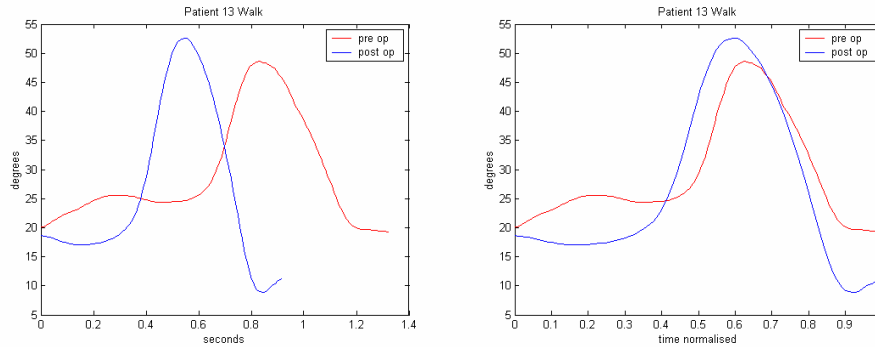
Figure 4.26 Flexion angle during level walking in subject 13

During level walking, subject 13 increased their maximum flexion angle from 48° preoperatively to 52° postoperatively. Minimum flexion angle decreased from 19° to 9°, resulting in an increased range of motion of 14°. Time taken to take one step decreased by 0.4 seconds postoperatively, with no change in time to maximum flexion (figure 4.26).
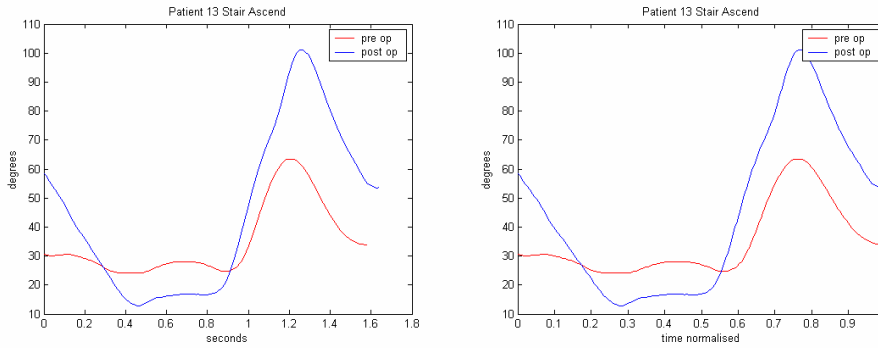
Figure 4.27 Flexion angle during stair ascent in subject 13

When ascending a staircase, subject 13 increased maximum flexion angle from 63° preoperatively to 101° postoperatively, and decreased their minimum flexion angle from 24° to 12°. The resultant 50° increase in range of motion is due to the change in method of ascending the stair, as preoperatively subject 13 could only climb the staircase one at a time, whereas postoperatively, they could clear each step (figure 4.27).
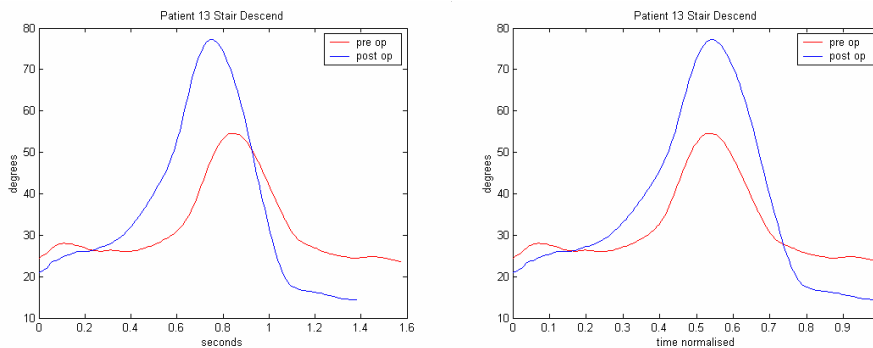
Figure 4.28 Flexion angle during stair descent in subject 13

When descending a staircase, subject 13 had a preoperative maximum flexion angle of 54° that increased to 77° postoperatively. Minimum flexion decreased by 9° to 14° postoperatively. As in stair ascent, the large

improvement in range of motion, this time of 32°, was again due to the subject being able to clear each step (figure 4.28).
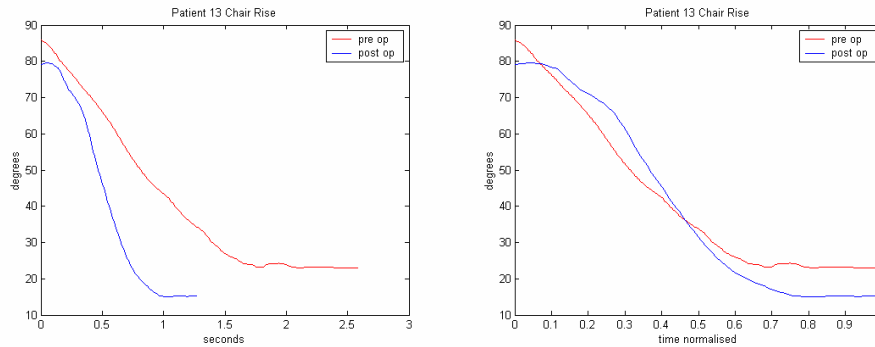
Figure 4.29 Flexion angle during chair rise in subject 13

When rising from a chair, subject 13 showed a slight decrease in maximum flexion angle of 6° to 79° postoperatively, but a decrease in minimum flexion angle of 7° to 15° resulted in a small increase in range of motion of 1° (figure 4.29).

Figure 4.30 Pre and post operative angles in 3 planes for subject 11 during level walking (a) stair ascent (b) stair descent (c) and chair rise (d)

In both pre and postoperative conditions, subject 13 had a varus rotation at heel strike during level walking, that rotated into valgus at maximum flexion. The knee was internally rotated at heel strike and rotated externally at maximum flexion, with less variation in the rotation postoperatively (figure 4.30a).

When ascending a staircase, subject 13 was in varus rotation throughout the motion preoperatively. Postoperatively, the knee was in valgus until after maximum flexion where the knee rotated into varus. Internal rotation was close to neutral in both conditions, but rotated more internally at maximum flexion postoperatively (figure 4.30b).

When descending a staircase, the knee was in varus preoperatively and valgus postoperatively. The knee rotated from neutral to a slight external rotation during flexion, before rotating internally during extension, only with less external rotation postoperatively (figure 4.30c).

When rising from a chair, the knee was in varus and internally rotated preoperatively, rotating towards neutral during the motion. Postoperatively, the knee was slightly valgus and internally rotated when seated, and rotated into valgus before rotating back to neutral in both planes (figure 4.30d).

4.1.7 Subject 14

Subject 14 was fitted with a cruciate sacrificing (size 2) rotating platform (size 2.5) knee from DePuy with a 10mm tibial spacer sized to the femur.
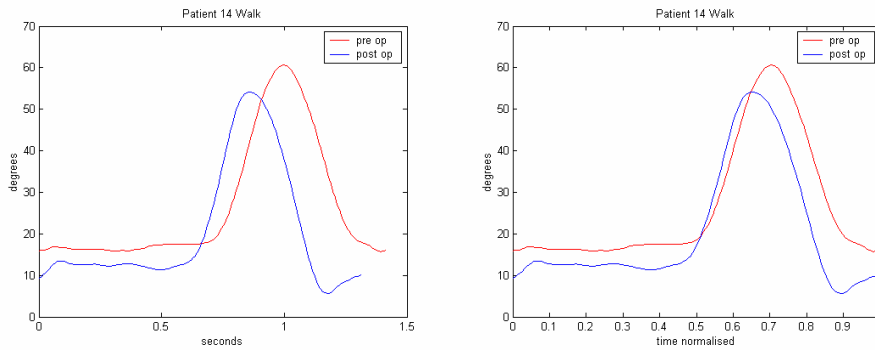
Figure 4.31 Flexion angle during level walking for subject 14

During level walking, subject 14 decreased their maximum flexion angle from 60° preoperatively to 54° postoperatively. A decrease in minimum flexion angle from 15° preoperatively to 5° postoperatively ensured an increase in range of motion of 4° (figure 4.31).
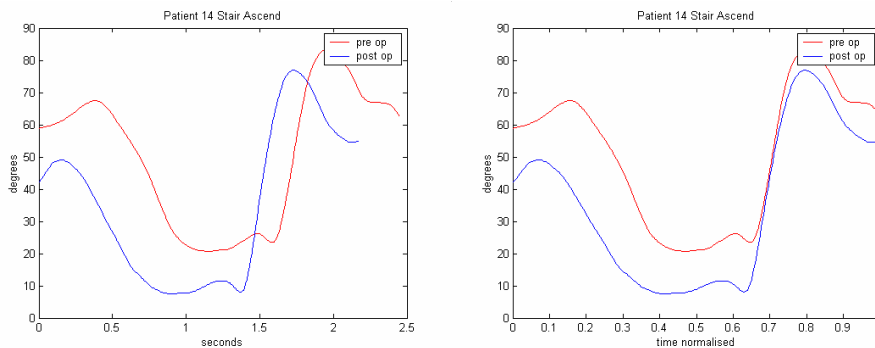
Figure 4.32 Flexion angle during stair ascent for subject 14

When ascending a staircase, subject 14 reduced maximum flexion angle by 6° to 77° postoperatively, and decreased minimum flexion angle from 21° to 7°, again resulting in an overall increase in range of motion of 8°. There was a slight increase in walking speed (figure 4.32).
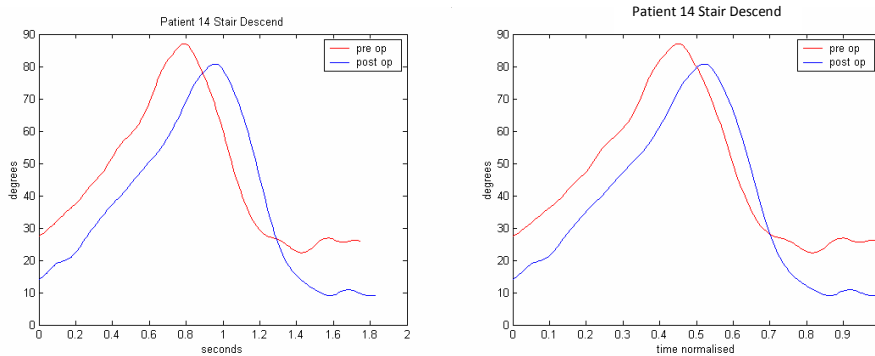
Figure 4.33 Flexion angle during stair descent for subject 14

When descending a staircase, again there was a decrease in both maximum and minimum flexion angles, this time of 6° to 81° for maximum angle and from 23° to 9° for minimum flexion angle. Range of motion increased by 8° (figure 4.33).
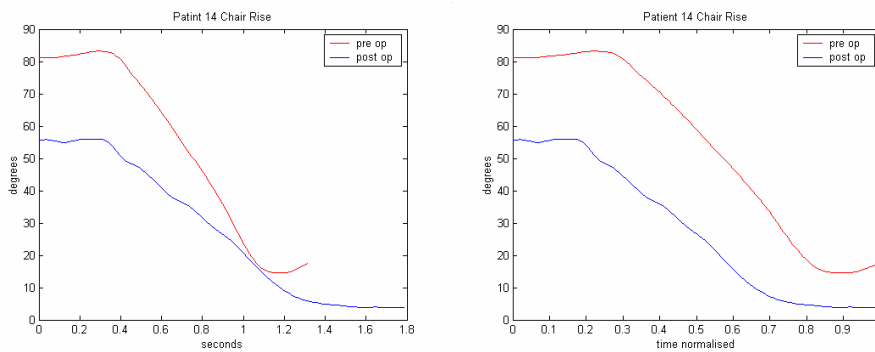
Figure 4.34 Flexion angle during chair rise for subject 14

There was a large change in foot positioning prior to rising from a chair postoperatively, resulting in a much reduced maximum flexion angle of 27° from 83° preoperatively. Minimum flexion angle also reduced, from 14° preoperatively to 3° postoperatively. On this occasion there was a decrease in range of motion of 16° (figure 4.34).
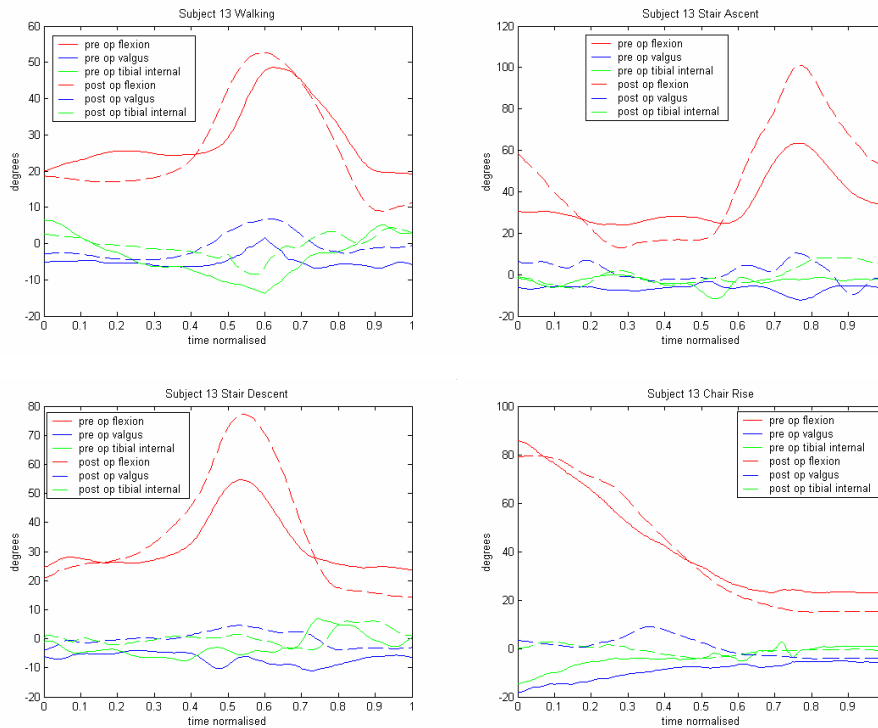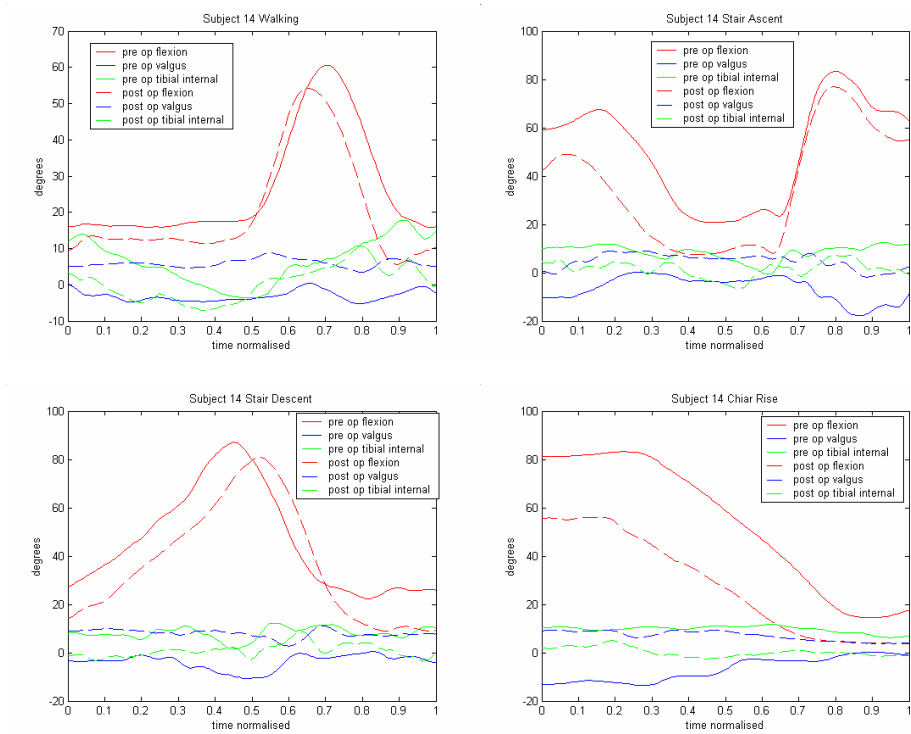

Figure 4.35 Pre and post operative angles in 3 planes for subject 11 during level walking (a) stair ascent (b) stair descent (c) and chair rise (d)

During level walking, the knee was in varus preoperatively, but a valgus rotation postoperatively. Preoperatively, at heel strike the knee is internally rotated, and rotated externally until the beginning of flexion where it rotated

internally again. The pattern of motion is similar postoperatively, but started in an external position and did not internally rotate to the same degree (figure 4.35a).

When ascending a staircase, the knee was mostly in varus and internal rotation preoperatively, and valgus and external rotation postoperatively. In both conditions the knee rotated to valgus and externally with extension and to varus and internally with flexion (figure 4.35b).

When descending a staircase (figure 4.35c) and rising from a chair (figure 4.35d), the varus and internal rotations are similar to ascending a staircase, in that the knee is mostly in varus and internal rotation preoperatively and valgus and external rotation postoperatively. Again, the pattern of motion is similar pre and postoperatively, although with a lesser range of motion postoperatively.

4.2 Group results

Implants
Subject 2 was fitted with a cruciate retaining femoral component, all other subjects had a cruciate sacrificing femoral component. Subjects 1, 2, 3 and 5 were fitted with a fixed bearing tibial component, subjects 11, 13 and 14 were fitted with a rotating platform tibial component. All sizes were decided by the surgeon based on the anatomy of each individual subject. All tibial spacers were 10mm, and were sized to the femur if the tibial implant was a rotating platform, and to the tibia if the tibial implant was a fixed bearing component.

4.2.1 Flexion

Walking trial
The maximum flexion angles seen during level walking show an increase postoperatively in 5 of the 7 subjects (figure 4.36). All 5 had pre operative maximum flexion angles of less than 50°. The 2 subjects who displayed a decrease in maximum flexion angle post operatively had a preoperative flexion angle greater than 60°. The difference was not related to the type of implant, as one had a fixed bearing implant, and the other had a rotating platform. The variation in maximum flexion angle for the group decreased from 29.8° preoperatively to 17.5° postoperatively.

Walking Maximum Flexion
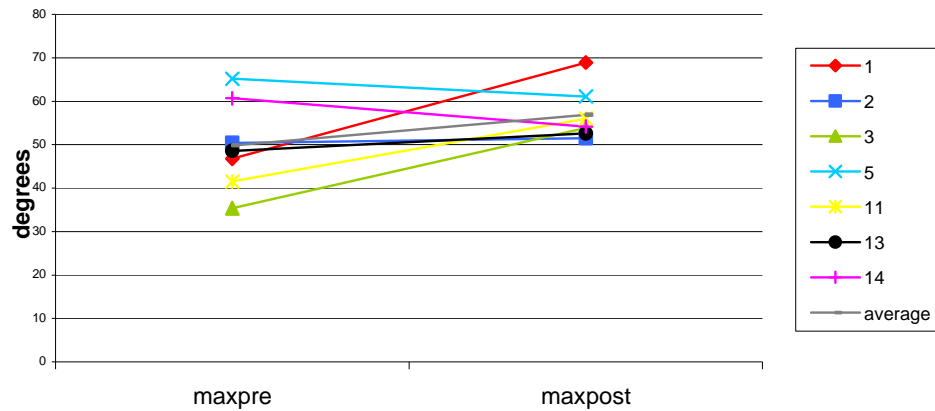
Figure 4.36 Maximum flexion Angles During Level Walking

The minimum flexion angles during extension decreased for 4 subjects, all of whom had a preoperative extension at or above $15°$ flexion (figure 4.37). The three remaining subjects had a preoperative extension angle at $0°$ or into hyperextension. The three subjects with hyperextension preoperatively were fitted with a fixed baring tibial implant, and had an increase in their minimum flexion angle postoperatively. Due to the combination of high flexion angles in some subjects and hyperextension in others, the variation of minimum flexion angles during walking within the group decreased considerably from $40.4°$ preoperatively to only $4.7°$ postoperatively.

Walking Minimum Flexion
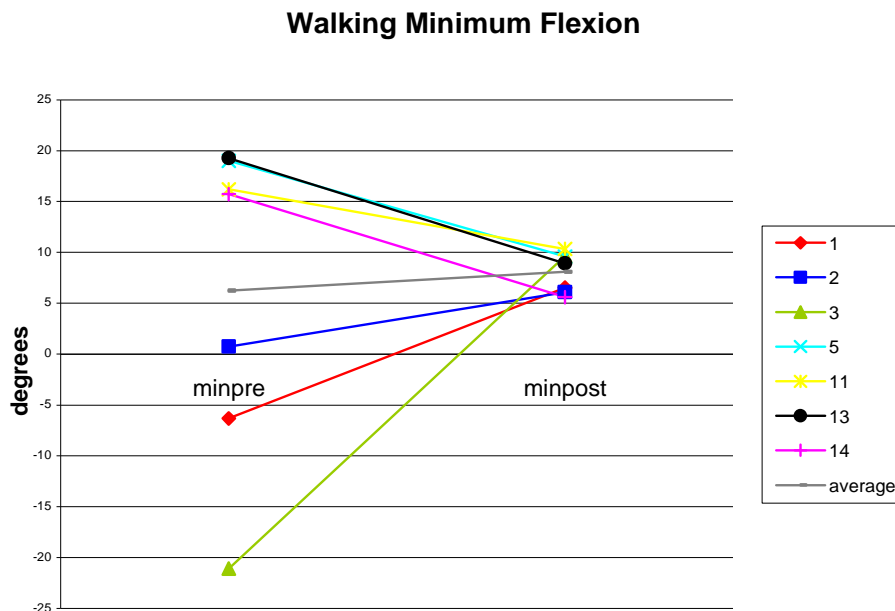
Figure 4.37 Minimum Flexion angles during level walking

The range of motion seen during level walking increased for 5 of the 7 subjects in this study. Of the 2 who showed a decrease, one was due to the removal of a 20° hyperextension, whilst the other had a small reduction in their extension and little change in their maximum flexion values.   The variation in the range of motion decreased during level walking from 31.2° preoperatively to 18.7° postoperatively (figure 4.38). This suggests that the larger variation in range of motion seen preoperatively has been brought closer to a more normal or standardised range of motion postoperatively with less individual variation.
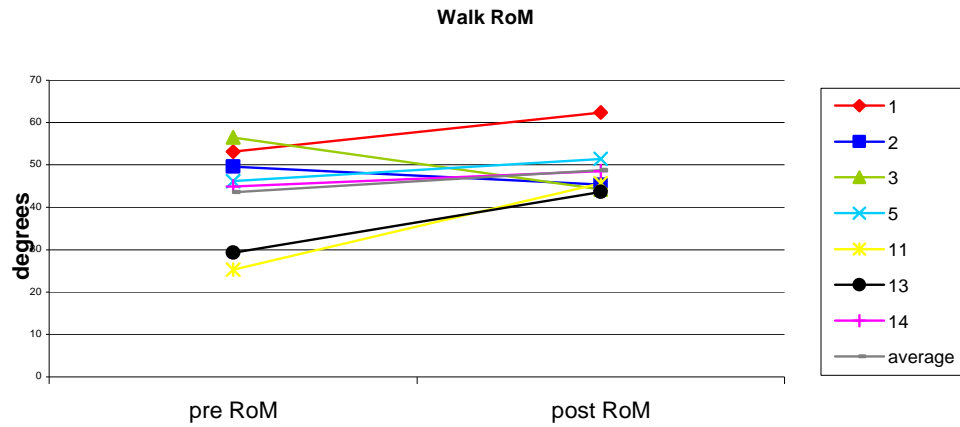
Figure 4.38 Range of motion during level walking
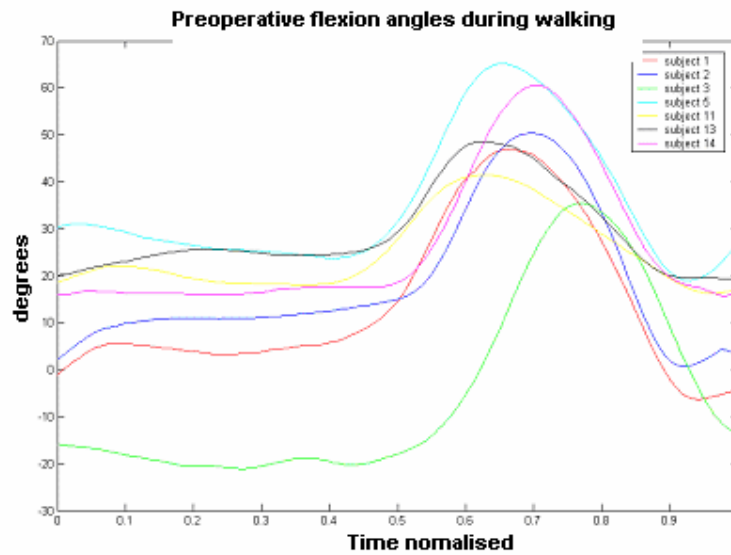
Figure 4.39 Preoperative angles of flexion during level walking

Figures 4.39 and 4.40 show the pattern of flexion angle for the group preoperatively and post operatively respectively. These graphs further

illustrate the change in pattern for the group as a whole, towards a more normal pattern of gait.
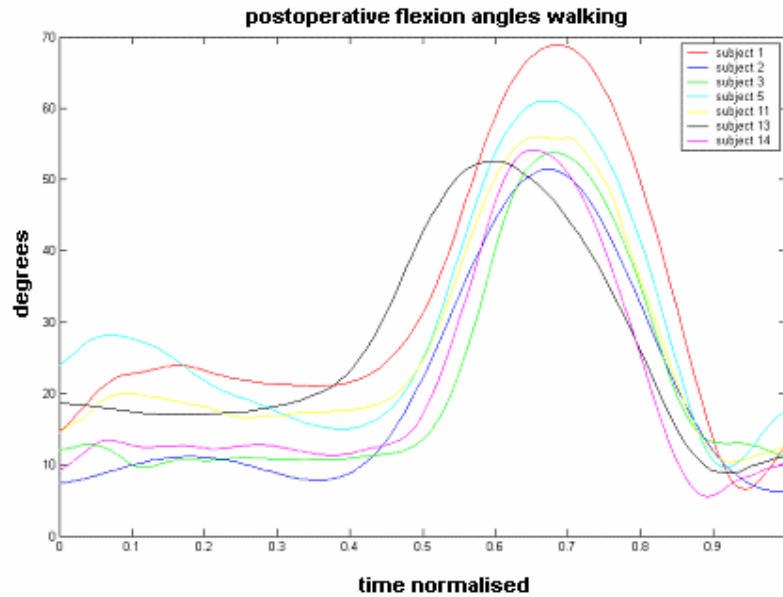
Figure 4.40 Postoperative angles of flexion during level walking

Gait adaptations in the elderly are associated with a decrease in muscle strength due to a loss of motor neurone function, muscle fibres, and aerobic activity (Prince et al 1997). The elderly maintain a slight knee flexion at the end on the swing phase, and have a range of motion reduced by 4° in comparison to young subjects. This makes comparisons with the vast majority of published data difficult. Kaufman et al (2001) reported on knee flexion angles in OA compared to normal age matched subjects. They found that there was no significant difference in the maximum flexion angles when walking on a level surface, with OA subjects having 6° less maximum flexion than the control group. However, this was most likely due to the early stage of the disease that was being studied. The current study would be expected to differ from this due to the advanced stage of the disease being studied. Figure 4.41 shows maximum flexion angles from the current study pre and postoperatively compared to data previously reported by Myles et al (2002).

The maximum flexion angles in the current study preoperatively lie within one standard deviation of the mean value for maximum preoperative flexion angle as reported by Myles et al (2002).

**Maximum Flexion Angles During Level Walking
Compared with the literature**

Figure 4.41 Comparison of maximum flexion angles with Myles et al (2002)

Similarly, the postoperative values in the current study lie within one standard deviation of the mean for postoperative flexion angles previously reported. Nadeau et al (2003) reported that maximum flexion angles during level walking for healthy adults over the age of 40 was 67°(3.1°SD). The

improvement in maximum flexion angle is therefore comparable to data previously reported in the literature.

The preoperative minimum flexion angles for the group in the current study appear to be separated into two distinct groups: those with high preoperative minimum flexion angles and those who hyperextend the knee. The three subjects who hyper-extended preoperatively were all fitted with fixed bearing tibial implants, and only one had a cruciate retaining femoral implant. The variation seen in minimum preoperative flexion angles between the subjects in the current study is wider than those previously reported by Myles et al for preoperative TKR subjects, and by Rowe et al (2000) for healthy age matched subjects. Postoperatively, all seven subjects minimum flexion angles were higher than the mean value reported by Myles et al for postoperative subjects, but were still within one standard deviation of the mean. The postoperative minimum flexion angle was also higher than that reported for healthy adults over 40 by Nadeau et al (2003) of $1.1°(5.1°SD)$, but again within two standard deviations. This is a higher minimum flexion angle than the data reported for minimum flexion angles, but not significantly so (figure 4.42).

Minimum Flexion Angles During Level Walking Compared with the Literature
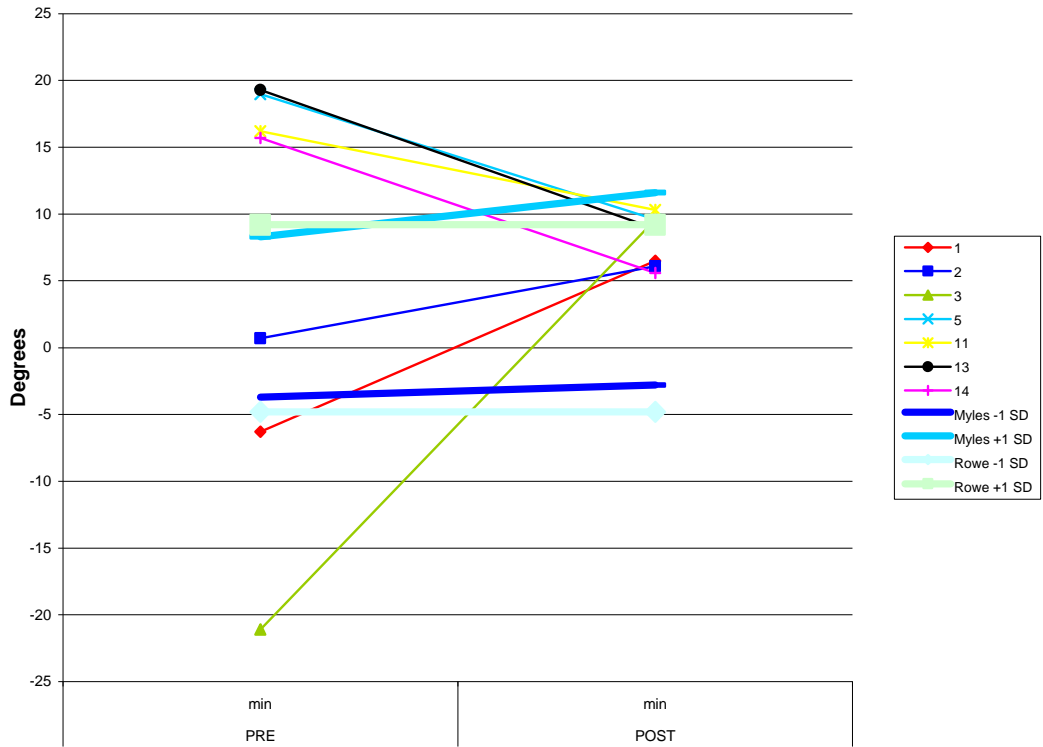
Figure 4.42 Comparison of minimum flexion angles with Myles et al (2002) and Rowe et al (2000)

The data published by Myles et al (2002) that is being used for comparison was collected 18 – 24 months postoperatively. However, minimum flexion angle postoperatively was also recorded by Myles et al at 4 months after surgery. Minimum flexion angle at 4 months was lower than at 18 months, and can therefore not account for the higher minimum flexion angles reported here. The data in the current study is still within one standard deviation of the mean of the data reported by Myles et al.

The range of motion seen in flexion during level walking decreased in two of the seven subjects. These two subjects hyper-extended preoperatively, and so the overall reduction seen in the range of motion is largely due to the correction of the hyper-extension. Five of the subjects preoperative range of motion fell within one standard deviation of the mean for the group studied by Myles et al (2002). Postoperatively, the range seen was similar to that reported for the postoperative group in the study by Myles et al. The postoperative group in Myles study were tested at 18-24 months postoperatively. The present study tested after 12 months, and this may account for the slight discrepancy seen in the data.   The mean range of motion 12 months postoperatively in the current study for level walking was 48.8°, compared with 54.6° at 18-24 months postoperatively in the Myles study. The results from the current study are closer to the mean at 4 months postoperatively in the Myles study of 51.4°, and 53° reported by Wilson et al (1996) for subjects with a posterior stabilised TKR. Myles et al reported that there is a significant difference in the pre and post operative excursion flexion angles in their study group. The results of the current study fall within the spread of data from the Myles study, but does not match the 61° reported by Wilson et al (1996) for healthy age matched controls.

Stair Ascent

All subjects showed an increase in their maximum flexion angles during stair ascent with the exception of subject 14 (figure 4.43).   However, this difference was only a 6° that this is part of a shift of the whole pattern of movement that ultimately reduces the minimum flexion angle.

Stair Ascent Maximum Flexion
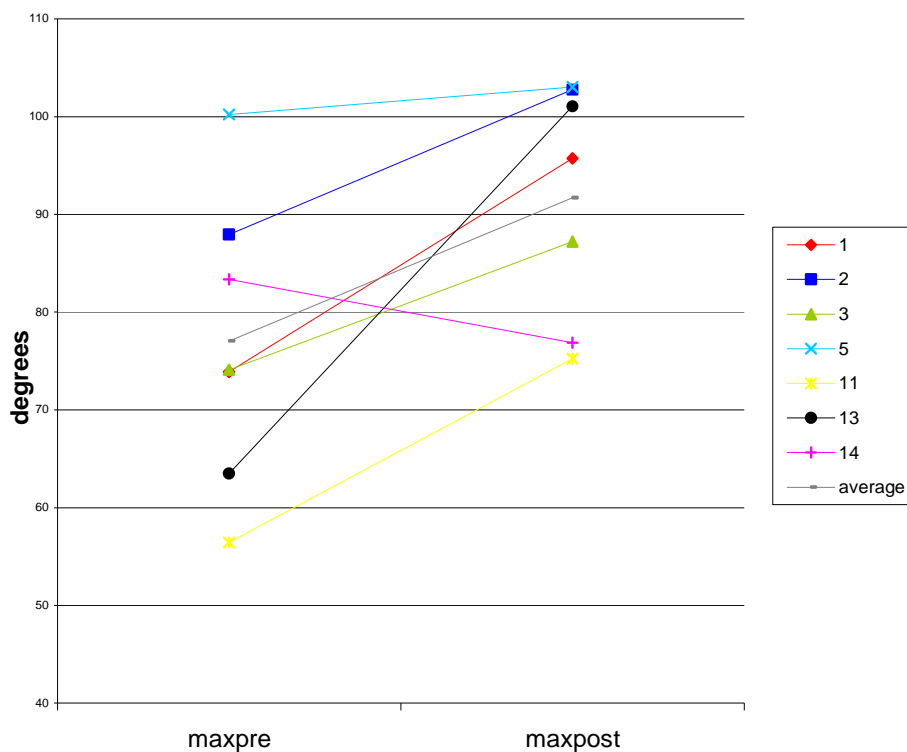
Figure 4.43 Maximum flexion angles during stair ascent

The variation in maximum flexion angle during stair ascent for the group decreased from $43.8°$ to $27.8°$. The graph shows that the subject with the highest preoperative flexion angle increased the least, and the subject with the lowest preoperative value increased the most.

The minimum flexion angle decreased for the 3 subjects who had a minimum flexion greater than $20°$. Conversely, the minimum flexion angle increased for the other 4 subjects that had a minimum flexion angle lower than $20°$.

This has the net effect for the group of reducing the variation in minimum flexion angle seen from 43.1° to just 9° postoperatively (figure 4.44).

Stair Ascent Minimum Flexion
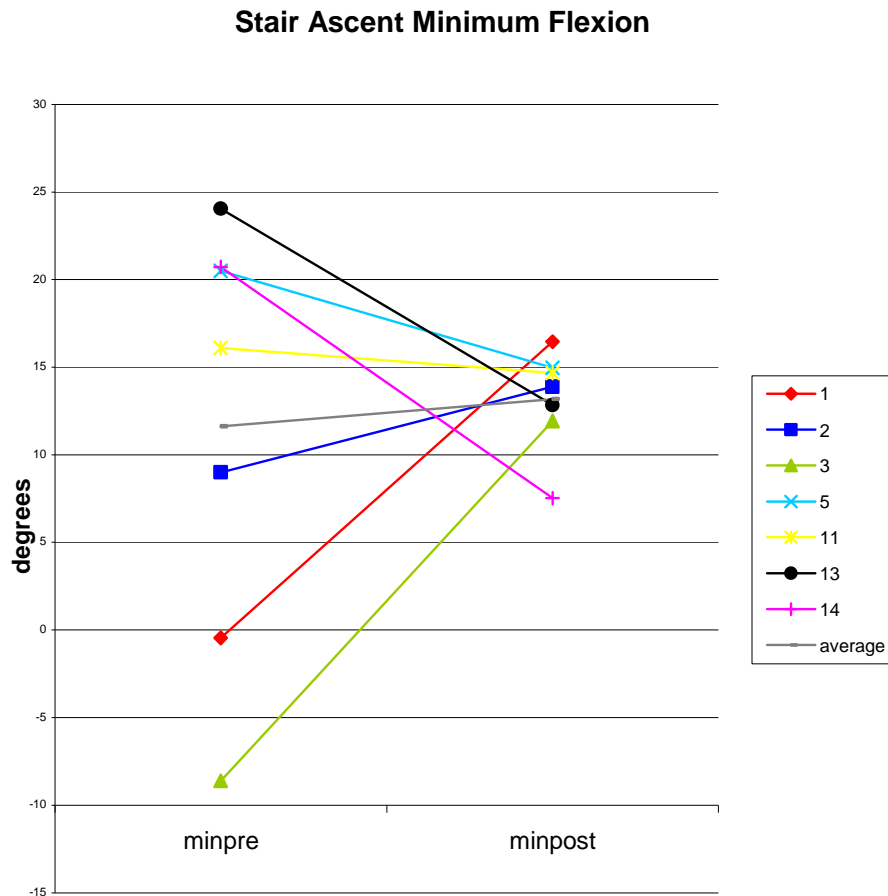
Figure 4.44 Minimum flexion angles during stair ascent

All subjects show an increase in their range of motion during stair ascent with the exception of subject 3 (figure 4.45). This is due to the fact that

preoperatively this subject had a hyperextension of over 20°, which has been corrected postoperatively. The largest increases are seen in subjects 11 and 13. This is because preoperatively these two subjects could only climb stairs one step at a time, putting both feet on each step. Postoperatively all subjects could climb stairs in a normal full stride manner.
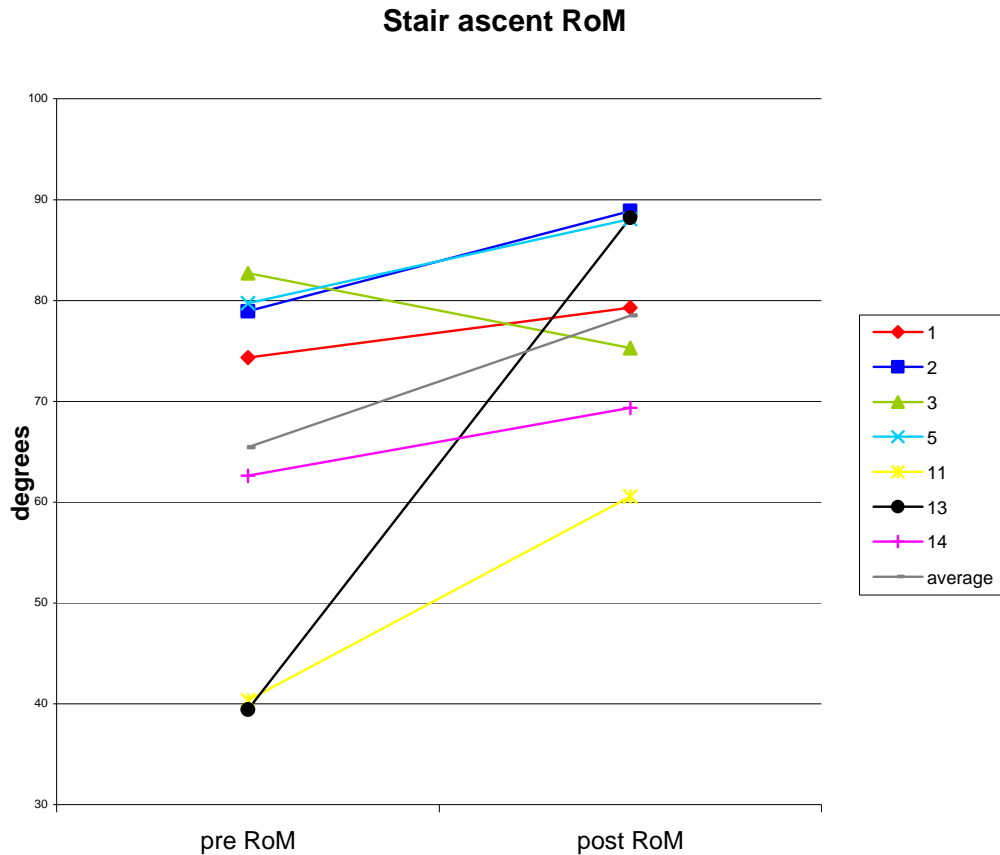
Stair ascent RoM

Figure 4.45 Range of motion during stair ascent

The change in motion patterns for the group as a whole, and especially subjects 11 and 13, are further confirmed by comparing their angles of knee

flexion throughout stair ascent preoperatively (figure 4.46) and postoperatively (figure 4.47).
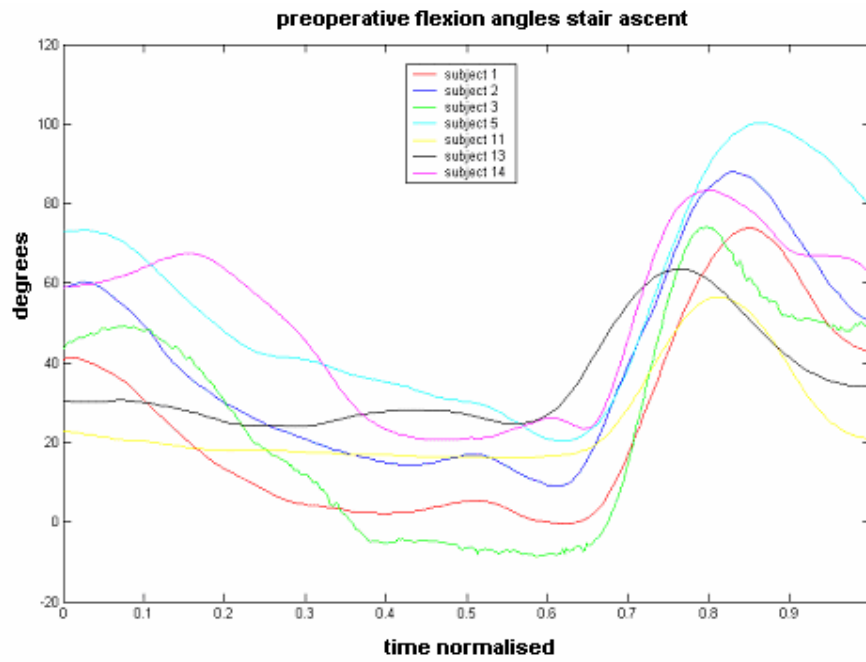
Figure 4.46 Flexion angles throughout stair ascent preoperatively
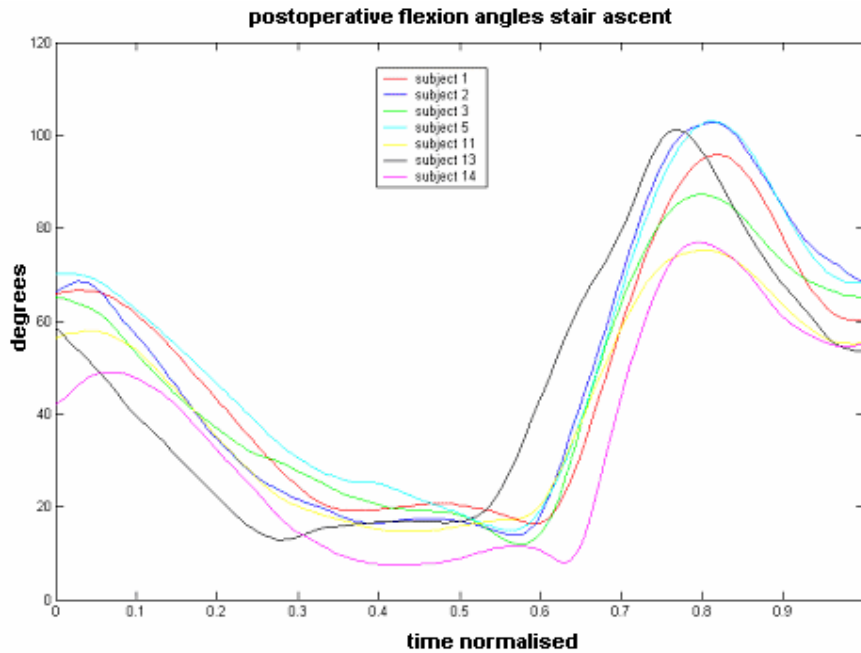
Figure 4.47 Flexion angles throughout stair ascent postoperatively

The ability to negotiate stairs has the potential to dramatically improve quality of life. Kaufman et al (2001) reported that subjects with mild OA only demonstrated an insignificant difference in range of motion of less than 2° compared to healthy aged matched subjects. A mild reduction in the range of motion of the knee, as is seen in OA, can dramatically reduce the functionality and performance of the knee (Nadeu et al 2003). For stair climbing, a larger range of motion is required than that for level walking, with maximum flexion angles in normal subjects being in the range of 80° to 100°. One subject in the current study, and a further 2 that were tested preoperatively but not postoperatively, could only ascend the stairs one at a time due to a reduced range of motion at the knee preventing them from being able to clear a step in the swing phase.

A large variation was seen in the maximum flexion angles preoperatively. Only subject 5 was not within one standard deviation of the mean of maximum flexion reported by Myles et al (2002). The lowest maximum postoperative flexion angle was the same as the average reported by Catani et al (2003). Four subjects had a postoperative maximum flexion angle higher than the range seen postoperatively by Myles et al. The subjects with the five highest flexion angles postoperatively were similar to that of age matched healthy subjects as reported by Rowe et al (2000). For ascending stairs, the maximum flexion angles for the group were therefore at worst comparable with previously reported data by Catani (2003) and Myles (2002), and the best results exceeded maximum flexion angles previously reported for postoperative TKR subjects, matching healthy aged-matched subjects, such as in the study by Nadeau (2003), who reported a maximum flexion angle of 93.1°(3.1°SD).

The preoperative minimum flexion angles when ascending a staircase in the current study ranged from 19° hyperextension to a flexion angle of 24.1°. This variation in the minimum flexion angle is far greater than the mean (SD) reported by Myles et al (2002) of 6.3°(6.3°), and by Thambyah et al (2004) of 2°(5°) for healthy subjects and 6°(5°) for subjects with ACL deficiency. Postoperatively, the minimum flexion angle when ascending a staircase varied from 7.5° to 16.5°, agreeing with the postoperative results of Myles et al of a mean minimum flexion angle of 11.5°(6.4°). The minimum flexion angle when ascending a staircase for healthy age matched subjects as reported by Rowe et al (2000) was slightly higher than the values reported here and by Myles et al for postoperative TKR, but the difference was not significant.

The variation in the range of motion when ascending a staircase for the current study fell within two standard deviations of the mean as reported by Myles et al (2002), both pre and postoperatively.

Stair Descent

Five of the seven subjects showed an increase in maximum flexion when descending a staircase (figure 4.48). As with stair ascent, subject 14's reduction was slight, and part of a reduction in the overall pattern of motion. In this situation, subject 5 also shows a slight reduction, but postoperatively still has the highest maximum flexion angle. The variation in maximum flexion angle across the group decreased considerably from 61.6° preoperatively to 24.8° postoperatively.

Stair Descent Maximum Flexion
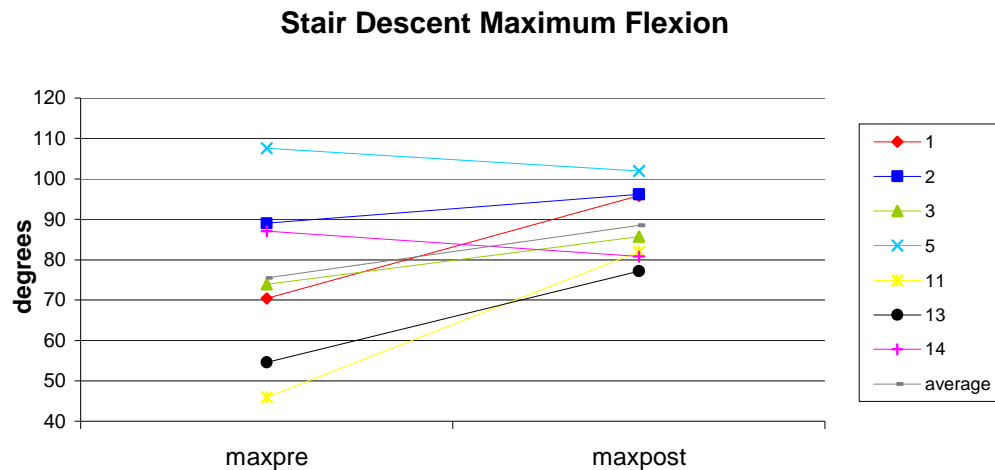
Figure 4.48 Maximum flexion angles when descending a staircase

As with walking and stair ascent, there is again a cut off value for an increase or decrease in minimum flexion angle. Subjects with a minimum flexion

angle above 10° showed a decrease in flexion angle postoperatively, whereas those with a minimum flexion angle below 10° increased their flexion angle (figure 4.49). Yet again this split in the group is mainly due to the difference in subjects who tend to hyperextend preoperatively and those who do not. As such, the variation in minimum flexion angles during stair descent changes markedly from 42.9° to 5.6°.

Stair Descent Minimum Flexion
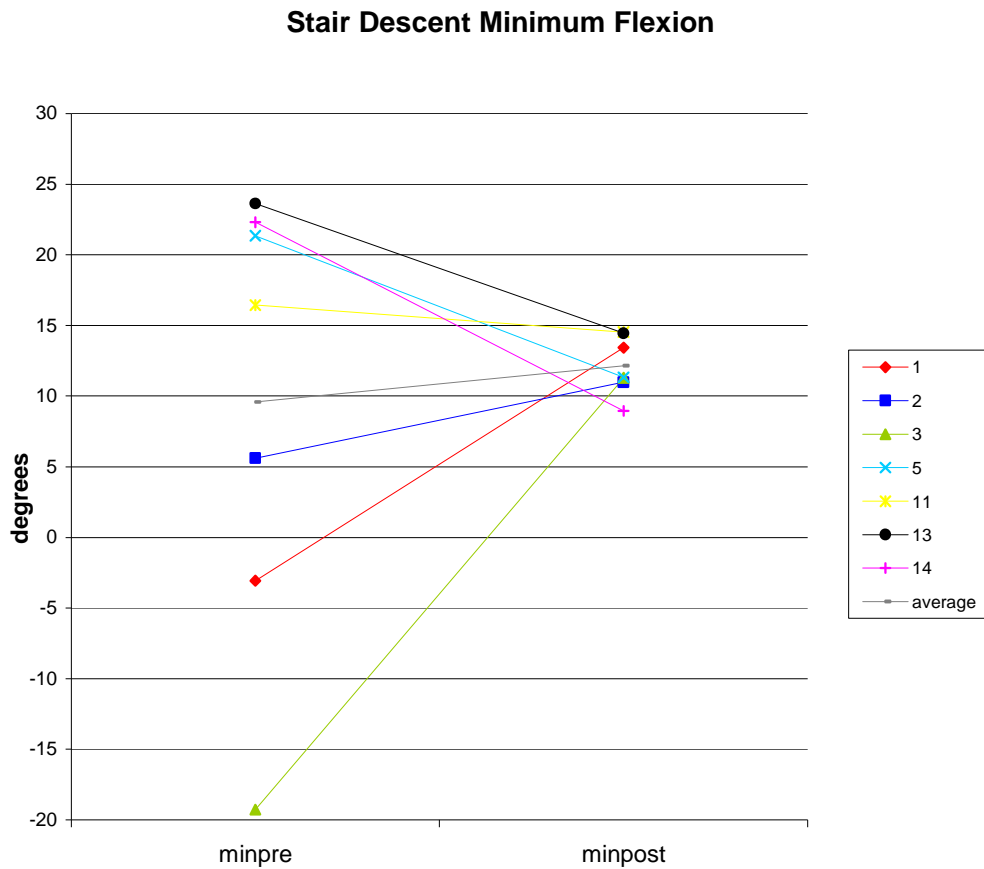
Figure 4.49 Minimum flexion angles when descending a staircase

Again, as seen in stair ascent, all the subjects show an increase in the range of motion (figure 4.50) with the exception of subject 3, because of the

correction for the large hyperextension. The difference in range of motion for the group reduces from 63.7° preoperatively to 27.9° postoperatively.
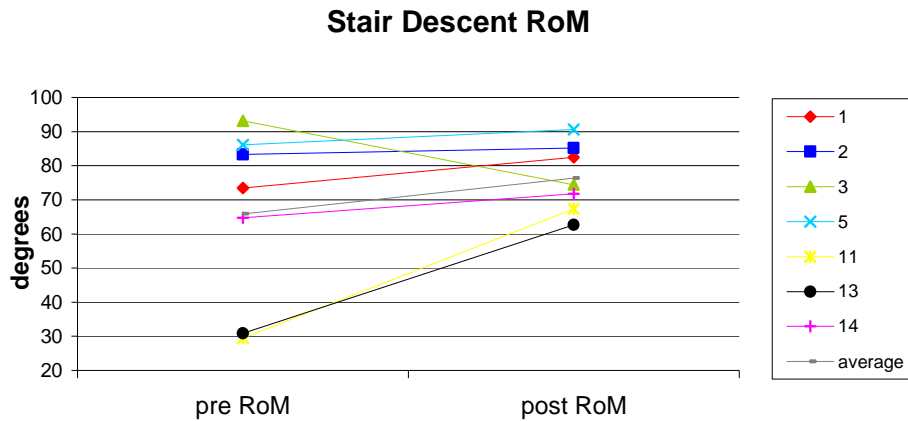
Stair Descent RoM

Figure 4.50 Range of motion for flexion when descending a staircase

As with stair ascent, the variance seen in pattern of motion preoperatively (figure 4.51) is large. This is again brought into line with a more normal pattern during stair descent postoperatively (figure 4.52). Again, the biggest change in motion is seen in subjects 11 and 13. This is due to the change in taking steps one at a time preoperatively to descending the staircase in a consecutive manner.
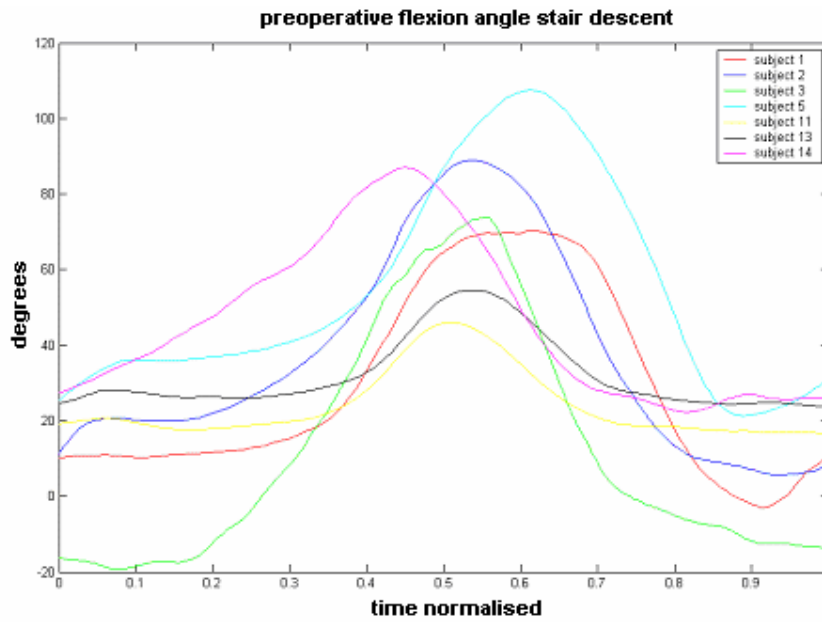
Figure 4.51 Preoperative flexion angles when descending a staircase
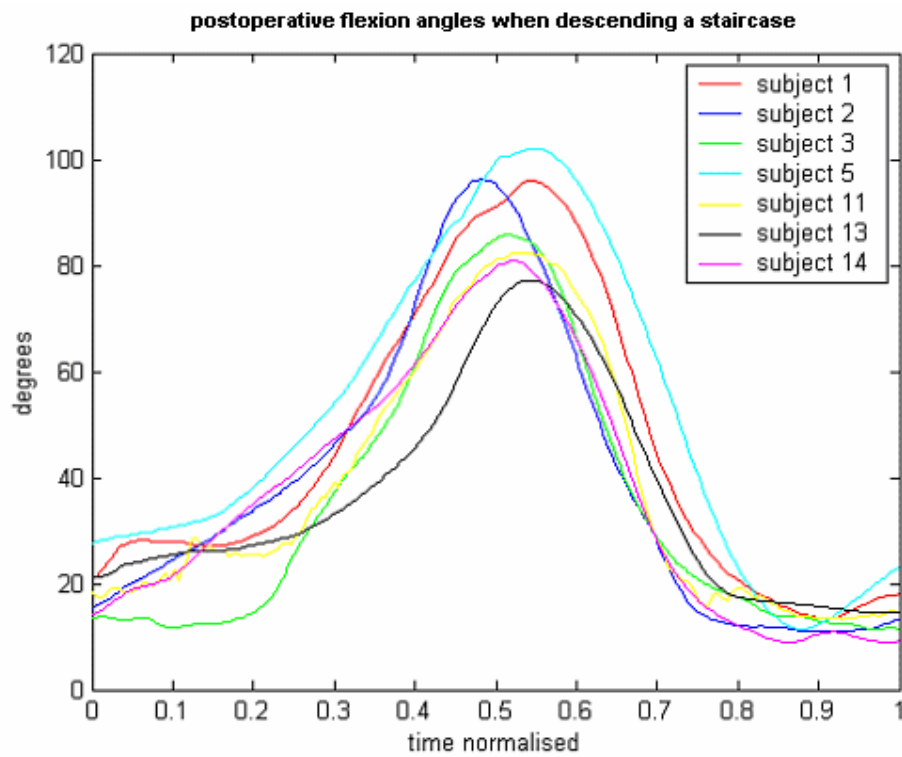
Figure 4.52 postoperative flexion angles when descending a staircase

As with stair ascent, the variation of both maximum and minimum preoperative flexion angles was out-with one standard deviation of the mean in the Myles study, but still within the normal variation of two standard variations. Postoperatively, the minimum flexion angles agreed with the postoperative minimum values in the Myles study. Maximum flexion angles when descending a staircase were higher than both the results of postoperative maximum flexion angles in the study by Myles et al (2002) and the results for normal healthy age matched subjects reported by Rowe et al (2000).

As the maximum flexion angles reported here are larger than maximum flexion angles in the Myles et al study, it follows that the range of motion when descending a staircase will also be larger. The mean range of motion in the current study of 78.5° is larger than the 64.9° range of motion reported by Myles et al, but all subjects in the present study fall within two standard deviations of the mean from the Myles et al study.

Chair Rise

When sitting, 5 of the subjects increased their maximum flexion angles postoperatively. Subjects 13 and 14 did not (figure 4.53). These 2 subjects had the largest preoperative flexion angles, and while subject 13 was mid-range for this group postoperatively, subject 14 went from second highest to the lowest flexion angle postoperatively. Subsequently, the variance of the maximum flexion angle for the group only showed a modest decrease from 40.6° to 34.9°.

Chair Rise Maximum Flexion
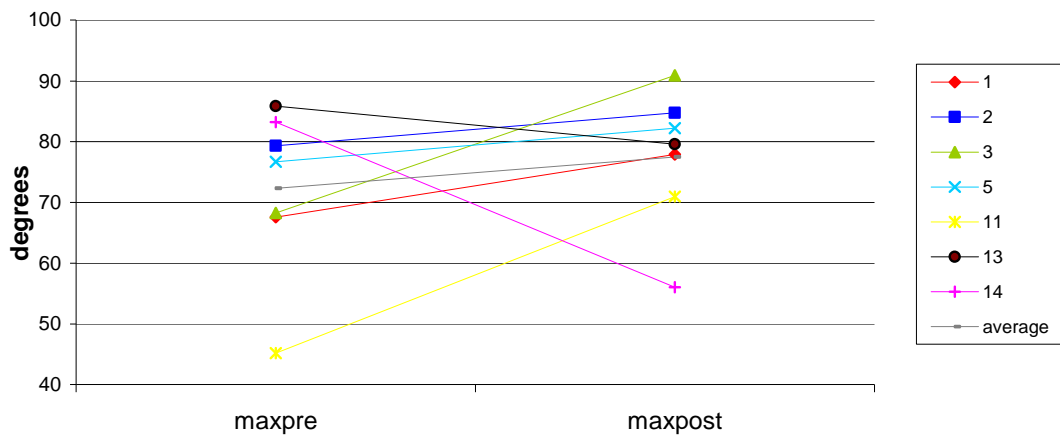
Figure 4.53 Maximum flexion angles when rising from a chair

As with the previous 3 tasks, the minimum flexion angle when rising from a chair increases in the subjects who have a preoperative flexion less than 10° and decreases for those with flexion values over 10°. This again has the effect of reducing the range throughout the group from 42.2° preoperatively to 11.4° postoperatively (figure 4.54).

Chair Rise Minimum Flexion
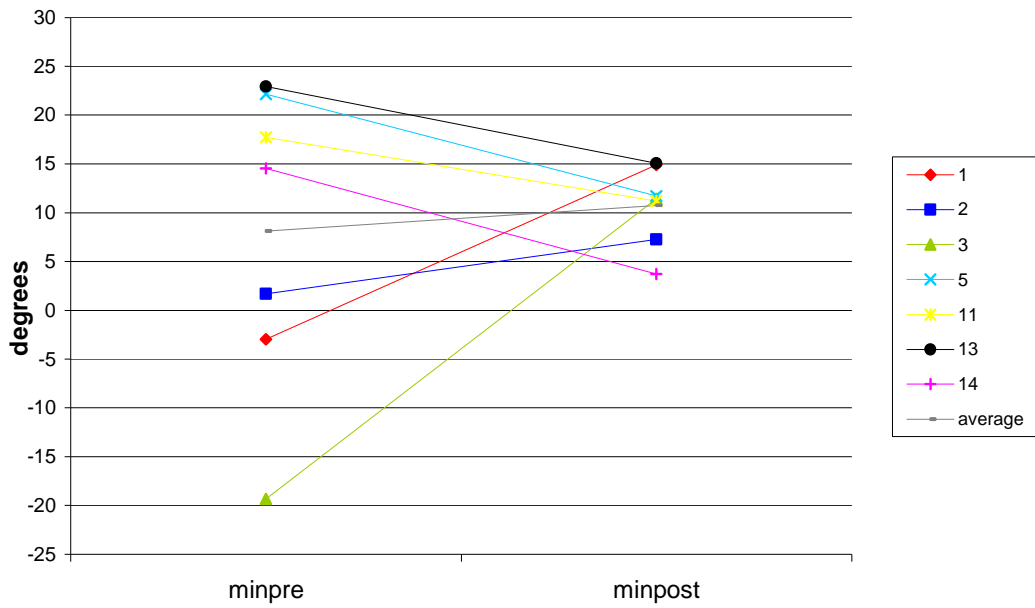
Figure 4.54 Minimum flexion angles when rising from a chair

The difference in range of motion decreased from 64.4° to 27.2°, however there is no discernable pattern to the changes in the range of motion (figure 4.55). This may be due to the methods used to stand, and will be discussed later.

Chair Rise RoM
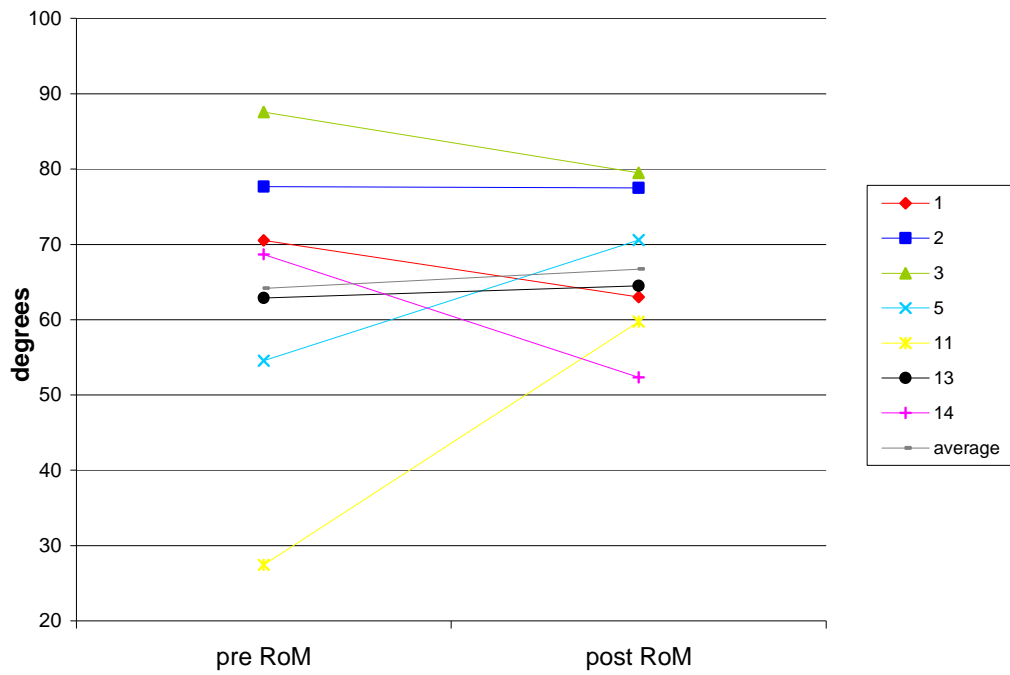
Figure 4.55 Changes in range of motion when rising from a chair

The improvement in overall pattern of motion seen in the other three activities is not as marked in rising from a chair (figures 4.56 and 4.57). This may be mostly due to the placement of the foot when sitting, thus affecting the starting flexion angle.
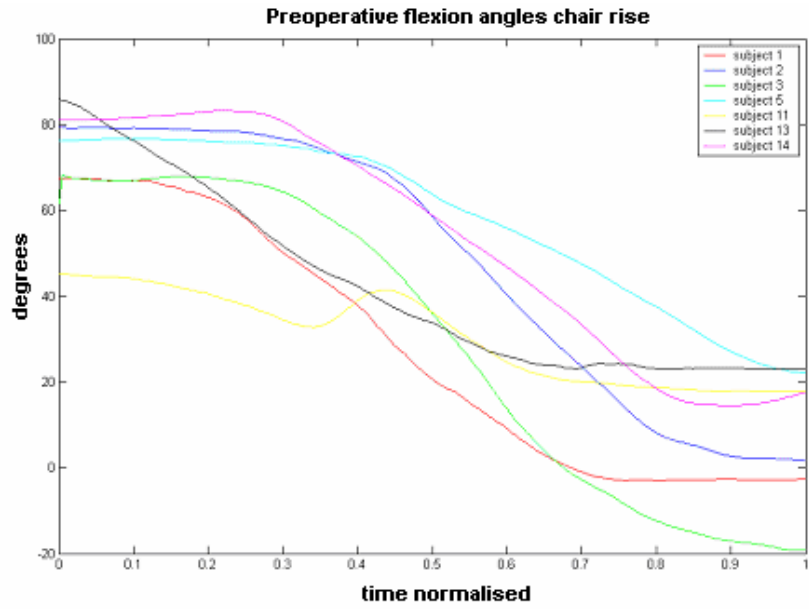
Figure 4.56 Preoperative flexion angles when rising from a chair
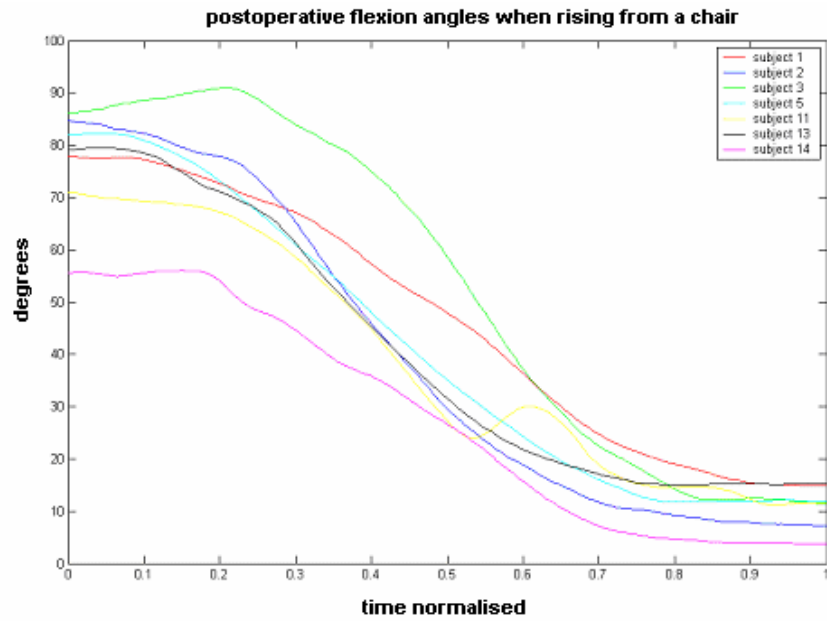
Figure 4.57 Postoperative flexion angles when rising from a chair

The minimum and maximum flexion angles both pre and postoperatively show a wider variation in the present study with respect to the results presented by Myles et al (2002). Only the postoperative maximum flexion angle range can be described as falling within the normal distribution reported by Myles et al. This is the only discrepancy between the two studies in all the data presented. In the study by Myles et al, the preoperative range of motion is higher than the range of motion 4 months postoperatively. The range of motion returns to the preoperative values by 18 – 24 months. In the current study, the range of motion when rising from a chair is unchanged postoperatively compared to their preoperative values. This is in agreement with the results presented by Myles et al. The difference in values of the range of motion may be attributed to the methods utilised by the subjects for rising from a chair.

Saari et al (2004) reported on flexion angles when rising from a chair for subjects with either a cruciate retaining flat tibial plateau, cruciate retaining concave tibial plateau, cruciate sacrificing flat tibial plateau, cruciate sacrificing concave tibial plateau, and a control group. They reported no significant differences between the 5 groups, with maximum flexion ranging from 81° to 100°, and a hyperextension of between 13° and 26°.

No effort was made in the present study to control for foot placement, as it was decided that all data would be collected with the subjects acting as naturally as possible. Su et al (1998) analysed the different stages of rising from a chair. They concluded that the rising mechanism utilised after TKR is not the same as normal age matched subjects, but is better than subjects that had a mild OA, but who do not need surgical intervention.

4.2.3 Varus Valgus and Internal External Rotations

There was no discernable pattern in the change of motion in the frontal or transverse planes. Furthermore, there was no relation in the changes of rotation in the frontal plane with respect to the transverse plane.

There was a slight increase in the range of motion in the frontal plane during level walking (figure 4.58). There was a reduction from 16.2° to 10.7° in the range of motion in the frontal plane in ascending stairs (figure 4.59), and from 22.1° to 6.7° in the frontal plane when descending the staircase (figure 4.60). There was also a slight reduction in the range when rising form a chair, with the exception of subject 3 (figure 4.61).

Frontal Plane level Walking Range of Motion
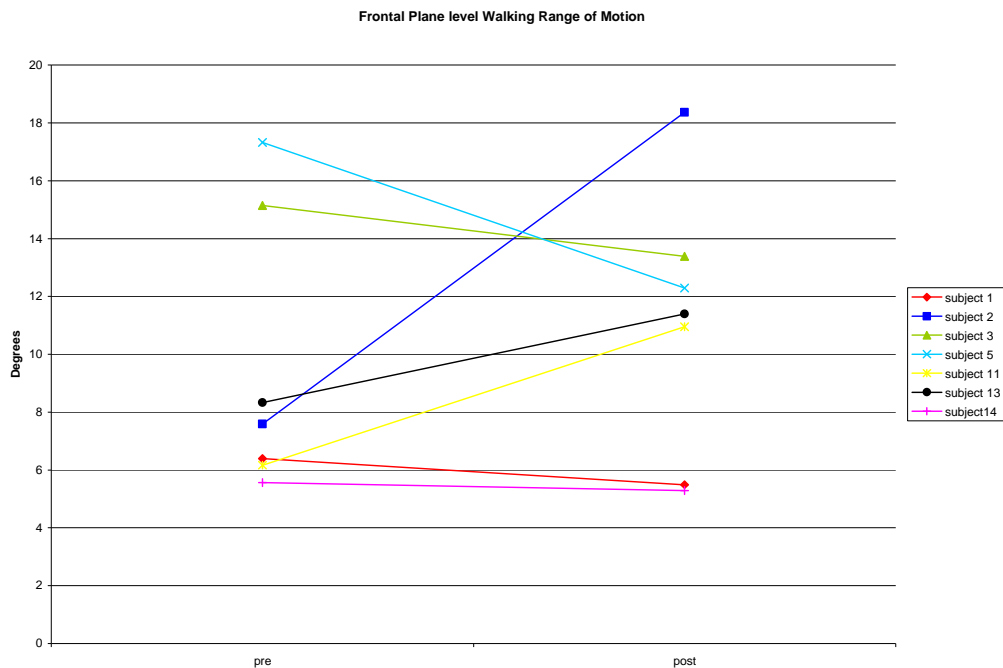
Figure 4.58 Frontal plane range of motion during level walking
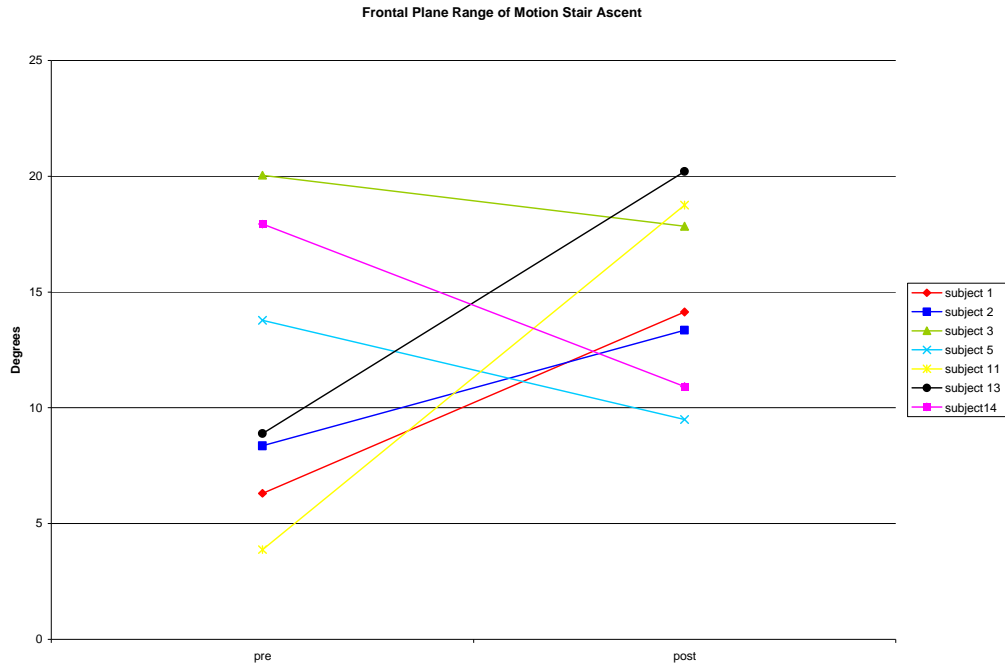
Figure 4.59 Frontal plane range of motion during stair ascent
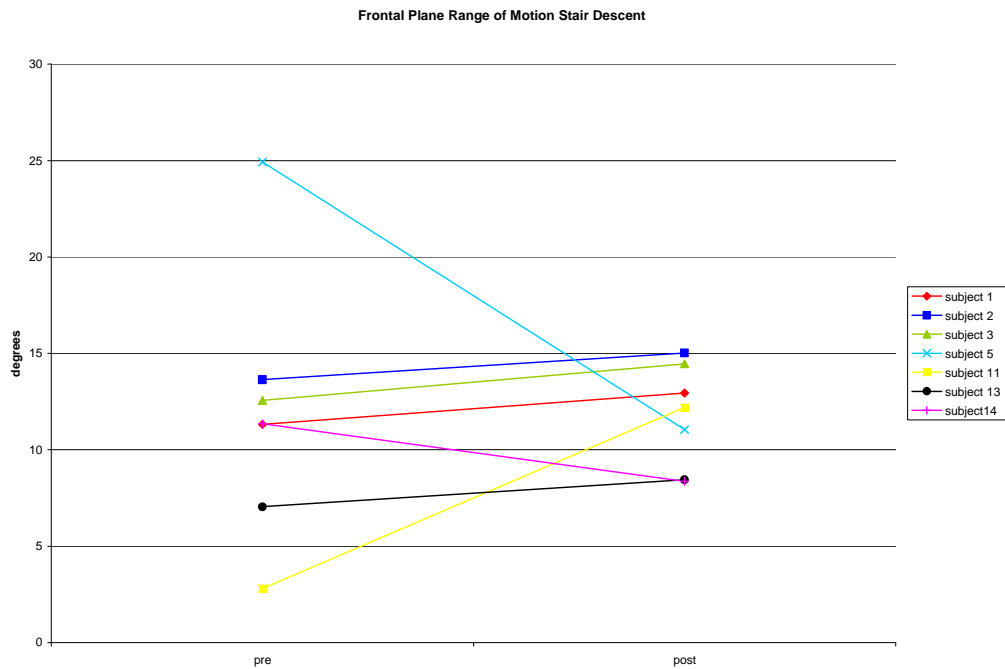
Figure 4.60 Frontal plane range of motion during stair descent
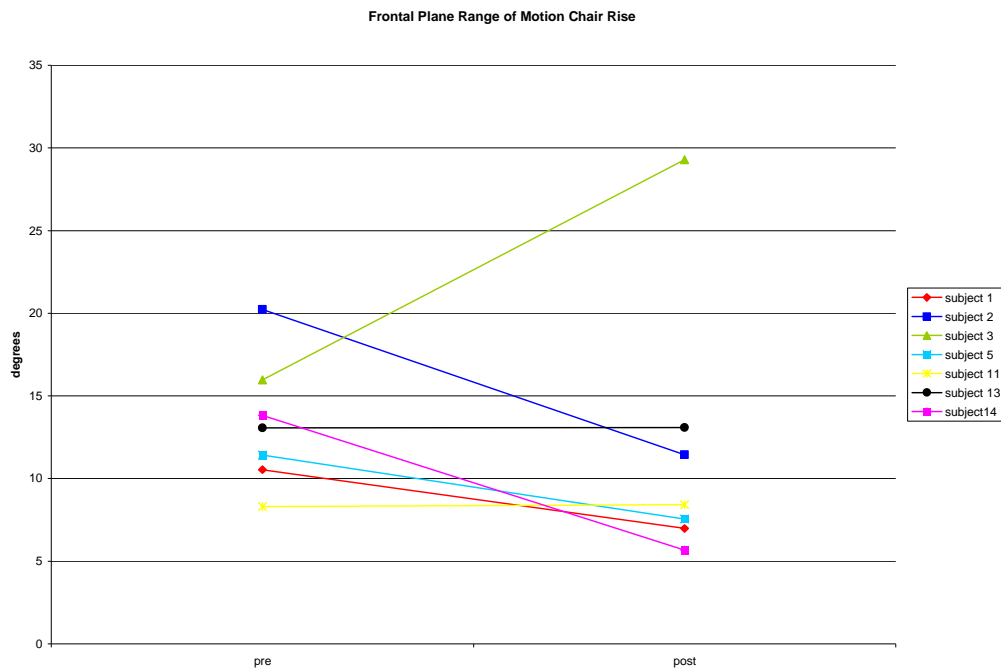
Figure 4.61 Frontal plane range of motion during chair rise

As with the frontal plane, in the transverse plane there was an increase in the range of rotation for the group in the transverse plane when walking on a level surface (figure 4.62). When ascending a staircase the range reduced from 11.2° preoperatively to 6.4° postoperatively (figure 4.63). When descending the staircase the range reduced from 19.5° preoperatively to 14.5 ° postoperatively (figure 4.64). There was a general reduction in the range of motion when rising from a chair in the transverse plane, with the exception of subject 11 (figure 4.65).

Transverse Plane Range of Motion Level Walking
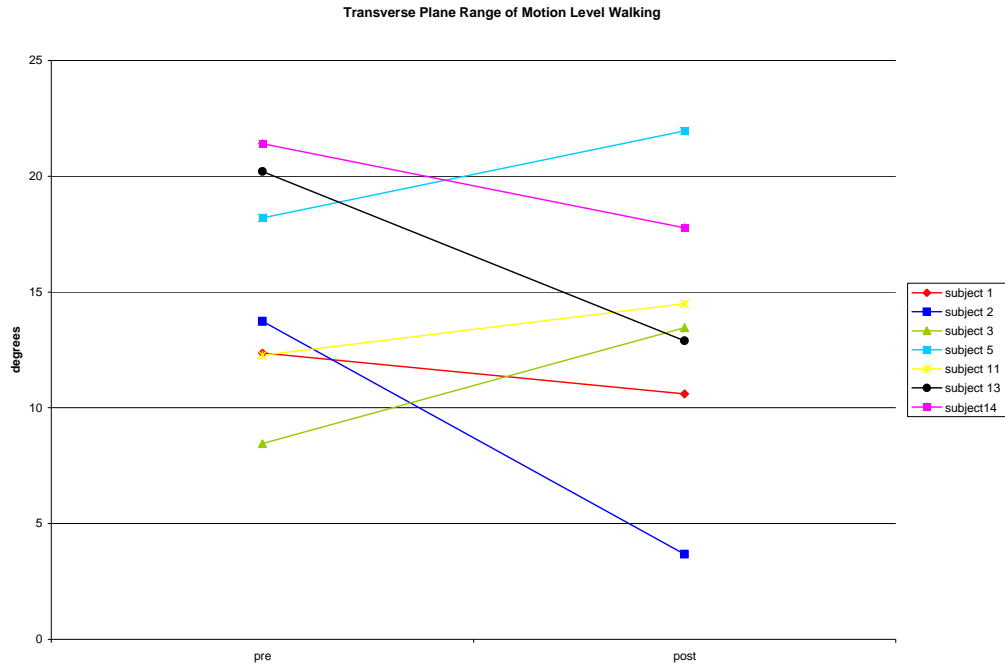
Figure 4.62 Transverse plane range of motion during level walking

Transverse Plane Range of Motion Stair Ascent
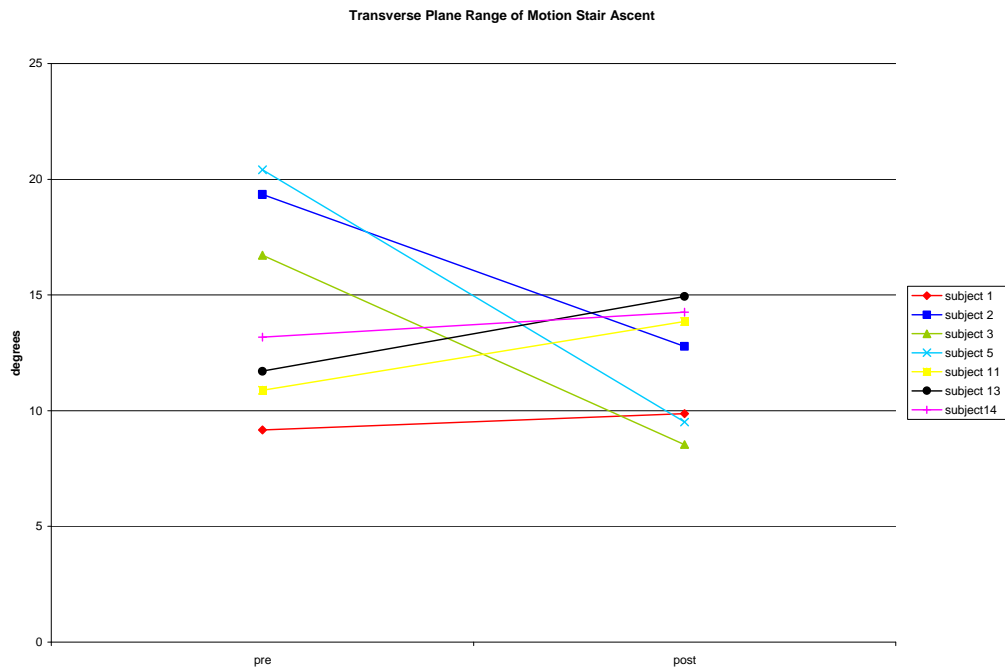
Figure 4.63 Transverse plane range of motion during stair ascent

Transverse Plane Range of Motion Stair Descent
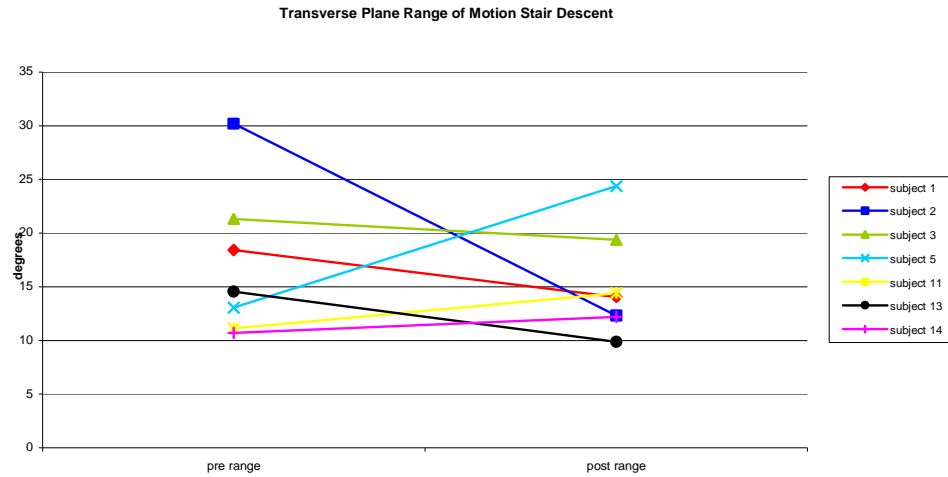
Figure 4.64 Transverse plane range of motion during stair descent

Transverse Plane Range of Motion chair Rise
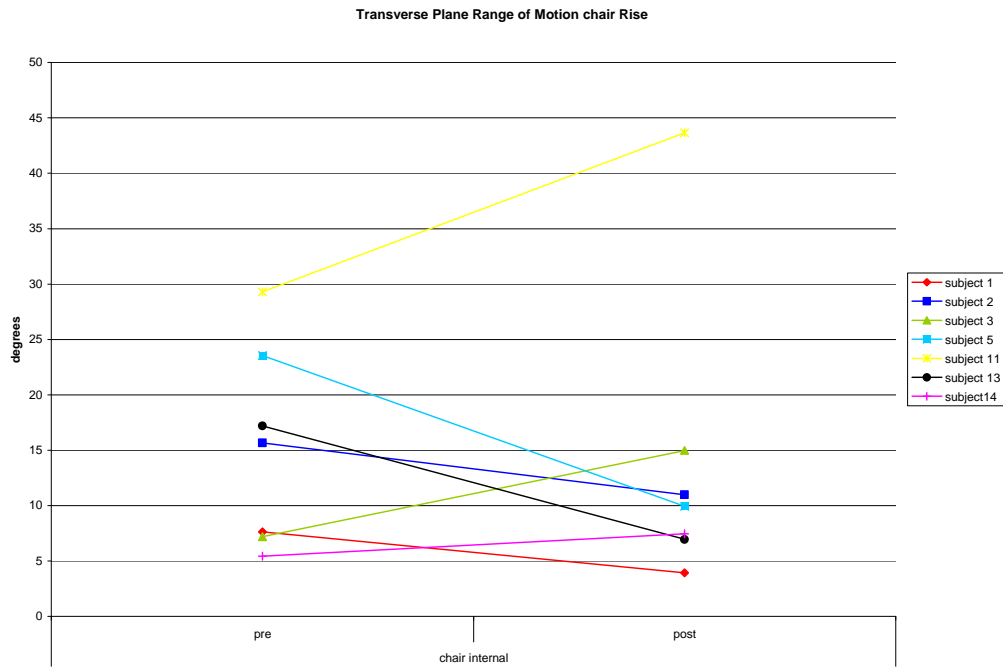
Figure 4.65 Transverse plane range of motion during chair rise

There is limited data in the literature on the rotations of the knee in the frontal or transverse planes, and the data that does exist is varied due to test conditions, such as age, disease, weight bearing, active or passive movement, and cadaveric studies. The main reason for limited amount of reliable data is because the smaller rotations seen in these planes are more susceptible to measurement errors than those measured in the sagittal plane, and errors can occur due to kinematic cross talk (Piazza and Cavanagh 2000). Nadeau et al (2003) reported a magnitude of movement of less than 10° in the frontal plane when level walking, valgus 5.8°(6.8°SD) to varus 4.6° (4.1°SD), and 15° negotiating a staircase, valgus 5° (7°SD) to varus 10.4° (7.1°SD) in healthy adults. Patel et al (2004) reported a valgus rotation of 10°-14° when the knee was flexed from 0°-65°. Mandeville et al (2008) reported that, during level walking, the knee is in valgus of between 2° and 7° for healthy subjects, whereas preoperative knee replacement subjects have a rotation in the A-P plane of between 3° valgus and 2° varus. Postoperatively, the subjects in the Mandeville study were in valgus of between 4° and 8° during level walking. A similar result is seen in ascending a staircase, with control subjects having a valgus angle of between 7° and 2°, preoperative subjects being between 1° valgus and 4° varus, and postoperatively being between 7° and 11° valgus.

 In supine weight bearing, Patel et al (2004) reported an internal rotation of 6° at 20° of flexion over a 45° motion. The average values seen both pre and postoperatively for the magnitude of movement in the frontal plane is slightly higher than 10° in all test situations. Some individual subjects have rotational differences up to 20°. The reason for this may be that the Nadeau study considered the rotations in healthy subjects over 40 years old with no pathological knee problems. Even though there are improvements seen in most cases in the current study postoperatively, the subjects may still suffer from changes in muscular structure and function associated with OA.

Johal et al (2005) studied the lateral motion of the epicondyles in young healthy knees. They reported that the lateral condyle translates more than the medial, resulting in an internal rotation of the tibia of approximately 20° between 0° and 120° of flexion. However, they also point out that this is in contract to a previous study by Ando (1994) that found the tibia to rotate externally. Zurcher et al (2008) also reported contradictory results for rotation around the S-I plane. They reported that, when rising from a chair, healthy subjects showed a rotation of between 11.8° internally and 1.7° externally resulting in a range of motion of 13.5°. However, when the same subjects were rising from a chair into a turn, the knee rotated 14.8° internally to 6.7° externally, a range of motion of 20.9°. They noted that previous reports by Ranawat et al (2004) reported a difference in internal rotation between fixed platform (4.1°) and mobile bearing (7.3°) knee implants, whereas Denis et al reported no difference, with both groups having a range of 5.5° internal to 2.1° external rotation. Komistek et al (2003) used fluoroscopy and volume data from CT scans to assess the normal human knee. They reported that during deep flexion activities the lateral condyle experiences significantly more anteroposterior translation leading to axial rotation of the tibia relative to the femur, being greater than 13° in deep flexion compared to less than 5° in level walking. The same group (Ranawat et al 2004) also used fluoroscopy to compare kinematics for mobile and fixed bearing posterior stabilised knees. 19/20 subjects in both groups experienced posterior femoral roll back of the lateral condyles. 9 of the 20 subjects with a mobile bearing prosthesis and 12 of the 20 with a fixed bearing prosthesis had condylar lift off. Results from tests conducted on a young healthy subject within the current study showed that, when manipulated, a healthy knee can rotate in the frontal and transverse planes by up to 50°. It is feasible therefore that subjects with OA of the knee may have rotations considerably larger than the 10° presented by Nadaeu et al.

Seisler and Sheehan (2007) developed a normative database for knee kinematics. The group used fast-PC MRI to investigate patellofemoral and tibiofemoral kinematics. In this study, subjects lay supine in the MRI scanner and were asked to flex and extend their knee at 35bpm. Although MRI images were only taken in one plane, the 3D reconstruction of these images allowed for collection of rotational data in the S-I and A-P axes with respect to flexion angle. The method utilised is seen as a gold standard as it has been shown to be precise to $1.2°$ in flexion/extension, $1.5°$ in internal/external rotation, and $0.7°$ in varus/valgus rotation.

Graphs 4.66 and 4.67 show internal rotation with respect to flexion in the current study, compared to the Seisler and Sheehan database in pre and postoperative conditions. It can be seen that most, but not all, of the data in the present study falls within 2SD of the gold standard database. As flexion approaches $44°$, the SD of the database narrows. This is because only 2 of the 34 knees in the Seisler and Sheehan study could flex to this angle. Flexion was constrained by a combination of leg length and scanner dimensions. Also, the data collected for the database was done in a non weight-baring condition, using healthy subjects. In the current study, all subjects are over 50 years old, and are either suffering from OA in the preoperative tests, or have underwent TKR in the postoperative tests. Nonetheless, it is encouraging that the majority of results in the current study fall within the normal range of the database. Graphs 4.66 and 4.67 are representative of all testing conditions, which are included in appendix VI.
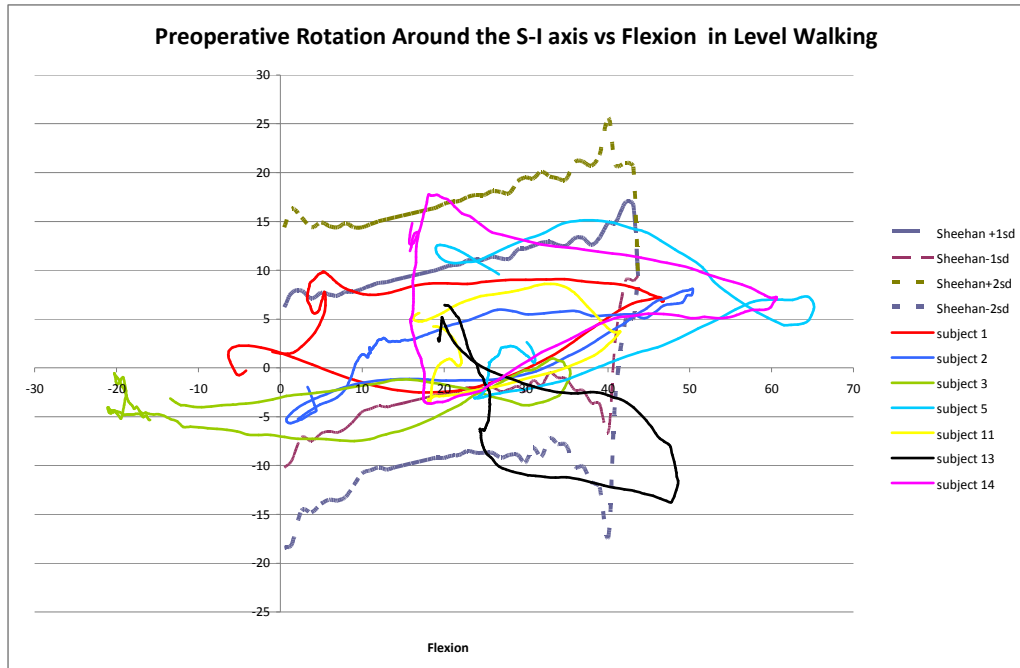
Figure 4.66 Preoperative internal rotation against flexion
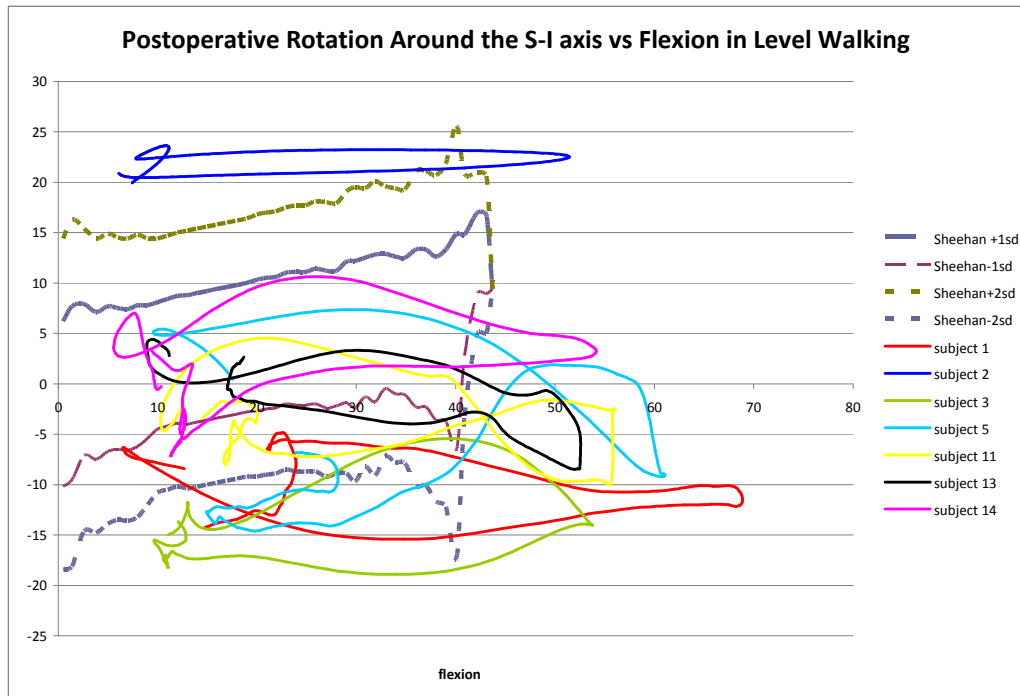
figure 4.67 Postoperative internal rotation against flexion

4.2.4 Tibiofemoral Translations

The 3 dimensions of translation, medio-lateral shift, distal-proximal lift, and femoral roll back, were analysed. Translations have been reported by Iwaki et al (2000) as being predominantly as a result of rotations of the knee, and not pure translations. However, as previous studies have not made any allowance of the rotational affect on translations, the data was presented as pure translation for comparison reasons. Of the 84 possible results in the current study, (seven subjects by four trials by three degrees of freedom), 44% showed translations greater than 20mm preoperatively, with 36% of translations greater than 25mm. Postoperatively, this reduced to 25% and 16% respectively. Figure 4.68 shows the change in femoral roll back during level walking. The preoperative range is vastly reduced postoperatively. This general improvement is seen during stair ascent (figure 4.69), stair descent (figure 4.70), and chair rise (figure 4.71). Six of the seven subjects showed a reduced level of femoral roll back during level walking. The remaining subject had an increased femoral roll back, which postoperatively was within the range for the group.

Femoral Roll Back Walking
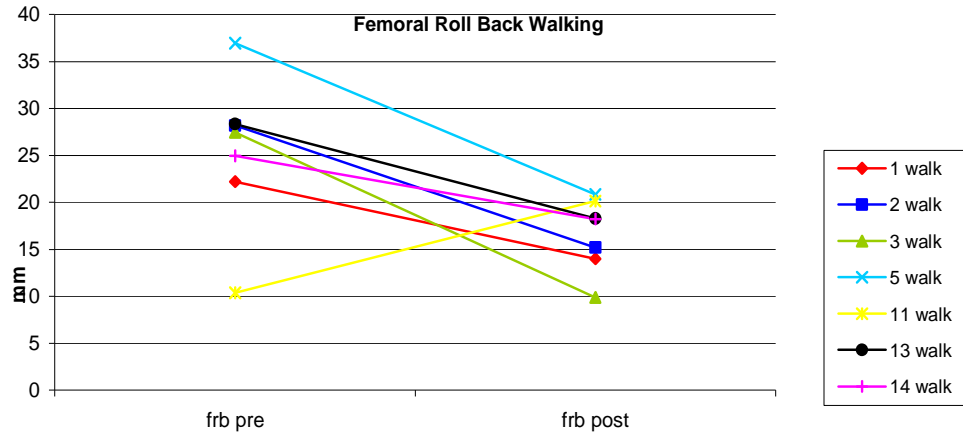
Figure 4.68 Femoral roll back when walking

Femoral Roll Back Stair Ascent
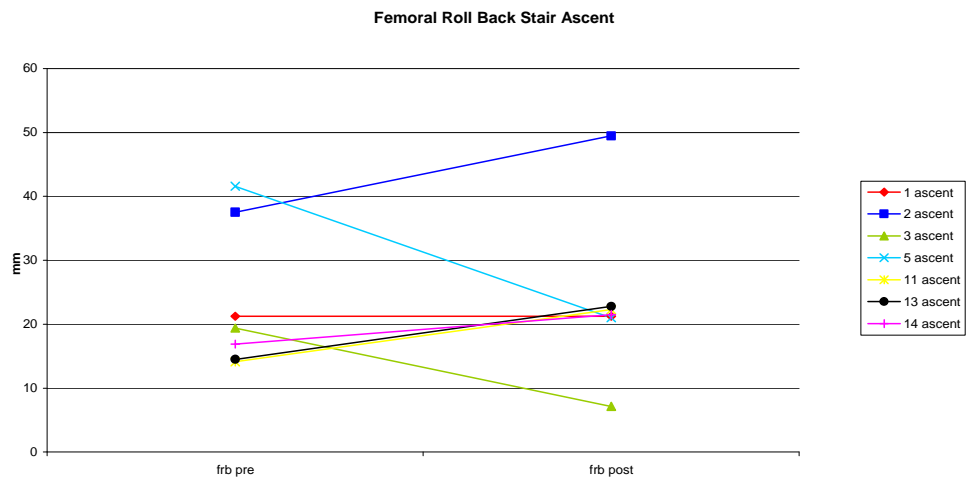
Figure 4.69 Femoral roll back when ascending stairs

femoral Roll Back Stair Descent
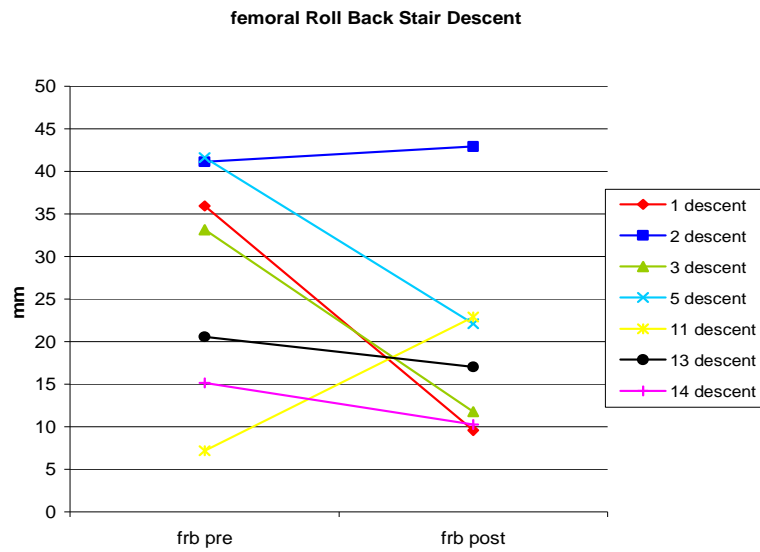
Figure 4.70 Femoral roll back when descending stairs

Femoral Roll Back Chair Rise
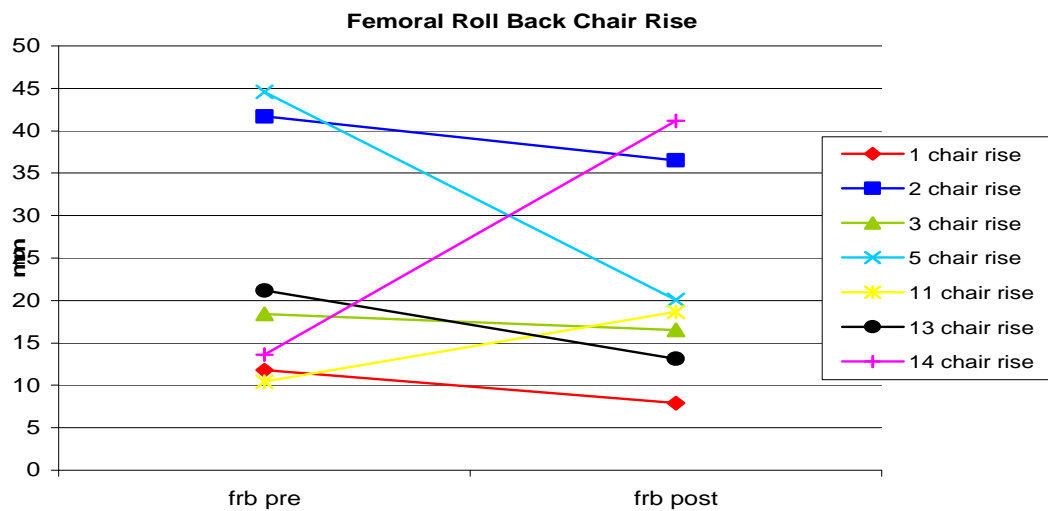
Figure 4.71 Femoral roll back when rising from a chair

There was no pattern in the changes or magnitude of distal-proximal lift. This is demonstrated in figure 4.72, which shows distal-proximal lift during rising from a chair. This is typical for the rest of the trials.

Distal-Proximal Lift chair Rise
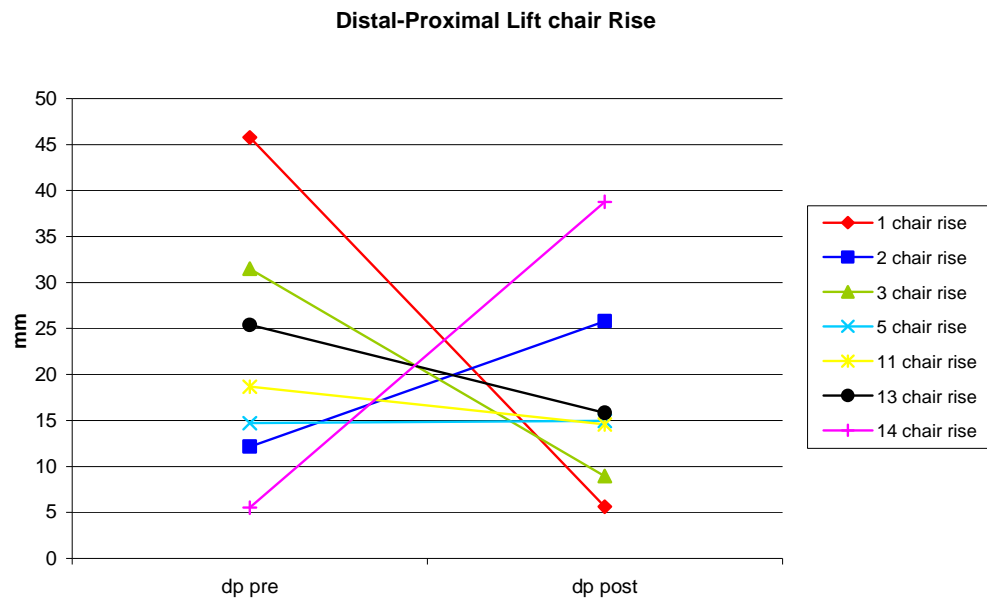
Figure 4.72 Distal-proximal lift during rising from a chair

Imaging studies by Patel et al (2004) and von Eisenhart-Rothe et al (2004) have investigated the translations of the knee. More recently, Johal et al (2005) have studied tibiofemoral movement of the healthy knee in vivo. These studies have been conducted on young healthy volunteers in, at best, quasi-static weight bearing. Nonetheless, the results presented here are

favourable with respect to the imaging studies. The study by Johal et al utilised developments in MRI technology that allows images to be taken in an open scanner in a static weight bearing position. In healthy subjects of mean age 25 years, movement from 5° of hyperextension to 120° of flexion resulted in an anteroposterior translation of the lateral condyle of 21.1+/-4.7mm of the femur relative to the tibia. Further movement to 140° causes an additional translation of 9.8 +/-2.1mm. In movement from hyperextension to 30° flexion, the medial condyle translates anteriorly by 1.7 +/-1.3mm, 2.2 +/-1.5mm to 90° flexion, and posteriorly by 3.6+/-2mm in further flexion to 120° (Johal et al 2005). The results of this include femoral roll back, distal proximal lift, and internal tibial rotation to 20°. In tibial internal rotation the knee behaves as in neutral. Other studies such as Wretenberg et al (2002) agree with the Johal study in that the lateral condyle translates more than the medial. However, Ando et al (1994) states that the medial side translates more than the lateral side. As all these studies used healthy subjects, it is feasible that the diseased knee as seen in the present study could have varying degrees of translations and internal rotations as their disease dictates. The largest tibial rotations are seen over the early stage of the flexion range, and so are comparable to the data in the present study.

Seisler and Sheehan (2007) created a database of translations of the tibiofemoral joint. Again, the data collected here was with young healthy subjects in non weight bearing conditions. The range of motion reported was 35.4mm in A-P, 10.8 in L-M, and 15.8 in S-I. When the data is viewed with +/-2SD, the range increases to 50.5mm, 23.7mm and 22.9mm respectively. The majority of ranges from the current study fall within 2SD of the ranges of the gold standard developed by Seisler and Sheehan. However, 32 of the 112 minimum and maximum values of translations in the M-L plane in the current study are out with the values of the gold standard (figure 4.72), and this is representative of the other 2 planes. The differences in values could

be due to one of 2 reasons: firstly, as the absolute differences between the minimum and maximum values in the current study are comparable to those of the Seisler and Sheehan study, the difference in actual values could be due to the methods of identifying the centres of the femur and tibia in the two studies. The differences could however be due to inherent errors in the methods of data collection in the current study, which will be discussed later.
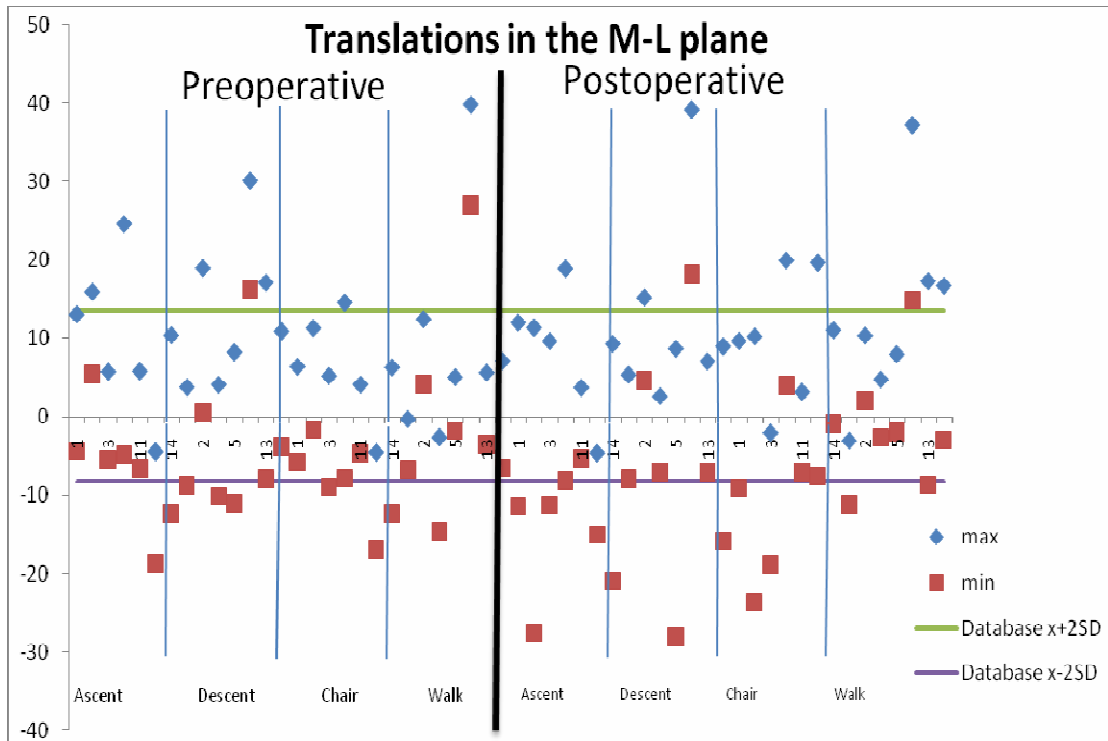
Figure 4.72 Minimum and maximum translations in the M-L plane

4.3 Animations

Animations were made for each subject for level walking, ascending and descending a staircase, and rising from a chair, in both pre and postoperative conditions. 52 animations are available for viewing in the appendix CD. 4 animations (subject 5 preoperative) are not included due to technical difficulties with the scan. For subject 5 the 3D reconstruction is included. The animations are not yet of clinical usefulness, and are prone to a number of errors. However, they do show promise for the future and with proper constraints in future studies could yield clinical usefulness.

Preoperatively, when level walking subject 1 shows wear on the lateral side of the tibia. The wear on the tibia is more profound during stair ascent and more so during stair descent. Conversely, when rising from a chair the contact and wear on the tibia is on the medial side. Subject 1 was the youngest of the subjects tested, and was fitted with a cruciate sacrificing fixed bearing implant. There appears to be no noticeable wear patterns on the tibial component postoperatively.

During walking and stair ascent preoperatively, subject 2 displays femur contact on the tibia causing wear on the lateral side. When descending a staircase, the knee appears to buckle, causing an increase in wear on the lateral side, with added wear anteriorly. When rising from a chair, as with subject 1, the contact appears to be on the medial side, resulting in medial tibial wear.

Subject 2 was the only subject in the present study to be fitted with a cruciate retaining femoral component, with a fixed bearing tibial component. There is

wear of the tibial component on the anterior of the medial side, and a slight gap appearing between the tibial implant and the bone on the lateral side. It can be seen in the animation rising from a chair that most of the contact is on the medial side. When examining the 3D reconstruction of the tibia, a gap can be seen between the bone and the implant on the lateral side. On the medial side the implant appears to be compressed into the bone, and the tibia can be seen to be above the line of the base of the implant.

Subject 3 has a large amount of bone deformation, with wear on the anteriolateral side due to the large hyperextension and on the medial side during flexion. The preoperative animations for subject 3 are the most affected by error, as the bones pass through each other during deeper flexion. Subject 3 was fitted with a cruciate sacrificing fixed bearing implant. In all 4 situations the hyperextension is seen to be removed, however the abnormal contact on the posteriolateral side is already causing wear to the tibial implant.

The preoperative animations from subject 5 are incorrect due to a technical fault. The static image from the preoperative scan produced an unexplained mirror image of the joint. While the wear patterns on the tibia can be clearly seen in the 3D image, they cannot be used for animation purposes.

Subject 5 was fitted with a cruciate sacrificing fixed bearing implant. There does not appear to be any wear caused by abnormal loading in any of the 4 situations studied. The tibial component appears to be shifting medially relative to the bone. There is a gap appearing between the bone and implant on the medial side and the tibial implant is hanging over the edge of the tibia, leaving a flat cut of the tibia on the lateral side not in contact with the tibia.

Preoperatively, subject 11 is grinding a pit in the medial side of the tibia with the medial femoral condyle during all walking tasks, and again this is more profound when descending a staircase. When rising from a chair, there is a momentary shift in contact to the lateral side that is causing wear from the centre of the lateral tibial plateau to the lateral edge of the tibia. Subject 11 was fitted with a cruciate sacrificing rotating platform implant. While there is no evidence of polythene wear on the tibial component, the component itself appears to have moved relative to the tibia. On the posterior it can be seen that there is a gap forming between the bone and implant, producing a "V" shaped area of no contact. The tibial implant is also sloping forward. As there is no wear marks on the implant to suggest abnormal loading, it is possible that in this subject the tibia itself is weak and is remoulding over time.

Preoperatively, subject 13 appears to load on the lateral side posteriorly during walking tasks. When sitting, the contact begins on the lateral side, and rocks onto the medial side, causing wear on the aneriolateral aspect. The animations for the tasks performed by subject 13 preoperatively are not correct as the posteriomedial side of the femur passes through the tibia. Subject 13 was fitted with a cruciate sacrificing rotating platform implant. There does not appear to be any wear of the implant or any shift in the implant from abnormal loading. The rotation of the joint during rising from a chair appears to be under poor control.

The preoperative animations for subject 14 show that the deeper flexion activities of stair ascent descent and rising from a chair all cause the medial femoral condyle to rub on the tibia, causing the bone to wear down. Subject 14 was fitted with a cruciate sacrificing rotating platform implant. The motion of the knee joint is still predominantly of medial loading.

By only assessing the kinematic results of TKR patients, it is easy to miss the effects that any malrotations have on the integrity of the implant. The animated 3D images give more meaning to the numbers produced in the gait lab, allowing the surgeon a better sense of what is happening in vivo. If future imaging techniques allow for the successful imaging of the polythene tray the potential of this technique could be realised. The kinematic data alone suggest that the postoperative results for the subjects are successful, however when the 3D reconstructions are viewed, problems that will ultimately lead to implant failure and revision surgery can be seen to be in the early stages. Without the 3D reconstruction of the knee and the animated motions, the issues will not be noticed until later in the life of the implant. If the reasons for the abnormal motions seen in the postoperative animations can be addressed the life and quality of the implant can be vastly improved, thus reducing the need for revision surgery.

Chapter 5. Discussion

Subject Recruitment

Subjects were recruited from the waiting list for TKR from Glasgow Royal Infirmary. 14 subjects were identified as being suitable for the study and were tested preoperatively. Five subjects had their operations rescheduled to a timescale out with the scope of this project due to the development of other health conditions. Two subjects decided to withdraw from the study due to feeling psychologically uncomfortable during the testing session. Two subjects were placed on the waiting list for revision surgery following complications after their original surgery. These are common problems in recruitment for patient groups, and as a result very few studies in knee replacement have a large patient group. The results herein are expected to be representative of the most successful operations, as no results of failures are included.

Error Analysis

Motion Analysis

The hardware in the Vicon motion analysis system was subject to a specific calibration procedure prior to each testing session. As part of the system requirements, the calibration of the system was accepted if the overall calibration was less than 1mm. In the current study each calibration was less than 0.75mm. The overall error in the hardware system is small, and continues to reduce as improvements are made to hardware systems. For example, in the current study the Vicon 612 system consisted in part of analogue cameras. Newer versions of the system include the Mx3 digital cameras, and system calibrations of under 0.1mm can be achieved. As only

one investigator was involved in the collection and processing of motion analysis data, there are no inter experimenter errors.

The CAST marker system of using marker clusters was utilised in this project (Cappozzo et al 1995). A cluster of markers can change shape by their position relative to each other, introducing errors into the estimation of underlying bone position (Lu and O'Connor 1999). Markers for the clusters were placed onto a rigid plastic backing attached to the limb segment via a neoprene strap. By placing the markers onto a plastic plate relative movement between markers in the clusters were removed. Any flicker of the markers should therefore be contained within the overall system error of 0.75mm. The neoprene strap serves two functions: firstly it provides a compression to the underlying soft tissue, helping to reduce motion of the cluster relative to the bone due to movement of skin and subcutaneous fat. Secondly, the nature of the material on the back of the neoprene strap prevents the strap and therefore the cluster from slipping during the motion tasks.

Skin Motion Artefact (SMA)

SMA is recognised as being the major source of error in motion analysis, with numerous studies attempting to quantify the errors involved (Peters et al 2010). The Bodybuilder model in this study was written for motion analysis in order to minimise the effects of SMA.

Stagni et al (2005) quantified soft tissue artefact by placing skin markers at various locations on the leg. Although the study was only conducted on two subjects, the results suggest that the best areas for marker placement in order to limit the skin motion artefact are on the anteriolateral aspect of the bottom third of the length of the thigh, and on the anterior of the bottom third of the shank. The positioning of the clusters in the current study agree with the results as described by Stagni et al.

In the current study an attempt was made at a double calibration technique similar to that subsequently demonstrated by Cappello et al (2005). The double calibration method was effective in the flexion extension axis, but errors were not quantifiable in the other two planes of motion or in any of the three directions of translation, possibly due to a combination of unquantifiable skin motion errors and abnormal motion of the knee joint due to the nature of the disease. On analysis of the double calibration, a marker placed directly over the lateral epicondyle of the femur resulted in artefact errors of approximately 40mm in 120° of flexion. When the epicondyles of the femur were marked in standing (0° flexion) and sitting (90° flexion), the calculated error was 5° for a single calibration method at the extreme ends of the range of motion. In the testing sessions, the anatomical landmarks were identified in a static standing position, and therefore the errors in the flexion extension axis are estimated to be 0° at 0° flexion, rising in a roughly linear manner to 5° at 90° flexion.

Errors in the S-I and A-P planes are harder to quantify. Cappozzo et al (1996) reported that errors in these planes due to skin motion can be at least an order of magnitude higher than errors due to stereophotogrammetry. Stagni et al (2005) also suggest that errors in gait analysis in the S-I and A-P planes are of a magnitude higher than that of the measured values, rendering the data collected in these two planes of no clinical use. During single calibration, rms errors in varus/valgus and internal/external rotation have been shown to be 3.7° (Cappello et al 2005).

Hip Joint Centre Location

The estimation of the hip joint centre is often a cause for concern in lower limb motion analysis. Estimation of the hip joint centre by the location of the greater trochanter can lead to errors due to the identification of the plane of the leg (Della Crosse et al 2005). Errors also occur due to the relatively large surface area of the greater trochanter compared to the size of the skin

marker. Gamage and Lasenby (2002) described a least squares algorithm to calculate the centre of rotation of a ball and socket joint, such as the hip joint. A similar method is utilised in computer aided TKR to identify the hip joint centre. The hip joint is rotated in a circular fashion, starting with small movements and gradually increasing the radius of the circle. During surgery this is relatively simple to do, as the patient is under anaesthetic and the surgeon controls the motion passively. However, replicating this in the motion analysis laboratory is more difficult as it relies on the subject to be physically able to replicate the movements (Stagni et al 2000). In the current study this method was impossible for the subjects to perform due to their age and state of disease. The hip joint centre was therefore estimated by the location of bony landmarks on the pelvis. The pelvis frame was defined by palpitation of the ASIS and PSIS, and the hip joint centre was calculated as a function of the distance between the left and right ASIS (Bell et al 1990). This method also has potential for error. The joint centre in the Bell et al method is calculated from MRI scans of cadavers, meaning the calculation is not based on the individual data. Also, placing the markers directly onto the bony landmarks can cause visibility problems in the obese patient. Using a belt strap and a rigid marker cluster resolves this issue, but introduces potential error in the movement of the belt strap during motion. Relative motion of the strap is not an issue on the thigh or shank, but is on the pelvis as the motion of the pelvis and abdominal fat and muscles can cause a large movement of the belt strap. Data in the current study processed when the belt strap was used during dynamic trials resulted in a change in measured length of the femur by as much as 15%. Changing the length of a bone in the measurements can have adverse effects in the resultant kinematic calculations. In the current study, a belt strap was used with a cluster of markers attached. Once the pelvis frame was identified and the hip joint centre was calculated in a static position, the hip joint centre was then reprocessed to be located in the thigh cluster reference frame. The belt strap was then removed for the capture of data in dynamic trials, as it was unnecessary for the motion analysis.

The Bell (1990) method of calculating the hip joint centre from anatomical landmarks based on anthropometric data has been shown to be as accurate as the functional method in patients with a limited range of motion (Stagni et al 2000) and has been extensively utilised in motion analysis. Stagni et al showed that an error of hip joint centre location, while critical to HJC kinematics and kinetics, has a limited effect on errors of knee kinematics. Errors of up to $1.5°$ can be expected in knee flexion of $68°$, internal/external rotations of $14°$ and varus/valgus rotations of $7.5°$. The majority of post operative trials in the current study are within or close to the range of motion described by Stagni, and the errors of calculated knee kinematics associated with HJC mislocation are therefore estimated at between $1.5°$ and $2.5°$ in all 3 planes.

Rotational Axis

The centre of rotation of the knee joint is calculated by the location of the anatomical landmarks on the femur. The first source of error in this method is in the identification and location of the landmarks. In an estimated marker placement error of 10mm, the marker can be placed 5mm in error in any direction. For an estimated knee width of 110mm and an error of 5mm placement in opposite directions either side, the calculated error of the axis would therefore be $5.2°$. The second error is the assumption that the centre of rotation of the knee joint is a midpoint between the epicondyles. Holzreiter (1991) demonstrated a method to calculate the instantaneous centre of rotation in a joint. In this method, a cluster of points similar to that used on the thigh and shank in the current study were used as reference points to calculate the centre of rotation at any given timeframe. A program was written in Matlab in the current study to calculate ICR in the knee joint. Initial tests on two planks of wood joined by a metal hinge showed a variation in the calculated centre of rotation of 1.5mm. When applied to the knee joint kinematic data the ICR varied by a maximum of 2.5mm. The total error in

estimated centre of location as a sum of marker placement and ICR variation is therefore within 8mm, with a resultant rotational error within 8.3°

Repeatability of Marker Placement

On each visit a calibration procedure was conducted to determine the relationship between the anatomical landmarks and segment tracking clusters. It is possible that by altering the placement of the anatomical landmarks, the rotations of the knee may be misrepresented. This may result in a change in reporting of absolute angles, while having a small effect on range of motion, making it difficult to distinguish between changes due to measurement errors and changes due to surgical procedure. An example of this in the current study can be seen when viewing the flexion angle during level walking in subject 3. The flexion curve postoperatively is similar in shape to the preoperative curve, with an approximate increase of 25°. It is unclear from the graphical representation how much of this change is due to a surgical correction of hyperextension and how much is due to calibration error. Any error of placement of anatomical landmark markers due to mis-palpation are expected to be within the parameters described as above. It is therefore expected that differences in placement of markers pre and post surgery could account for up to 8° of error in rota tions.

Imaging Techniques

Collection of the images was conducted by staff at the GRI hospital at the end of clinical appointment lists. The first source of error in the scanning technique derives from the slice thickness of the images taken. The equipment and setup available meant that the scans were not set to the same slice thickness or pixel size, but were both set to the same resolution. Images were therefore collected at a best available size of 2mm slices and a pixel size of 0.3516 in MRI and of 1mm and pixel size of 0.3867 in CT. The

slice thickness is of most importance at the interface of the two bones at the knee joint for visualisation in animation.

As medical imaging techniques have improved, medical imaging has been put at the forefront of orthopaedic surgery and research of the knee (Victor et al 2009). Wretenberg et al (2002) imaged in MRI in supine non-weight bearing conditions, manipulating the angle of the knee to investigate contact areas. More recently Johal et al (2005) used a 0.5T open MRI scanner to image the knee in a quasi-static weight bearing condition, and Sheehan et al (2009) recorded a cyclical motion while supine in a 1.5T dynamic MRI. Just as radiographic studies progressed from supine non-weight bearing to standing weight bearing studies as the development of radiographic equipment progressed, studies in MRI developed from the supine non-weight bearing as used in the present study to quasi-static and cyclic motion studies more recently, and to fluoroscopic analysis in real time 3D. The accuracy of the images will improve as further advances in medical imaging are made and the slice thickness decreases without increasing overall scan time. Since the conception of the present study, there have also been major developments in the use of fluoroscopy as an analytical tool in TKR. Dennis et al (2001) used fluoroscopy combined with CT to analyze the motion of the knee joint in 3D. They created volumetric 3D data from medical imaging, and overlaid the models onto the 2D fluoroscopic image. The group showed that 3D images could be combined with fluoroscopy to accurately describe motions at the knee joint, and did so successfully in healthy knees, UKR and TKR. In 2003 Fantozzi et al used a similar method to Dennis et al to compare two types of knee implants, additionally using gait analysis for control group comparison. The combination of imaging and kinematic analysis for individual subjects is the ultimate aim of both this and numerous other studies.

3D Reconstruction

The creation of the 3D images was done using MIMICS software. Although this software has numerous automated surface recognition tools, the best results were yielded when the author manually traced the outline of the bone in each slice of each scan. In the assessment of this method a scan of a healthy knee was used and was easy to surface. However the osteoarthritic knees under study in the present project were problematic due to the nature of the disease, making it difficult to differentiate between bone and cartilage. It is estimated that the error involved in the identification of the true edges of the bone segments would be under 5mm, and would have minimal impact on the effectiveness of the produced animations.

3D Animation.

When the 3D images are viewed without the kinematic data being applied, some of the subjects appear to have a gap between femur and tibia. The most likely reason for this is that when surfacing the DICOM images any cartilage that remained in the joint was not included. As the subjects were supine during the scan, there may also be a degree of joint laxity. As technology improves, and open scanners such as those used by Johal et al (2005) and fast cine phase MRI as used by Sheehan et al (2009) become more readily available, the ability to take scans in weight bearing will become commonplace.

Registration of Points from Gait Analysis to 3D Reconstruction

The anatomical landmarks were palpated in the gait laboratory. After the knees were scanned, these points had to be identified on the 3D images. Ideally, the subject would attend the scan immediately before or after motion analysis, and the scan would be conducted with the anatomical landmarks labelled in such a way as to be visible in the scanned image. As the scans were being done at the end of clinical lists in a separate location to the

motion analysis laboratory, this was not possible. Piazza and Cavanagh (2000) reported that kinematic crosstalk can be caused by misplacement of an anatomical landmark that describes a plane, resulting in rotations being described around the wrong axis. An attempt was made to register the anatomical points using a healthy subject for comparative purposes using markers the same size as those used in the motion analysis lab in a vial of copper sulphate solution, similar to that used by Sheehan et al (1997). However an unquantifiable image shift of the copper sulphate solution was seen in the image, and the data was not usable. The anatomical landmarks were therefore identified on the 3D images by virtual palpation. A virtual palpation tool was created in MATLAB and the femoral epicondyles were identified. An error is introduced by using a secondary method of locating the anatomical landmarks on the 3D image, and is expected to be similar to the error of identifying the anatomical landmarks on two separate occasions, as described above. The repeatability in calculating the virtual points from the 3D images is estimated to be within 1mm. This is in agreement with Victor et al (2009) who reported on errors in identifying anatomical landmarks from CT scans that were surfaced in MIMICS software.

Axis Definition

In gait analysis in the current study, the femur was defined as being from the centre of the distal femur to the hip joint centre, and the tibia was defined as being the centre of the proximal tibia to the ankle joint centre. When obtaining the medical images, the study was constrained by the time and equipment of the hospital department. As such, the area around the knee joint was imaged but the whole leg was not. The result of this methodology is that in the 3D reconstruction the axes of the knee joint had to be estimated from the limited images available. Most et al (2004) investigated the effect of different M-L axis definitions on kinematic results. They reported a significant difference in both femoral translation and tibial rotation, a difference that increased with flexion angle. For the purposes of the

animation the knee joint was assumed to be in a neutral position with the long axis of each of the segments parallel with the bed of the scanner, and the transverse plane identical to the transverse plane of the scanner. Although the scope for malalignment of these axes is small due to the physical constraint of the scanner and knee brace coil, there still exists the possibility that the subjects were not aligned with the bed. The errors associated with this are estimated to be no more than $10°$, with the largest error being translated to varus valgus rotation in the animation due to the likelihood that relative position of the hip and ankle in the mediolateral plane is most likely to be off neutral. Alignment errors can be reduced by taking a coarse scan of the whole leg from pelvis to foot, and a more detailed scan of the knee joint, allowing for the axes to be identified on the 3D image from anatomical landmarks.

In summary, there are a number of potential sources of error in the data collection process decribed in this study. The two largest contributers to potential error are within SMA and the registration of anatomical points to medical images. As part of a multi centre EU funded project titled Multimod, Leardini et al (2006) reported on the development of a system called Data Manager. Similar to that reported here, they aimed to provide a visualisation of joint mechanics in such a format that could be understood by any professional, and produced animations that demonstrated unrealistic penetration and separation of the bones. The inclusion of joint centre constraints in their animations resulted in a more physiological motion, and this would benefit the animations in the current study.

When collecting medical images, it is recommended that the scan incorporates as detailed a scan as possible at the tibiofemoral joint, and a coarse scan of the rest of the leg to include the hip and ankle joint locations. Although the scan must be taken with consideration to the comfort of the patient, faster and more powerful scanners that those utilised in the current study will be able to collect such a scan without increasing the time of scan or level of discomfort for the patient. As MRI technology continues to

improve, the scan could also be taken in a weight bearing position similar to that of the calibration position in the motion analysis system. It is also recommended that future studies incorporate a form of registration of points between the medical image and motion analysis system. Registration of points removes the errors associated with estimation of marker placement in the 3D image.

Animations

The animations produced in this study are not of a high enough quality or accuracy for clinical use. The main reasons for this are based in the measurement errors as described above. The largest errors associated with the acquisition of the scan are possibly also the most rectifiable. A scan that incorporates the lower limb from hip to ankle will provide reference points for joint centres within the animation, thus removing the error of malalignment in the scanner. The addition of markers of anatomical landmarks in the scanner will allow for the registration of points between the medical image and the motion analysis software.

In spite of the failure of the animations in the current study, the future of animation of motion has numerous advantages over graphical representation of kinematic data. Firstly, when calculating out the rotation of one segment around another into 3 resulting angular rotations, there is a tendency for cross talk to occur. The smaller angular rotations around varus and internal rotations are particularly susceptible to miscalculation due to cross talk from large flexion angles. When the knee is in deep flexion, rotation around varus can be misrepresented as a rotation around the internal axis, and vice versa. The method of calculation of the angles for animation purposes used in the current study calculates the overall rotational angle from Cardian angles in the specific order that they were first calculated out from in the motion analysis program. Any cross talk that is created from the kinematic analysis in the motion analysis system are removed by back calculating the data into one resultant angle. In future studies it will not be necessary to double handle the data in this way, as the raw data can also be used to control the animation. From a clinicians point of view, the animation does not need to distinguish between the three angles of rotation of the joint, as the important aspect is being able to visualise interactions of the two bones through the range of motion, a concept that is very difficult when interpreting graphs

(Baker 2006) The use of animation in disseminating results from the motion analysis lab to the clinician removes the need for training clinicians in the interpretation of 3D gait analysis results.   Furthermore, as the important aspect is the realistic visualisation of the movement, less emphisis needs to be placed on the accuracy of the kinematic data, as small errors in rotational calculations will be difficult to identify in an animation.

Technological Advances

The current study, although not yet of clinical usefulness, has the potential to be developed for a number of applications both pre and post surgery. It is recommended that the first stage of further work is to improve the accuracy of the methodology. Already the accuracy of motion analysis systems has improved at least by 10 fold from the system utilised in the current study. New cameras and software systems such as the Vicon MX cameras and Nexus software have a system accuracy of 0.1mm. Since the conception of the current study new open source software packages that are more user friendly than VRML have been developed, such as Python (www.python.org accessed May 2011). One of the benefits of such software is that the raw marker data exported from motion analysis software could be used to control the motion of the animation. Such a method would remove the cumbersome task of calculating absolute rotations from 3 angles. New technology will also improve the viewing experience for the clinician. Applications such as onhandviewXL available for use on the iPad (www.absolute-apps.com accessed May 2011) allows for the animations to be easily accessible, and more intuitive in their control.

Kinematic Changes Due to Surgical Intervention

In the current study, all knee replacements were conducted by two surgeons using either fixed or mobile bearing knees from DePuy. Although there was a large variation in preoperative kinematics, postoperatively the variation dramatically decreased, especially in minimum flexion angles. It is possible that small differences in total knee replacement design do not translate to differences in knee kinematics, resulting in a standardised flexion range of motion across most implant designs. Mobile bearing designs may yield different kinematics than fixed bearing designs in internal/external rotation, however these differences may be masked by errors in reporting in this plane due to errors inherent in gait analysis as described previously. Other aspects, such as muscle activation around the knee joint, may also contribute to the abnormal gait pattern seen in TKR patients (Benedetti et al 2003). The argument that prostheis design has an influence on knee kinematics is further evidenced by investigations into unicompartmental knee arthroplasty. By maintaining the anatomical integrity of the knee joint, normal knee kinematics can be maintained (Patil et al 2005).

Comparison of fixed vs mobile bearing knee replacements
In the current study 4 subjects were fitted with a fixed bearing tibial component and 3 subjects were fitted with a rotating platform mobile bearing tibial component. Fixed bearing knee replacements have been used since the 1970's and studies have shown them to provide durable and long term fixation with prosthetic survival rates over 90% up to 17 years after implant (Ladermann, et al 2008) Failure of a prosthesis can occur under high contact stress. The rotating platform mobile bearing knee designs allow for motion at the polyethylene-tibial tray interface, resulting in greater conformity between the tibial and femoral components and decreasing contact stress (Gioe, et al 2009). However there is limited evidence to support significant

difference in clinical outcomes between a fixed or mobile bearing tibial insert. Harrington et al (2009) investigated the difference between fixed and mobile bearing tibial implants in140 TKR patients with a 2 year follow up. They reported a significantly larger range of motion in the mobile bearing group at 6 weeks and 1 year post surgery, but no differences at 3 and 6 months or at 2 years. Furthermore they also reported no differences at any time up to 2 years in Knee Society, WOMAC, or SF-36 scores, or the rate of complications. Similarly, in a 2 year follow up of 312 TKR surgeries Gioe et al (2009) found no significant differences between fixed or mobile bearing knees in range of motion, KSS, SF-36 and WOMAC scores, and radiographic parameters. In a randomised study of 107 consecutive TKR surgeries Woolson and Northop (2004) found that although a significant difference in knee flexion range existed between patients who underwent TKR with a fixed and mobile bearing platform preoperatively, no difference in knee flexion range of motion, KS score, or radiological knee alignment existed postoperatively. This suggests that, similar to the current study, knee replacement surgery results in a 'standardised' range of functional motion irrespective of preoperative range of motion. In a 7 year follow up, Ladermann et al (2009) found no significant differences between fixed and mobile bearing knees with respect to KSS, pain, range of motion or complication rates. As the theoretical benefit of a mobile bearing platform is a reduction in contact stress, it is possible that potential benefits may not be seen until much later in the life of the implant.

Potential Benefits of the Animation System

The aim of TKR is to return function to a level deemed normal for the population. Although the subjects in the current study reach flexion angles comparable to previous studies, this does not mean that the subjects have a normal knee function. The subjects in the present study still avoid situations where they have to walk long distances or climb stairs. Also, two of the nine subjects who had the operation within the timescale of this project needed revision surgery. Any system that can improve the outcome of surgery will lead to a better quality of life for the patient. When the recommendations as described are met and a more meaningful animation can be produced, there are a number of potential applications for use.

Prehabilitation

Replacing the knee joint does not guarantee postoperative success. Symptoms of OA are present for a long time before the operation, and muscles are often wasted, contributing to an abnormal walking pattern (Mattsson et al 1990). Patients may benefit from physiotherapy before and after TKR, before altered walking patterns are developed. Inadequate rehabilitation has been suggested as being responsible to at least some degree for the variation seen in postoperative results (Moon and Moon, 2000). An example of this in the current study can be seen in the flexion angle for subject 11 during chair rise. The compensation method of changing foot placement during sit-to-stand preoperatively was still utilised by this subject postoperatively. Using the 3D images also gives the surgeon a much clearer image of the disease state than a simple 2D x-ray. For example, when viewing the static 3D image preoperatively for subject 3, the extent to which the anterior of the tibia is worn can clearly be seen. In addition to this, when the animations are viewed it is possible to identify the tasks that are causing the damage. Viewing the motion of the joint may help inform a prehabilitation plan. By being able to visualise the motion that is

causing wear and pain, an exercise and physiotherapy plan can be formed or adapted to avoid loading the joint under certain motions, while aiming to increase muscle strength and joint range of motion, which has been shown to improve postoperative results (Topp et al 2009).

Surgical Planning

The surgeon makes operative decisions based partly on preoperative assessment. During this the surgeon will assess passive range of motion and use questionnaire based data such as the Oxford Knee Scoring System. Testing passive range of motion will yield much different results to active range of motion.   Active range of motion includes the activation of surrounding soft tissue. One of the aspects of arthritis is that the pathology can affect the line of action of the muscles and can also induce muscle wastage. During passive motion the muscles are not active and hence do not have an impact on the range of motion of the joint. Passive motion also negates the effect of gravity on the range of motion of the joint. There are limited studies into the kinematics of the osteoarthritic knee joint, and these are restricted to motion in the plane of flexion. The surgeon will see little motion in the transverse or frontal plane during passive motion, and may only see a larger varus or valgus angle when assessing the patient standing still. While this will provide useful information, it does not give a full picture as to the range of motion in the transverse or frontal planes during activities of daily living.   The true effect of this can be seen in the preoperative animations where the loading and pattern of wear are markedly different when undertaking different tasks, especially the difference between the walking tasks and rising from a chair. The ability to predict the effect that TKR surgery will have on the kinematics of the knee joint in everyday living conditions will influence the outcome of the success of the operation.

A major part of planning for a TKR operation is where to make the bone cuts. Current techniques rely on the surgeon making the correct cuts by placement of a rig on the bone. Part of the surgical decision-making process involves

cutting the tibia at the deepest point in order to obtain a flat surface. The preoperative data obtained in the present study allows for the surgeon to identify the geometry of the bone surfaces without the patient being present. A more detailed view of the static joint in 3D afforded by the current methodology as opposed to conventional 2D radiographs can better inform the surgeon of the anatomy and abnormality of the joint. This may assist in the decision making process of where to make cuts, and what type of implant is most suitable for a particular patient before surgery. The main advantage of this type of view is that the tibia and femur can be viewed independently from each other, allowing the surgeon to view the articulating surfaces of the joint not normally visible until during surgery.

Any information that can improve the preoperative planning of an operation and therefore the postoperative results is of benefit for both the patient in terms of health and the NHS in terms of cost of revision surgery.

Computer Assisted and Virtual Surgery

The most recent development in Greater Glasgow Health Board's approach to TKR is the introduction of computer-assisted surgery. An anatomical landmark identification system very similar to the method described in the current study is used to define the mechanical axes of the femur and tibia, guiding the surgeon as to the placement and angles of the cuts and therefore the placement of the implant components. This is currently conducted intra-operatively, using patient specific data superimposed onto a standardised computer knee model. Inclusion of patient specific data from 3 dimension reconstructions of the preoperative knee joint has the potential to further improve this method of surgery.

The possibility also arises to allow the surgeon the option of virtual surgery, where different cuts can be made and different implant types and sizes placed onto the virtual bone to assist in the operative decision making process.

Standardising Treatment

A full 3D view of the knee joint may lead to a more standardised set of guidelines as to what stage of the disease would be most beneficial for operation. Currently, radiological measurements do not relate to severity of disease, and there are no set guidelines as to what stage of the disease to perform surgery (Kennedy et al 2003). A measurement of volume deformation or tibial wear caused by grinding by the femur may assist in the development of guidelines for optimal stage of disease for surgical intervention.

Quantification of Design Aspects.

The animation method described in the current study provides an opportunity to determine if the theoretical advantages of increased motion and contact areas provided by a mobile bearing knee joint are a physical reality in vivo. As numerous studies have failed to show an advantage of mobile bearing over fixed bearing knees in standard clinical and range of motion outcomes, the method of viewing a patient specific animation of the knee joint as described in the current study may help provide evidence of early indicators of abnormal wear of the prosthetic joint. Firstly, by viewing separate components of the static 3D image, it is possible to visualise component wear, separation between implant and bone, or migration of implant. By viewing the surface interactions of the knee joint under every day activities, it is then possible to determine what motions of the joint are causing the abnormal wear, separation or migration. By viewing the joint in 3D animation the detail is far superior to that of a radiograph or slide by slide CT/MRI scan, and is in an anatomical format easily recognisable and understandable to the practitioner. This eliminates the need for interpreting and understanding complex graphical representations of knee rotation around 3 axes. Visualisation of the in vivo knee replacement joint may also help inform manufacturers of potential issues of interest to the design of the prosthesis, if

the 3D scan identifies that daily motion at the joint differs from that expected by the manufacturers.

Reporting of Component Wear and Loosening

Attempts to predict wear patterns in the tibial component by computational modelling have been shown by Fregley et al (2005). The computed model was based on CAD model provided by the prosthetic manufacturer, and fluoroscopic data from treadmill walking for one subject. The animations produced in the current study have two main advantages over this process. Firstly, the motions are taken from every day activities, and do not need to be extrapolated from treadmill data. Secondly, the images are patient specific, and so do not rely on standardised CAD designs. The individualised images therefore show areas of wear and loosening under real conditions. An example of this can be seen when viewing subject 11's postoperative image. The angle of the tibial implant in the A-P plane can be seen to tilt downwards anteriorly, with the result that there is separation of the implant and tibial bone posteriorly. Harman et al (2001) reported direct effects of wear on tibial inserts, however this was done by retrieving implants from cadavers or from revision surgeries on subjects who had previously undergone fluoroscopic analysis. The availability of such studies would therefore be extremely limited, and of no benefit to the patients in the study.

Rehabilitation

Similar to potential benefits of prehabilitation, identification of potential problems at the knee joint after TKR may be beneficial in the rehabilitation setting. If for example it can be seen from an animation that when walking there is an abnormal contact on the medial component, this may inform a physiotherapy or temporary orthotic intervention to help the knee joint into a more valgus position, with the potential correction of the varus knee and resulting in a more even distribution of the contact surface.

Chapter 6. Conclusion

TKR patients reach a standardised level of function, which may not be their optimum. This may be due to the geometrical constraints of the implant, despite different designs being used.

Patient specific animations of the knee joint pre and post TKR surgery can be produced. Although the animations produced in this project are not accurate enough for clinical use, the combination of technological advances and addition of joint constraints could result in clinically meaningful and useful images.

Animations have advantages over graphical representation of data as the element of crosstalk is removed and specialised training for their interpretation is not needed.

The possible application of the animated joint is widespread, and can help inform decision making for the physiotherapist, surgeon, and design engineer.

References

Ando, Y., Fukatsu, H., Ishigaki, T., Aoki, I., & Yamada, T. (1994). Analysis of knee movement with low-field MR equipment--a normal volunteer study. *Radiation medicine, 12*(4), 153.

Andriacchi, T., Galante, J., & Fermier, R. (1982). The influence of total knee-replacement design on walking and stair-climbing. *The Journal of Bone and Joint Surgery, 64*(9), 1328.

Andriacchi, T. P., & Alexander, E. J. (2000). Studies of human locomotion: past, present and future. *Journal of Biomechanics, 33*(10), 1217-1224.

Andriacchi, T. P., Lang, P. L., Alexander, E. J., & Hurwitz, D. E. (2000). Methods for evaluating the progression of osteoarthritis. *Journal of Rehabilitation Research and Development, 37*(2), 163-170.

Asano, T., Akagi, M., Tanaka, K., Tamura, J., & Nakamura, T. (2001). In vivo three-dimensional knee kinematics using a biplanar image-matching technique. *Clinical Orthopaedics and Related Research, 388*, 157.

Astephen, J. L., Deluzio, K. J., Caldwell, G. E., Dunbar, M. J., & Hubley-Kozey, C. L. (2008). Gait and neuromuscular pattern changes are associated with differences in knee osteoarthritis severity levels. *Journal of Biomechanics, 41*(4), 868-876.

Baker, R. (2006). Gait analysis methods in rehabilitation. *Journal of NeuroEngineering and Rehabilitation, 3*(1), 4.

Ball, S. T., Sanchez, H. B., Mahoney, O. M., & Schmalzried, T. P. (2010). Fixed Versus Rotating Platform Total Knee Arthroplasty: A Prospective, Randomized, Single-Blind Study. *The Journal of Arthroplasty*.

Bell, A. L., Pedersen, D. R., & Brand, R. A. (1990). A comparison of the accuracy of several hip center location prediction methods. *Journal of Biomechanics, 23*(6), 617-621.

Benedetti, M., Catani, F., Bilotta, T., Marcacci, M., Mariani, E., & Giannini, S. (2003). Muscle activation pattern and gait biomechanics after total knee replacement. *Clinical Biomechanics, 18*(9), 871-876.

Berman, A. T., Zarro, V., Bosacco, S., & Israelite, C. (1987). Quantitative gait analysis after unilateral or bilateral total knee replacement. *The Journal of Bone and Joint Surgery, 69*(9), 1340.

Bourne, R. B. (2008). Measuring tools for functional outcomes in total knee arthroplasty. *Clinical Orthopaedics and Related Research®, 466*(11), 2634-2638.

Buckland-Wright, C. (1999). Radiographic assessment of osteoarthritis: comparison between existing methodologies. *Osteoarthritis and Cartilage, 7*, 430-433.

Cappello, A., Cappozzo, A., La Palombara, P. F., Lucchetti, L., & Leardini, A. (1997). Multiple anatomical landmark calibration for optimal bone pose estimation. *Human Movement Science, 16*(2-3), 259-274.

Cappello, A., Stagni, R., Fantozzi, S., & Leardini, A. (2005). Soft tissue artifact compensation in knee kinematics by double anatomical landmark calibration: performance of a novel method during selected motor tasks. *Biomedical Engineering, IEEE Transactions on, 52*(6), 992-998.

Cappozzo, A. (1984). Gait analysis methodology. *Human Movement Science, 3*(1-2), 27-50.

Cappozzo, A., Catani, F., Della Croce, U., & Leardini, A. (1995). Position and orientation in space of bones during movement: anatomical frame definition and determination. *Clinical Biomechanics, 10*(4), 171-178.

Cappozzo, A., Catani, F., Leardini, A., Benedetti, M., & Della Croce, U. (1996). Position and orientation in space of bones during movement: experimental artefacts. *Clinical Biomechanics, 11*(2), 90-100.

Carpenter, R. D., Brilhault, J., Majumdar, S., & Ries, M. D. (2009). Magnetic resonance imaging of in vivo patellofemoral kinematics after total knee arthroplasty. *The Knee, 16*(5), 332-336.

Catani, F., Benedetti, M., De Felice, R., Buzzi, R., Giannini, S., & Aglietti, P. (2003). Mobile and fixed bearing total knee prosthesis functional comparison during stair climbing. *Clinical Biomechanics, 18*(5), 410-418.

Chao, E., Laughman, R., & Stauffer, R. (1980). Biomechanical gait evaluation of pre and postoperative total knee replacement patients. *Archives of Orthopaedic and Trauma Surgery, 97*(4), 309-317.

Culliford, D., Maskell, J., Beard, D., Murray, D., Price, A., & Arden, N. K. (2010). Temporal trends in hip and knee replacement in the United Kingdom: 1991 to 2006. *Journal of Bone and Joint Surgery-British Volume, 92*(1), 130.

Curtis, C. L., Harwood, J. L., Dent, C. M., & Caterson, B. (2004). Biological basis for the benefit of nutraceutical supplementation in arthritis. *Drug discovery today, 9*(4), 165-172.

Davies, A. P., & Glasgow, M. M. S. (2000). Imaging in osteoarthritis: a guide to requesting plain X-rays of the degenerate knee. *The Knee, 7*(3), 139-143.

Della Croce, U., Leardini, A., Chiari, L., & Cappozzo, A. (2005). Human movement analysis using stereophotogrammetry:: Part 4: assessment of anatomical landmark misplacement and its effects on joint kinematics. *Gait & Posture, 21*(2), 226-237.

Delp, S. L., Stulberg, D. S., Davies, B., Picard, F., & Leitner, F. (1998). Computer Assisted Knee Replacement. *Clinical Orthopaedics and Related Research, 354*, 49-56.

Deluzio, K., & Astephen, J. (2007). Biomechanical features of gait waveform data associated with knee osteoarthritis:: An application of principal component analysis. *Gait & Posture, 25*(1), 86-93.

Deluzio, K. J., Wyss, U. P., Costigan, P. A., Sorbie, C., & Zee, B. (1999). Gait assessment in unicompartmental knee arthroplasty patients: Principal component modelling of gait waveforms and clinical status. *Human Movement Science, 18*(5), 701-711.

Dennis, D., Komistek, R., Scuderi, G., Argenson, J. N., Insall, J., Mahfouz, M., et al. (2001). In vivo three-dimensional determination of kinematics for subjects with a normal knee or a unicompartmental or total knee replacement. *The Journal of Bone and Joint Surgery, 83*(Supplement 2, Part 2), S104.

Dennis, D. A., Mahfouz, M. R., Komistek, R. D., & Hoff, W. (2005). In vivo determination of normal and anterior cruciate ligament-deficient knee kinematics. *Journal of Biomechanics, 38*(2), 241-253.

Depuy.com. (Accessed March 2011). http://www.depuy.com/sites/default/files/products/files/0612-86-510%20(2)_0.pdf.

Desailly, E., Daniel, Y., Sardain, P., & Lacouture, P. (2009). Foot contact event detection using kinematic data in cerebral palsy children and normal adults gait. *Gait & Posture, 29*(1), 76-80.

Dieppe, P. (2000). Towards a better understanding of osteoarthritis of the knee joint. *The Knee, 7*(3), 135-137.

DiGioia III, A. M., Jaramaz, B., & Colgan, B. D. (1998). Computer assisted orthopaedic surgery: image guided and robotic assistive technologies. *Clinical Orthopaedics and Related Research, 354*, 8.

Duffy, P., Petrie, D. P., Leighton, R. K., & Collier, K. (2008). A randomized single blinded clinical trial comparing posterior cruciate retaining vs posterior cruciate sacrificing total knee replacements - results after two years. *J Bone Joint Surg Br, 90-B*(SUPP_I), 51-.

Fantozzi, S., Benedetti, M. G., Leardini, A., Banks, S. A., Cappello, A., Assirelli, D., et al. (2003). Fluoroscopic and gait analysis of the functional performance in stair ascent of two total knee replacement designs. *Gait & Posture, 17*(3), 225-234.

Felson, D. T. (2006). Clinical Practice: Osteoarthritis of the Knee. *New England Journal of Medicine, 354*(8), 841-848.

Felson, D. T., Lawrence, R. C., Dieppe, P. A., Hirsch, R., Helmick, C. G., Jordan, J. M., et al. (2000). Osteoarthritis: New Insights. Part 1: The Disease and Its Risk Factors. *Annals of Internal Medicine, 133*(8), 635-646.

Fregly, B. J., Sawyer, W. G., Harman, M. K., & Banks, S. A. (2005). Computational wear prediction of a total knee replacement from in vivo kinematics. *Journal of Biomechanics, 38*(2), 305-314.

Gamage, S. S., & Lasenby, J. (2002). New least squares solutions for estimating the average centre of rotation and the axis of rotation. *Journal of Biomechanics, 35*(1), 87-93.

Gibson, S., Samosky, J., Mor, A., Fyock, C., Grimson, E., Kanade, T., et al. (1997). *Simulating arthroscopic knee surgery using volumetric object representations, real-time volume rendering and haptic feedback*.

Gioe, T. J., Glynn, J., Sembrano, J., Suthers, K., Santos, E. R. G., & Singh, J. (2009). Mobile and fixed-bearing (all-polyethylene tibial component) total knee arthroplasty designs. A prospective randomized trial. *The Journal of Bone and Joint Surgery, 91*(9), 2104.

Gray, H. (1918). *Anatomy of the human body*: Lea & Febiger.

Grood, E. S., & Suntay, W. J. (1983). A joint coordinate system for the clinical description of three-dimensional motions: application to the knee. *Journal of Biomechanical Engineering, 105*, 136.

Harman, M. K., Banks, S. A., & Hodge, W. A. (2001). Polyethylene damage and knee kinematics after total knee arthroplasty. *Clinical Orthopaedics and Related Research, 392*, 383.

Harrington, M. A., Hopkinson, W. J., Hsu, P., & Manion, L. (2009). Fixed-vs Mobile-Bearing Total Knee Arthroplasty:: Does It Make a Difference?--A Prospective Randomized Study. *The Journal of Arthroplasty, 24*(6), 24-27.

Holzreiter, S. (1991). Calculation of the instantaneous centre of rotation for a rigid body. *Journal of Biomechanics, 24*(7), 643-647.

Hossain, M. A., Fukunaga, M., & Hirokawa, S. (2008). A Kinematic Assessment of Knee Prosthesis from Fluoroscopy Images. *Memoirs of the Faculty of Engineering, Kyushu University, 68*(1), 19-30.

Hunt, M. A., Birmingham, T. B., Skarakis-Doyle, E., & Vandervoort, A. A. (2008). Towards a biopsychosocial framework of osteoarthritis of the knee. *Disability & Rehabilitation, 30*(1), 54-61.

Iwaki, H., Pinskerova, V., & Freeman, M. A. R. (2000). Tibiofemoral movement 1: the shapes and relative movements of the femur and tibia in the unloaded cadaver knee. *J Bone Joint Surg Br, 82-B*(8), 1189-1195.

Johal, P., Williams, A., Wragg, P., Hunt, D., & Gedroyc, W. (2005). Tibio-femoral movement in the living knee. A study of weight bearing and non-weight bearing knee kinematics using interventional MRI. *Journal of Biomechanics, 38*(2), 269-276.

Jones, L., & Holt, C. (2008). An objective tool for assessing the outcome of total knee replacement surgery. *Proceedings of the Institution of Mechanical Engineers, Part H: Journal of Engineering in Medicine, 222*(5), 647-655.

Kaufman, K. R., Hughes, C., Morrey, B. F., Morrey, M., & An, K.-N. (2001). Gait characteristics of patients with knee osteoarthritis. *Journal of Biomechanics, 34*(7), 907-915.

Kennedy, L. G., Newman, J. H., Ackroyd, C. E., & Dieppe, P. A. (2003). When should we do knee replacements? *The Knee, 10*(2), 161-166.

Khanna, A. J., Cosgarea, A. J., Mont, M. A., Andres, B. M., Domb, B. G., Evans, P. J., et al. (2001). Magnetic resonance imaging of the knee: Current techniques and spectrum of disease. *The Journal of Bone and Joint Surgery, 83*(Supplement 2, Part 2), S128.

Komistek, R. D., Dennis, D. A., & Mahfouz, M. (2003). In vivo fluoroscopic analysis of the normal human knee. *Clinical Orthopaedics and Related Research, 410*, 69.

Komistek, R. D., Kane, T. R., Mahfouz, M., Ochoa, J. A., & Dennis, D. A. (2005). Knee mechanics: a review of past and present techniques to determine in vivo loads. *Journal of Biomechanics, 38*(2), 215-228.

Kurtz, S. (2005). Prevalence of primary and revision total hip and knee arthroplasty in the United States from 1990 through 2002. *Journal of Bone and Joint Surgery; American volume, 87*(7), 1487.

Lädermann, A., Lübbeke, A., Stern, R., Riand, N., & Fritschy, D. (2008). Fixed-bearing versus mobile-bearing total knee arthroplasty: A prospective randomised, clinical and radiological study with mid-term results at 7 years. *The Knee, 15*(3), 206-210.

Leardini, A., Belvedere, C., Astolfi, L., Fantozzi, S., Viceconti, M., Taddei, F., et al. (2006). A new software tool for 3D motion analyses of the musculo-skeletal system. *Clinical Biomechanics, 21*(8), 870-879.

Leardini, A., Chiari, L., Croce, U. D., & Cappozzo, A. (2005). Human movement analysis using stereophotogrammetry:: Part 3. Soft tissue artifact assessment and compensation. *Gait & Posture, 21*(2), 212-225.

Li, J., Wyss, U., Costigan, P., & Deluzio, K. (1993). An integrated procedure to assess knee-joint kinematics and kinetics during gait using an optoelectric system and standardized X-rays. *Journal of biomedical engineering, 15*(5), 392-400.

Liu, H., Holt, C., & Evans, S. (2007). Accuracy and repeatability of an optical motion analysis system for measuring small deformations of biological tissues. *Journal of Biomechanics, 40*(1), 210-214.

Longstaff, L. M., Sloan, K., Stamp, N., Scaddan, M., & Beaver, R. (2009). Good alignment after total knee arthroplasty leads to faster rehabilitation and better function. *The Journal of Arthroplasty, 24*(4), 570-578.

Lu, T. W., & O'connor, J. (1999). Bone position estimation from skin marker co-ordinates using global optimisation with joint constraints. *Journal of Biomechanics, 32*(2), 129-134.

Ma, Y. Y., Zhang, H., & Jiang, S. W. (2004). Realistic modeling and animation of human body based on scanned data. *Journal of Computer Science and Technology, 19*(4), 529-537.

Mahfouz, M. R., Hoff, W. A., Komistek, R. D., & Dennis, D. A. (2005). Effect of segmentation errors on 3D-to-2D registration of implant models in X-ray images. *Journal of Biomechanics, 38*(2), 229-239.

Majeed, A., & Aylin, P. (2005). The ageing population of the United Kingdom and cardiovascular disease. *BMJ, 331*(7529), 1362.

Mandeville, D., Osternig, L. R., Lantz, B. A., Mohler, C. G., & Chou, L. S. (2008). The effect of total knee replacement on the knee varus angle and moment during walking and stair ascent. *Clinical Biomechanics, 23*(8), 1053-1058.

Marin, F., Allain, J., Diop, A., Maurel, N., Simondi, M., & Lavaste, F. (1999). On the estimation of knee joint kinematics. *Human Movement Science, 18*(5), 613-626.

Matsuda, S., Matsuda, H., Miyagi, T., Sasaki, K., Iwamoto, Y., & Miura, H. (1998). Femoral condyle geometry in the normal and varus knee. *Clinical Orthopaedics and Related Research, 349*, 183.

Matsuda, S., Miura, H., Nagamine, R., Mawatari, T., Tokunaga, M., Nabeyama, R., et al. (2004). Anatomical analysis of the femoral condyle in normal and osteoarthritic knees. *Journal of Orthopaedic Research, 22*(1), 104-109.

Mattsson, E., Broström, L., & Linnarsson, D. (1990). Changes in walking ability after knee replacement. *International orthopaedics, 14*(3), 277-280.

McGinley, J. L., Baker, R., Wolfe, R., & Morris, M. E. (2009). The reliability of three-dimensional kinematic gait measurements: a systematic review. *Gait & Posture, 29*(3), 360-369.

McPherson, A., Kärrholm, J., Pinskerova, V., Sosna, A., & Martelli, S. (2005). Imaging knee position using MRI, RSA/CT and 3D digitisation. *Journal of Biomechanics, 38*(2), 263-268.

Mills, C., Pain, M., & Yeadon, F. (2005). *Modeling the gymnast-mat interaction during vault landings.*

Mizner, R. L., & Snyder-Mackler, L. (2005). Altered loading during walking and sit-to-stand is affected by quadriceps weakness after total knee arthroplasty. *Journal of Orthopaedic Research, 23*(5), 1083-1090.

Moon, M. S., & Moon, J. L. (2000). Range of motion after total knee replacement: a review from the East. *Current Orthopaedics, 14*(4), 302-308.

Most, E., Axe, J., Rubash, H., & Li, G. (2004). Sensitivity of the knee joint kinematics calculation to selection of flexion axes. *Journal of Biomechanics, 37*(11), 1743-1748.

Myles, C. M., Rowe, P. J., Walker, C. R. C., & Nutton, R. W. (2002). Knee joint functional range of movement prior to and following total knee arthroplasty measured using flexible electrogoniometry. *Gait & Posture, 16*(1), 46-54.

Nadeau, S., McFadyen, B. J., & Malouin, F. (2003). Frontal and sagittal plane analyses of the stair climbing task in healthy adults aged over 40 years: what are the challenges compared to level walking? *Clinical Biomechanics, 18*(10), 950-959.

Ng, C., Ballantyne, J., & Brenkel, I. (2007). Quality of life and functional outcome after primary total hip replacement: a five-year follow-up. *Journal of Bone and Joint Surgery-British Volume, 89*(7), 868.

Öberg, U., Öberg, T., & Hagstedt, B. (1996). Functional improvement after hip and knee arthroplasty: 6-month follow-up with a new functional assessment system. *Physiotherapy Theory and Practice, 12*(1), 3-13.

onhandviewXL. (Accessed May 2011). www.absolute-apps.com.

Otake, Y., Suzuki, N., Hattori, M., Sugano, N., Hagio, K., Yonenobu, S., et al. (2002). 4-dimensional visualization of gait and the clinical application. *Clinical Orthopaedic Surgery, 37*(11), 1279-1286.

Patel, V. V., Hall, K., Ries, M., Lotz, J., Ozhinsky, E., Lindsey, C., et al. (2004). A three-dimensional MRI analysis of knee kinematics. *Journal of Orthopaedic Research, 22*(2), 283-292.

Patil, S., Colwell Jr, C. W., Ezzet, K. A., & D'Lima, D. D. (2005). Can normal knee kinematics be restored with unicompartmental knee replacement? *The Journal of Bone and Joint Surgery, 87*(2), 332.

Peters, A., Galna, B., Sangeux, M., Morris, M., & Baker, R. (2010). Quantification of soft tissue artifact in lower limb human motion analysis: A systematic review. *Gait & Posture, 31*(1), 1-8.

Piazza, S. J., & Cavanagh, P. R. (2000). Measurement of the screw-home motion of the knee is sensitive to errors in axis alignment. *Journal of Biomechanics, 33*(8), 1029-1034.

Prince, F., Corriveau, H., Hébert, R., & Winter, D. A. (1997). Gait in the elderly. *Gait & Posture, 5*(2), 128-135.

Pudlo, P., Lempereur, M., Lepoutre, F., & Gorce, P. (2009). A new method for simulating the car-entering movement. *International Journal of Vehicle Design, 51*(3), 341-358.

Python.org. (Accessed May 2011). www.python.org.

Ranawat, C. S., Komistek, R. D., Rodriguez, J. A., Dennis, D. A., & Anderle, M. (2004). In Vivo Kinematics for Fixed and Mobile-Bearing Posterior Stabilized Knee Prostheses. *Clinical Orthopaedics and Related Research, 418*, 184-190.

Rovati, L. (1999). Radiographic assessment. Introduction: existing methodology. *Osteoarthritis and Cartilage, 7*(4), 427-429.

Rowe, P., Myles, C., Walker, C., & Nutton, R. (2000). Knee joint kinematics in gait and other functional activities measured using flexible electrogoniometry: how much knee motion is sufficient for normal daily life? *Gait & Posture, 12*(2), 143-155.

Saari, T., Tranberg, R., Zügner, R., Uvehammer, J., & Kärrholm, J. (2004). The effect of tibial insert design on rising from a chair; motion analysis after total knee replacement. *Clinical Biomechanics, 19*(9), 951-956.

Sandilands, V., Brocklehurst, S., Sparks, N., Baker, L., McGovern, R., Thorp, B., et al. (2011). Assessing leg health in chickens using a force plate and gait scoring: how many birds is enough? *Veterinary Record, 168*(3), 77.

Schep, N. W. L., Broeders, I., & van der Werken, C. (2003). Computer assisted orthopaedic and trauma surgery:: State of the art and future perspectives. *Injury, 34*(4), 299-306.

Schwartz, M. H., Trost, J. P., & Wervey, R. A. (2004). Measurement and management of errors in quantitative gait data. *Gait & Posture, 20*(2), 196-203.

Seisler, A. R., & Sheehan, F. T. (2006). A Visualization Tool to convey Quantitative in vivo, 3D Knee Joint Kinematics.

Seisler, A. R., & Sheehan, F. T. (2007). Normative three-dimensional patellofemoral and tibiofemoral kinematics: a dynamic, in vivo study. *Biomedical Engineering, IEEE Transactions on, 54*(7), 1333-1341.

Sharkey, P. F., Hozack, W. J., Rothman, R. H., Shastri, S., & Jacoby, S. M. (2002). Why are total knee arthroplasties failing today? *Clinical Orthopaedics and Related Research, 404*, 7.

Sheehan, F. T., Derasari, A., Brindle, T. J., & Alter, K. E. (2009). Understanding patellofemoral pain with maltracking in the presence of joint laxity: complete 3D in vivo patellofemoral and tibiofemoral kinematics. *Journal of Orthopaedic Research, 27*(5), 561-570.

Sheehan, F. T., & Drace, J. E. (2000). Human patellar tendon strain: a noninvasive, in vivo study. *Clinical Orthopaedics and Related Research, 370*, 201.

Sheehan, F. T., & Mitiguy, P. (1999). In regards to theISB recommendations for standardization in the reporting of kinematic dataa. *Journal of Biomechanics, 32*(1135), 1136.

Sheehan, F. T., Seisler, A. R., & Alter, K. E. (2008). Three-dimensional In Vivo Quantification of Knee Kinematics in Cerebral Palsy. *Clinical Orthopaedics and Related Research®, 466*(2), 450-458.

Sheehan, F. T., Zajac, F. E., & Drace, J. E. (1997). Using cine phase contrast magnetic resonance imaging to non-invasively study in vivo knee dynamics. *Journal of Biomechanics, 31*(1), 21-26.

Shiozaki, H., Koga, Y., Omori, G., & Tamaki, M. (1999). Obesity and osteoarthritis of the knee in women: results from the Matsudai Knee Osteoarthritis survey. *The Knee, 6*(3), 189-192.

Sibanda, N., Copley, L. P., Lewsey, J. D., Borroff, M., Gregg, P., MacGregor, A. J., et al. (2008). Revision Rates after Primary Hip and Knee Replacement in England between 2003 and 2006. *PLoS Med, 5*(9), e179.

Silman, A. J., & Hochberg, M. C. (1993 (reprint 2001)). *Epidemiology of the rheumatic diseases*: Oxford University Press.

Simon, S. R. (2004). Quantification of human motion: gait analysis--benefits and limitations to its application to clinical problems. *Journal of Biomechanics, 37*(12), 1869-1880.

Singh, J., O'Byrne, M., Harmsen, S., & Lewallen, D. (2010). Predictors of moderate-severe functional limitation after primary Total Knee Arthroplasty (TKA): 4701 TKAs at 2-years and 2935 TKAs at 5-years. *Osteoarthritis and Cartilage, 18*(4), 515-521.

Stagni, R., Fantozzi, S., & Cappello, A. (2006). Propagation of anatomical landmark misplacement to knee kinematics: Performance of single and double calibration. *Gait & Posture, 24*(2), 137-141.

Stagni, R., Fantozzi, S., Cappello, A., & Leardini, A. (2005). Quantification of soft tissue artefact in motion analysis by combining 3D fluoroscopy and stereophotogrammetry: a study on two subjects. *Clinical Biomechanics, 20*(3), 320-329.

Stagni, R., Leardini, A., Cappozzo, A., Grazia Benedetti, M., & Cappello, A. (2000). Effects of hip joint centre mislocation on gait analysis results. *Journal of Biomechanics, 33*(11), 1479-1487.

statistics.gov.uk. (accessed March 2011).

Stulberg, S. D., Loan, P., & Sarin, V. (2002). Computer-assisted navigation in total knee replacement: results of an initial experience in thirty-five patients. *The Journal of Bone and Joint Surgery, 84*(Supplement 2), S90.

Su, F., Lai, K., & Hong, W. (1998). Rising from chair after total knee arthroplasty. *Clinical Biomechanics, 13*(3), 176-181.

Tanaka, S., Kubota, K., Yoshimura, O., Kobayashi, R., Minematsu, A., Hosoda, M., et al. (2000). Gait Analysis after Total Knee Arthroplasty-Comparison of Cemented Type and Cementless Type. *Journal of Physical Therapy Science, 12*(2), 101-105.

Teichtahl, A., Wluka, A., Davies-Tuck, M., & Cicuttini, F. (2008). Imaging of knee osteoarthritis. *Best Practice & Research Clinical Rheumatology, 22*(6), 1061-1074.

Thambyah, A., Thiagarajan, P., & Goh Cho Hong, J. (2004). Knee joint moments during stair climbing of patients with anterior cruciate ligament deficiency. *Clinical Biomechanics, 19*(5), 489-496.

Topp, R., Swank, A. M., Quesada, P. M., Nyland, J., & Malkani, A. (2009). The effect of prehabilitation exercise on strength and functioning after total knee arthroplasty. *PM&R, 1*(8), 729-735.

Tortora, G. J., & Derrickson, B. (2008). *Principles of Anatomy and Physiology [With A Brief Atlas of the Skeleton, Surface Anatomy,]*: John Wiley & Sons.

Uvehammer, J., Karrholm, J., & Carlsson, L. (2007). Cemented versus hydroxyapatite fixation of the femoral component of the Freeman-Samuelson total knee replacement: a radiostereometric analysis. *Journal of Bone and Joint Surgery-British Volume, 89*(1), 39.

Victor, J., Van Doninck, D., Labey, L., Innocenti, B., Parizel, P., & Bellemans, J. (2009). How precise can bony landmarks be determined on a CT scan of the knee? *The Knee, 16*(5), 358-365.

Vignon, E., Conrozier, T., Piperno, M., Richard, S., Carrillon, Y., & Fantino, O. (1999). Radiographic assessment of hip and knee osteoarthritis. Recommendations: recommended guidelines. *Osteoarthritis and Cartilage, 7*(4), 434-436.

von Eisenhart-Rothe, R., Siebert, M., Bringmann, C., Vogl, T., Englmeier, K. H., & Graichen, H. (2004). A new in vivo technique for determination of 3D kinematics and contact areas of the patello-femoral and tibio-femoral joint. *Journal of Biomechanics, 37*(6), 927-934.

Whittle, M. (2002). *Gait analysis: an introduction* (Vol. 1): Butterworth-Heinemann Medical.

Wilson, S. A., McCann, P. D., Gotlin, R. S., Ramakrishnan, H., Wootten, M. E., & Insall, J. N. (1996). Comprehensive gait analysis in posterior-stabilized knee arthroplasty. *The Journal of Arthroplasty, 11*(4), 359-367.

Woolf, A. D., & Pfleger, B. (2003). Burden of major musculoskeletal conditions. *Bulletin of the World Health Organization, 81*, 646-656.

Woolson, S. T., & Northrop, G. D. (2004). Mobile-vs. fixed-bearing total knee arthroplasty: a clinical and radiologic study. *The Journal of Arthroplasty, 19*(2), 135-140.

Wretenberg, P., Ramsey, D. K., & Németh, G. (2002). Tibiofemoral contact points relative to flexion angle measured with MRI. *Clinical Biomechanics, 17*(6), 477-485.

Wu, G., & Cavanagh, P. R. (1995). ISB recommendations for standardization in the reporting of kinematic data. *Journal of Biomechanics, 28*(10), 1257-1262.

Zürcher, A., Wolterbeek, N., Harlaar, J., & Pöll, R. (2008). Knee rotation during a weightbearing activity: Influence of turning. *Gait & Posture, 28*(3), 472-477.

Appendix I – Patient Information Sheet

Patient specific total knee replacement (TKR) in osteoarthritis

You are being invited to take part in a research study. Before you decide, it is important for you to understand why the research is being done and what it will involve. Please take time to read the following information carefully and discuss it with others if you wish. Ask us if there is anything that is not clear or if you would like more information. Take time to decide whether or not you wish to take part.

Thank you for reading this.

_____

Purpose of the study

Current gait analysis of TKR involves measuring movements of the whole leg. This study aims to measure the movements and interactions at the bones of the knee joint.

Why have I been chosen?

You have been selected as suitable to take part in this study by the surgeon who will conduct the operation. You have been selected because you are about to undergo knee replacement surgery as a result of osteoarthritis, and have no other conditions that affect your ability to walk.

Do I have to take part?

Taking part in this research is entirely voluntary. It is up to you to decide whether or not to take part. If you decide to take part you will be given this information sheet to keep and you will be asked to sign a consent form. If you decide to take part you are free to withdraw at any time and without giving a reason. A decision to withdraw or not to take part will in no way affect the standard of care that you receive.

What will happen to me if I take part?

This research project will take approximately three years to complete. If you decide to take part in this study, you will be involved in this research twice, with a year interval

between tests. You will be asked to have a medical scan taken of your knee, and to partake in some simple walking exercises at Strathclyde University prior to your operation. This involves a series of reflective markers being placed on your leg and waist, and images of the markers being captured whilst you walk in a straight line, up and down stairs, and squatting, if possible.

One year after your operation, you will again be asked to attend the hospital, and another scan of your knee will be taken. Shortly after this you will again be asked to partake in the same walking exercises as before at Strathclyde University.

What do I have to do?

You are requested to be present at Strathclyde University for half a day before your operation, and for another half day approximately one year afterwards, and also at Glasgow Royal Infirmary for medical scans. Your physiotherapy and rehabilitation is unaffected by this study, and as such will continue as normal.

What are the possible disadvantages of taking part?

This study does not entail you doing any activities that you would not normally undertake on a daily basis. Your treatment is not affected in any way by this study.

The pre-operative medical imaging used will be an MRI scan. This is non-invasive and will not harm you in any way. The one-year post-operative imaging will be a CT scan (a series of x-rays). As with all x-rays, there is use of radiation, which can be dangerous if exposed to large doses over a long timescale. However, as you will only be scanned once, the risk to you is minimal.

What are the possible benefits of taking part?

There will be no immediate clinical benefit to you as a result of this trial. However, the information gained from this trial may help us develop improved techniques for operating on patients with osteoarthritis in the future.

What if something goes wrong?

This study should not put you at risk in any way. However, if you are harmed due to someone's negligence, then you may have grounds for legal action, but you will have to pay for it. Regardless of this, if you wish to complain, or have any concerns about any

aspect of the way that you have been approached or treated during the course of this study, the normal National Health Service complaints mechanisms may be available to you.

Will my taking part in this study be kept confidential?

All information collected about you throughout the course of this study will be kept strictly confidential. Any information which leaves the hospital will have your name and address removed from it so that you cannot be recognised from it.

What will happen to the results of this study?
This study is intended as part of a Ph.D. study, and as such the results will be contained in the thesis, due for completion by the end of 2005. This will be published for use in the University of Strathclyde library. If you would like to see results from this study, please contact the researchers. You will not be identified in any way in the published results.

Who is organising and funding the research?
This research project is being conducted by the bioengineering unit of the University of Strathclyde, and is funded by the Engineering and Physical Sciences Research Council (EPSRC).

Who has reviewed the study?
This study has been approved by the Ethics committee at the Glasgow Royal Infirmary, and the University of Strathclyde.

Contact for further information
If you require any further information regarding this study, please feel free to contact:

Christopher Barr

Bioengineering unit

University of Strathclyde

106 Rottenrow East

Glasgow

G4 0NW

Phone: 0141-548 3136

E-mail: Christopher.barr.100@strath.ac.uk

May I take this opportunity to thank you for your involvement in this study. Please keep this information sheet for future reference, along with a copy of the consent form.

Appendix II – Consent Form

Study Number:

Patient Identification Number for this trial:

CONSENT FORM

Title of Project:

Patient Specific Total Knee Replacement (TKR) in Osteoarthritis

Name of Researcher:

A.C. Nicol

C. Barr

Please initial box

1. I confirm that I have read and understand the information sheet dated......19.02.2003.... (version..1.0......) for the above study and have had the opportunity to ask questions.

    [ ]

2. I understand that my participation is voluntary and that I am free to withdraw at any time, without giving any reason, without my medical care or legal rights being affected.

    [ ]

3. I understand that sections of any of my medical notes may be looked at by responsible individuals from [company name] or from regulatory authorities where it is relevant to my taking part in research. I give permission for these individuals to have access to my records.

    [ ]

4. I agree to take part in the above study.

    [ ]

_____   _____   _____

Name of Patient   *Date*   *Signature*

_____   _____   _____

Name of Person taking consent   *Date*   *Signature*
(if different from researcher)

_____   _____   _____

Researcher   *Date*   *Signature*

1 for patient; 1 for researcher; 1 to be kept with hospital notes

Appendix III - BodyBuilder Code

!MKR#2

[autolabel]

Pointer1

Pointer2

PELA

PELB

PELC

PELD

TTHIA

TTHIB

BTHIA

BTHIB

TSHAA

TSHAB

BSHAA

BSHAB

TTHIA,BTHIA

BTHIA,BTHIB

BTHIB,TTHIB

TTHIB,TTHIA

TSHAA,BSHAA

BSHAA,BSHAB

BSHAB,TSHAB

TSHAB,TSHAA

PELA,PELB

PELB,PELC

PELC,PELD

PELD,PELA

Waist=PELA,PELB,PELC,PELD

Thigh=TTHIA,TTHIB,BTHIA,BTHIB

Shank=TSHAA,TSHAB,BSHAA,BSHAB

Waist,Thigh

Thigh,Shank

CalMFEP

CalLFEP

CalMTEP

CalLTEP

CalMMAL

CalLMAL

CalLASI

CalRASI

CalLPSI

CalRPSI

CalGTCH

Waist

Thigh

Shank

[points from model]

SACR   Sacral

LASI   left asis

RASI   right asis

LPSI   left psis

RPSI   right psis

PELF   front of pelvis

FEMH   virtualpoint head of femur

LFEP   lateral femoral epicondyle wand marker

MFEP   medial femoral epicondyle wand marker

DFEM   distal centre of femur

GTCH   greater trochanter

LTEP   lateral tibial epicondyle

MTEP   medial tibial epicondyle

PTIB   Proximal cente of tibia

DTIB   distal centre of tibia

MMAL   Medial malleolus

LMAL   lateral malleolus

FEMH,DFEM

PTIB,DTIB

LASI,RASI

RASI,RPSI

RPSI,LPSI

LPSI,LASI

MMALCalib

LFEPCalib

LMEPCalib

MFEPCalib

MTEPCalib

LMALCalib

LPSICalib

RPSICalib

LASICalib

RASICalib

GTCHCalib

FEMHCalib

Pelvis

Tibia

Femur

%Translation

ORIGINFemur

XAXISFemur

YAXISFemur

ZAXISFemur

MODEL

{*Start of macro section*}

{*=====================*}

macro REPLACE4(p1,p2,p3,p4)

{*Replaces any point missing from set of four fixed in a segment*}

s234 = [p3,p2-p3,p3-p4]

p1V = Average(p1/s234)*s234

```
s341 = [p4,p3-p4,p4-p1]

p2V = Average(p2/s341)*s341

s412 = [p1,p4-p1,p1-p2]

p3V = Average(p3/s412)*s412

s123 = [p2,p1-p2,p2-p3]

p4V = Average(p4/s123)*s123

p1 =  p1 ? p1V

p2 =  p2 ? p2V

p3 =  p3 ? p3V

p4 =  p4 ? p4V



endmacro



macro SEGVIS(Segment)

ORIGIN#Segment=0(Segment)

XAXIS#Segment=0(Segment)+(1(Segment)*100)

YAXIS#Segment=0(Segment)+(2(Segment)*100)

ZAXIS#Segment=0(Segment)+(3(Segment)*100)

output  (ORIGIN#Segment,XAXIS#Segment,YAXIS#Segment,ZAXIS#Segment)

endmacro



Macro POINTER(Anatomy,Segment)

direct1=((Pointer1-Pointer2)/dist(Pointer1,Pointer2))

Anatomy#Calib=Pointer1+123*direct1

OUTPUT(Anatomy#Calib)
```

PARAM(Anatomy#Calib)

%#Anatomy#Calib=Anatomy#Calib/Segment

PARAM(%#Anatomy#Calib)

EndMacro

Macro DYNPOINTER(AnatPoint,Segment)

AnatPoint=%#AnatPoint#Calib*Segment

OUTPUT(AnatPoint)

PARAM(AnatPoint)

EndMacro

{* End of macro section *}

{*KINEMATICS*}

{*=========*}

OptionalPoints (LASI,RASI,RPSI,LPSI)

OptionalPoints (FEMH,LFEP,MFEP,DFEM,GTCH,LTEP,MTEP, PTIB, DTIB, MMAL,LMAL)

OptionalPoints (Pointer1, Pointer2)

OptionalPoints (CalMFEP, CalLFEP, CalGTCH)

OptionalPoints (CalRASI, CalLASI, CalRPSI, CalLPSI)

OptionalPoints (CalMTEP, CalLTEP, CalMMAL, CalLMAL)

OptionalPoints (CalMFEPsit, CalLFEPsit, CalGTCHsit)

OptionalPoints (CalRASIsit, CalLASIsit, CalRPSIsit, CalLPSIsit)

OptionalPoints (CalMTEPsit, CalLTEPsit, CalMMALsit, CalLMALsit)

OptionalPoints (LASIsit,RASIsit,RPSIsit,LPSIsit)

OptionalPoints (FEMHsit,LFEPsit,MFEPsit,DFEMsit,GTCHsit,LTEPsit,MTEPsit, PTIBsit, DTIBsit, MMALsit,LMALsit)

OptionalPoints (TTHIA, TTHIB, BTHIA, BTHIB)

OptionalPoints (TSHAA, TSHAB, BSHAA, BSHAB)

OptionalPoints (PELA,PELB,PELC,PELD)

REPLACE4(TTHIA, TTHIB, BTHIA, BTHIB)

REPLACE4(TSHAA, TSHAB, BSHAA, BSHAB)

REPLACE4(PELA,PELB,PELC,PELD)

{*Marker cluster axis definitions*}

Waist = [PELB, PELB-PELC, PELC-PELD, xyz]

Thigh = [TTHIA, TTHIA-BTHIB, BTHIA-TTHIA, xyz]

Shank = [TSHAA, TSHAA-BSHAB, BSHAA-TSHAA, xyz]

{*static calibrations*}

If $Static == 1

If EXIST(CalMFEP)

Pointer (MFEP, Thigh)

EndIf

If EXIST (CalGTCH)

Pointer (GTCH, Thigh)

EndIf

If EXIST(CalLFEP)

Pointer (LFEP, Thigh)

EndIf

If EXIST(CalMTEP)

Pointer (MTEP, Shank)

EndIf

If EXIST(CalLTEP)

Pointer (LTEP, Shank)

EndIf

If EXIST(CalMMAL)

Pointer (MMAL, Shank)

EndIf

If EXIST (CalLMAL)

Pointer (LMAL, Shank)

EndIf

If EXIST (CalLASI)

Pointer (LASI, Waist)

EndIf

If EXIST (CalRASI)

Pointer (RASI, Waist)

EndIf

If EXIST (CalLPSI)

Pointer (LPSI, Waist)

EndIf

If EXIST (CalRPSI)

Pointer (RPSI, Waist)

EndIf

If EXIST (CalGTCH)

DYNPOINTER (RPSI, Waist)

DYNPOINTER (LPSI, Waist)

DYNPOINTER (RASI, Waist)

DYNPOINTER (LASI, Waist)

{*additional pelvis points*}

PELF = (LASI+RASI)/2

SACR= (LPSI+RPSI)/2

Pelvis = [PELF, PELF-SACR, LASI-RASI, xyz]

InterASISDist = DIST (LASI, RASI)

HJC= (InterASISDist*$%HipOffsetFactor)*Pelvis

OUTPUT (HJC)

PARAM (HJC)

FEMHCalib=HJC

PARAM (FEMHCalib)

%FEMHCalib=FEMHCalib/Thigh

PARAM (%FEMHCalib)

EndIf

EndIf

If $Static == 0

FEMH=%FEMHCalib*Thigh

OUTPUT (FEMH)

PARAM (FEMH)

DYNPOINTER (MMAL,Shank)

DYNPOINTER (MTEP, Shank)

DYNPOINTER (LTEP,Shank)

DYNPOINTER (MFEP,Thigh)

DYNPOINTER (LFEP,Thigh)

DYNPOINTER (LMAL, Shank)

{*centres of femur and tibia*}

DFEM= (MFEP+LFEP)/2

PTIB= (MTEP+LTEP)/2

DTIB= (MMAL+LMAL)/2

OUTPUT (DFEM, PTIB, DTIB)

{*bone definitions*}

{*Now altered for LEFT leg*}

Femur = [DFEM, FEMH-DFEM, LFEP-MFEP, zyx]

SEGVIS (Femur)

OUTPUT (ORIGINFemur, XAXISFemur, YAXISFemur, ZAXISFemur)

Tibia = [PTIB, PTIB-DTIB, LTEP-MTEP, zyx]

{*Output for calculating CoR in MATLAB*}

tranone = TTHIA-PTIB

trantwo = TTHIB-PTIB

tranthree = BTHIA-PTIB

tranfour = PTIB-DFEM

hiptranone=TTHIA-PELC

hiptrantwo=TTHIB-PELC

hiptranthree=BTHIA-PELC

OUTPUT (tranone,trantwo,tranthree,tranfour)

OUTPUT (hiptranone, hiptrantwo,hiptranthree)

{*Relative rotations*}

KNEE=<Femur,Tibia, xyz>

OUTPUT (KNEE)

Translation = DFEM/Tibia

OUTPUT (Translation)

EndIf

Appendix IV – MRI Checklist

Safety Questionnaire for **MRI** scanning

Surname _____ First name _____
Date-of-Birth _____ Weight _____

Have you had a **CT or MRI** scan before? Yes No
Have you had any operations on your **HEAD**? Yes No
Have you had any operations on your **SPINE**? Yes No
Have you had any operations on your **CHEST or HEART**? Yes No
Have you had any operations involving the use of
METALLIC CLIPS, PINS or PLATES? Yes No
Do you have a **Cardiac Pacemaker**? Yes No
Do you have an **Aneurysm Clip**? Yes No
Do you have a **Cochlear implant**? Yes No
Have you ever worked with metal? Yes No
Is there any possibility that you could have **metal in your eye**? Yes No
Have you ever had a shrapnel or bullet injury? Yes No
Are you wearing a **CARDIAC / HRT / NICOTINE** patch? Yes No
Do you suffer from any allergies? Yes No

LADIES:
Is there any possibility that you may be pregnant? Yes No
Are you breast-feeding? Yes No

ALL metal worn or carried on your person is to be removed.
Pens, Spectacles, Keys, Money, Jewellery, Watches, Hairgrips, Dentures, Scissors, Credit Cards, Hearing Aids, Bra, Surgical Supports, etc.

Do not sign this form yet. A radiographer will go through the form with you and explain the MRI scan procedure.

I understand the procedure of a MRI examination. I also understand the above questions.
I give permission for the use of an intravenous contrast agent if it is deemed necessary.

Patient's Signature: _____ Date: _____
RDA Signature: _____Date: _____
PLEASE COMPLETE

This form helps us to give you an appointment that is convenient for you, and makes the best use of the MRI scanner.

1. WHAT DAYS OF THE WEEK ARE MORE SUITABLE FOR YOU TO ATTEND FOR YOUR MRI SCAN?
2. WHAT TIME OF THE DAY IS MORE CONVENIENT FOR YOU TO ATTEND?
3. HAVE YOU ANY HOLIDAYS IN THE NEAR FUTURE?
PLEASE NOTE THE DATES YOU CANNOT ATTEND.
4. DAYTIME TELEPHONE NUMBER : -
EVENING TELEPHONE NUMBER : -

Appendix V – VRML Code

```
#VRML V2.0 utf8


Viewpoint {

position  0 400 -200

orientation   0.0370408 0.8519395 0.5223285 3.020909

description "anterior"}


Viewpoint {

position 400 0 0

orientation 0.6153782 0.6153782 0.4925641 1.8307247

description "left"}


Viewpoint {

position 0 -400 200

orientation   1 0 0 0.9

description "posterior"}


Viewpoint {

position -400 0 0

orientation 0.6153782 -0.6153782 -0.4925641 1.8307247

description "right"}
```

```
Viewpoint {

position 0 0 -400

orientation 0.9950087 0.0705609 -0.0705609 3.1315851

description "distal"}


Viewpoint {

position 0 0 400

description "proximal"}



WorldInfo {

title ""

info [

"By Chris Barr"

]

}


Background {

skyColor  [ 0.3 0.3 0.5


                                    ]

}



DEF femur Transform {
```

center -93.7558 -80.1316 -12.7051

children [

Shape {

appearance Appearance {

material Material {

}

}

geometry IndexedFaceSet {

coord Coordinate {

point [

********Insert Coordinate point for Femur Here*******

]

}

coordIndex [

*************Insert Coordinate linkages for Femur Here***************

```
                    ]

                            }

                    }

            ]

            }




DEF tibia Transform {

        children [

                Shape {

                        appearance Appearance {




                        material Material {

                                }

                        }




geometry IndexedFaceSet {

                                coord Coordinate {




point [

        ********Insert Coordinare Points for Tibia Here*****************

                                ]
```

```
                              }



        coordIndex [



*************Insert Coordinare Linkages For Tibia Here***************************

                              ]
                      }




}
        ]
        }




        # animation clock

                DEF Clock TimeSensor {

                        cycleInterval 1.55 # make timelength of data set



                        loop TRUE

                }



                # animation path
```

```
                    DEF femurmovement OrientationInterpolator {

                        key [

**********Insert decimal breakdown of time here*************************

]

                        keyValue [


**********Insert Dizzy Rotations Here*************

                            ]

                        }




ROUTE Clock.fraction_changed TO femurmovement.set_fraction

ROUTE femurmovement.value_changed TO femur.set_rotation
```

Appendix VI – Additional Graphs

Preoperative Rotation Around the S-I axis vs Flexion in Level Walking

Preoperative Rotation Around the S-I axis vs Flexion in Stair Ascent

Preoperative Rotation Around the S-I axis vs Flexion in Stair Descent

Preoperative Rotation Around the S-I axis vs Flexion in Sit to Stand

Preoperative Rotation Around the A-P axis vs Flexion in Level Walking

Preoperative Rotation Around the A-P axis vs Flexion in Stair Ascent

Preoperative Rotation Around the A-P axis vs Flexion in Stair Descent

Legend:
- Sheehan +1sd
- Sheehan-1sd
- Sheehan+2sd
- Sheehan-2sd
- subject 1
- subject 2
- subject 3
- subject 5
- subject 11
- subject 13
- subject 14

flexion

Preoperative Rotation Around the A-P axis vs Flexion in Sit to Stand

Legend:
- Sheehan +1sd
- Sheehan-1sd
- Sheehan+2sd
- Sheehan-2sd
- subject 1
- subject 2
- subject 3
- subject 5
- subject 11
- subject 13
- subject 14

flexion

Postoperative Rotation Around the S-I axis vs Flexion in Level Walking

Legend: Sheehan +1sd, Sheehan-1sd, Sheehan+2sd, Sheehan-2sd, subject 1, subject 2, subject 3, subject 5, subject 11, subject 13, subject 14

flexion

Postoperative Rotation Around the S-I axis vs Flexion in Stair Ascent

Legend: Sheehan +1sd, Sheehan-1sd, Sheehan+2sd, Sheehan-2sd, subject 1, subject 2, subject 3, subject 5, subject 11, subject 13, subject 14

flexion

Postoperative Rotation Around the S-I axis vs Flexion in Stair Descent

flexion

Legend:
- Sheehan +1sd
- Sheehan-1sd
- Sheehan+2sd
- Sheehan-2sd
- subject 1
- subject 2
- subject 3
- subject 5
- subject 11
- subject 13
- subject 14

Postoperative Rotation Around the S-I axis vs Flexion in Sit to Stand

flexion

Legend:
- Sheehan +1sd
- Sheehan-1sd
- Sheehan+2sd
- Sheehan-2sd
- subject 1
- subject 2
- subject 3
- subject 5
- subject 11
- subject 13
- subject 14

207

Postoperative Rotation Around the A-P axis vs Flexion in Level Walking

Legend:
- Sheehan +1sd
- Sheehan-1sd
- Sheehan+2sd
- Sheehan-2sd
- subject 1
- subject 2
- subject 3
- subject 5
- subject 11
- subject 13
- subject 14

flexion

Postoperative Rotation Around the A-P axis vs Flexion in Stair Ascent

Legend:
- Sheehan +1sd
- Sheehan-1sd
- Sheehan+2sd
- Sheehan-2sd
- subject 1
- subject 2
- subject 3
- subject 5
- subject 11
- subject 13
- subject 14

flexion

Postoperative Rotation Around the A-P axis vs Flexion in Stair Descent

flexion

Legend:
- Sheehan +1sd
- Sheehan-1sd
- Sheehan+2sd
- Sheehan-2sd
- subject 1
- subject 2
- subject 3
- subject 5
- subject 11
- subject 13
- subject 14

Postoperative Rotation Around the A-P axis vs Flexion in Sit to Stand

flexion

Legend:
- Sheehan +1sd
- Sheehan-1sd
- Sheehan+2sd
- Sheehan-2sd
- subject 1
- subject 2
- subject 3
- subject 5
- subject 11
- subject 13
- subject 14

209